INFORMATION TO USERS

This material was produced from a microfilm copy of the original document. While the most advanced technological means to photograph and reproduce this document have been used, the quality is heavily dependent upon the quality of the original submitted.

The following explanation of techniques is provided to help you understand markings or patterns which may appear on this reproduction.

1. The sign or "target" for pages apparently lacking from the document photographed is "Missing Page(s)". If it was possible to obtain the missing page(s) or section, they are spliced into the film along with adjacent pages. This may have necessitated cutting thru an image and duplicating adjacent pages to insure you complete continuity.

2. When an image on the film is obliterated with a large round black mark, it is an indication that the photographer suspected that the copy may have moved during exposure and thus cause a blurred image. You will find a good image of the page in the adjacent frame.

3. When a map, drawing or chart, etc., was part of the material being photographed the photographer followed a definite method in "sectioning" the material. It is customary to begin photoing at the upper left hand corner of a large sheet and to continue photoing from left to right in equal sections with a small overlap. If necessary, sectioning is continued again -- beginning below the first row and continuing on until complete.

4. The majority of users indicate that the textual content is of greatest value, however, a somewhat higher quality reproduction could be made from "photographs" if essential to the understanding of the dissertation. Silver prints of "photographs" may be ordered at additional charge by writing the Order Department, giving the catalog number, title, author and specific pages you wish reproduced.

5. PLEASE NOTE: Some pages may have indistinct print. Filmed as received.

Xerox University Microfilms
300 North Zeeb Road
Ann Arbor, Michigan 48106

Downloaded from SHAREOK. Persistent Handle URL: https://hdl.handle.net/11244/4417

7817897

CONWAY, MICHAEL WAYNE
I. MECHANISM OF PHOTOLYSIS OF (9-ACRIDINYLMETHYL) QUATERNARY AMMONIUM SALTS. II. LUMINESCENCE CHARACTERISTICS OF 9-SUBSTITUTED ACRIDINE DERIVATIVES.

THE UNIVERSITY OF OKLAHOMA, PH.D., 1978

University Microfilms International 300 N. ZEEB ROAD, ANN ARBOR, MI 48106

THE UNIVERSITY OF OKLAHOMA

GRADUATE COLLEGE

I. MECHANISM OF PHOTOLYSIS OF (9-ACRIDINYLMETHYL) QUATERNARY AMMONIUM SALTS

II. LUMINESCENCE CHARACTERISTICS OF 9-SUBSTITUTED ACRIDINE DERIVATIVES

A DISSERTATION

SUBMITTED TO THE GRADUATE FACULTY

in partial fulfillment of the requirements for the

degree of

DOCTOR OF PHILOSOPHY

By

MICHAEL W. CONWAY

Norman, Oklahoma

1978

I. Mechanism of Photolysis of (9-acridinylmethyl) Quaternary Ammonium Salts.

II. Luminescence Characteristics of 9-substituted Acridine Derivatives.

APPROVED BY

DISSERTATION COMMITTEE

Dedication

To Judy, whose love, patience, understanding and assistance made this work possible.

Acknowledgements

The author wishes to express sincere appreciation to Dr. Roland E. Lehr for his direction and guidance throughout this course of study. To Dr. Pushkar N. Kaul, a continuing debt of gratitude is expressed. To my colleagues and friends, Dr. J. Michael Wilson, Patrick Cohenour, Lloyd Whitfield, Dr. Robert Allen, Dr. Tom Karns, Dr. Bob Hayes, Dr. Keith Hollenbeak, Dr. Hank Nichols, Dr. James Owens and Dr. Steve Elich, I wish to offer sincerest thanks for stimulating discussions, encouragement and assistance. To the Faculty and Staff of the Department of Chemistry, and all my friends too numerous to mention, appreciation is expressed for their willing assistance throughout my course of study in the Department. To my parents, Roscoe and Ida Mae Conway, and other family members, I wish to express warmest regards for understanding and encouragement.

TABLE OF CONTENTS

LIST OF TABLES vii

LIST OF FIGURES ix

PART I. MECHANISM OF PHOTOLYSIS OF (9-ACRIDINYLMETHYL QUATERNARY AMMONIUM SALTS 1

Chapter

1. INTRODUCTION 1

2. RESULTS AND DISCUSSION 7

3. EXPERIMENTAL 38

LITERATURE CITED 59

PART II. LUMINESCENCE CHARACTERISTICS OF 9-SUBSTITUTED ACRIDINE DERIVATIVES . 62

Chapter

1. INTRODUCTION 62

2. RESULTS AND DISCUSSION: GENERAL PROPERTIES OF ACRIDINE DERIVATIVES 92

3. RESULTS AND DISCUSSION: SPECTRAL CHARACTERISTICS OF ACRIDINE DERIVATIVES 107

TABLE OF CONTENTS, CONTINUED

4. EXPERIMENTAL 154

LITERATURE CITED 174

LIST OF TABLES

Table — Page

Part I

1. The Effect of Deuterated Methanol on the Photolysis of [10] 22

2. The Effect of Various Energy Transfer Agents on the rate of Photolysis of (9-acridinylmethyl) Trimethylammonium Bromide 24

3. The Effect of Reaction Medium on the Photolysis and Fluorescence of (9-acridinylmethyl) Trimethylammonium Bromide 23

4. Comparison of the Photolysis of Acridine Quaternary Salts Derived from Trimethylamine [10] and Chlorpromazine [15] 27

Part II

1. Colour of Fluorescence of Various Acridines in UV Light . 64

2. Effects of Substituents upon the Fluorescence of Aromatics 78

3. Effect of Water on the Fluorescence of Acridine 84

4. Effect of Temperature on Observed Quantum Yield of Fluorescence 85

5. Effect of Acid-base Properties on Fluorescence 87

6. Effect of Isomeric Substitution on the Fluorescence of Pyridine Derivatives 88

7. Fluorescence Characteristics of Isomeric Aminoacridines 88

List of Tables, Continued

8. Fluorescence Characteristics of Selected Aromatic Amines 89

9. Fluorescence Characteristics of Various (9-acridinyl)-thiourea Derivatives 91

10. Spectroscopic Characteristics for 9-acridinylmethyl Derivatives in Methanol 118

11. Spectroscopic Characteristics for 9-acridinylmethyl Derivatives in Water 119

12. Spectroscopic Characteristics of 9-acridinylmethyl Derivatives in Acidic Solvent 119

13. Hammett Substituent Constants for Selected Functional Groups 120

14. Relative Fluorescence Values for Selected 9-acridinyl Derivatives in Acidic Solvents 124

15. Fluorescence Characteristics in 12 N H_2SO_4 in Methanol of Quaternary Salts Derived from 9-bromomethylacridine .127

16. Fluorescence Characteristics of Selected Acridine Derivatives 130

17. Singlet-singlet Nonradiative Electronic Energy Transfer Mechanisms 132

18. Expected Spectral Characteristics of Encounter Complexes 137

LIST OF FIGURES

Figure Part I.		Page
1.	60 MHz PMR Spectrum ($CDCl_3$) of 1,2-bis-(9-acridinyl) Ethane [6]	12
2.	IR Spectrum (KBr) of 1,2-bis-(9-acridinyl) Ethane [6]	13
3.	Mass Spectrum (70 ev) of bis-(9-acridinyl) Ethane [6]	14
4.	Time Profiles for the Photolyses of 10^{-2} and 10^{-3} M Solutions of [10] in Degassed Methanol	17
5.	Time Profile for the Photolysis of [10] and [15] on a Silica Gel TLC Plate Using Broad Band Irradiation at 350 nm	32
6.	Potential Reaction Pathways for 9-acridinylmethyl Radical on Silica Gel TLC Plates	36
7.	60 MHz PMR Spectrum (CD_3OD) of (9-acridinylmethyl) Trimethylammonium Bromide [10]	41
8.	IR Spectrum of (9-acridinylmethyl) Trimethylammonium Bromide [10]	42
9.	60 MHz PMR Spectrum ($CDCl_3$) of (9-acridinylmethyl) (3-phenylpropyl) dimethylammonium Bromide [11]	44
10.	IR Spectrum (KBr) of (9-acridinylmethyl)(3-phenylpropyl) Dimethylammonium Bromide [11]	45
11.	60 MHz Spectrum ($CDCl_3$) of 9-(methoxymethyl)-acridine [5]	48
12.	IR Spectrum (KBr) of 9-(methoxymethyl)-acridine [5]	49
13.	Mass Spectrum (70 ev) of 9-(methoxymethyl)-acridine [5]	50

List of Figures, Continued

14. 60 MHz PMR (CF_3COOH) of [14] 57

Part II.

1. Potentially Useful Acridine Fluorescence Tagging Reagents 65

2. Potential Energy Diagram for the Ground State and the First Excited Singlet and Triplet States of a Representative Organic Molecule in Solution 67

3. Classification of Molecular Electronic Transitions by Approximate Correlation with Molar Absorption Coefficient, Oscillator Strength and Intrinsic Luminescence Lifetime . . 69

4. A Modified Jablonski Diagram Showing Various Radiative and Nonradiative Pathways 71

5. The Dependence of Vibrational Overlap Integral on the Energy Separation Between the Lowest Triplet and Ground States 75

6. Tertiary Amine Drugs Used to Prepare Quaternary Salts for Chemical and Spectral Characterization 99

7. 100 MHz PMR ($CDCl_3$) of the Chlorpromazine Quaternary Salt [15] 100

8. 100 MHz PMR ($CDCl_3$) of the Amitriptyline Quaternary [29] at Room Temperature 102

9. The Effect of Temperature on the N,N-dimethyl PMR Signal of [29] 103

10. Relative Fluorescence of 9-methylacridine [2] and (9-acridinylmethyl) Trimethylammonium Bromide [10] . . 108

11. Fluorescence Excitation and Emission Spectrum of 9-methylacridine in Water 110

12. The Effect of Acid Concentration on the Fluorescence of (9-acridinylmethyl) Trimethylammonium Bromide [10] . . 111

13. The Energy Distribution from two types of Commercial Point-source Lamps 112

List of Figures, Continued

14. Reflectance Curves for Spectrofluorometer Gratings . . . 113

15. Absorption Spectra for 9-methylacridine [2] in Ethanol and Ethanolic 2 N H_2SO_4 115

16. Energy Corrected Excitation Spectrum of Benzopyrene in Ethanol 116

17. Schematic Diagram of Potential Energy Curves Corresponding to the Charge Transfer Excited State and Ground State of the CT Complexes 139

18. Fluorescence Spectra of Anthracene Monomer, the Dimer B and the Excimer in Cyclohexane Matrix at 77°k . 141

19. 100 MHz PMR Spectra of 9-methylacridine in $CDCl_3$ . . . 145

20. First Order Splitting Diagram for 9-methylacridine . . . 146

21. The Effect of Chlorpromazine on the NMR Spectrum of the Trimethylamine Quaternary Salt [10] 148

22. Concentration Dependence in the NMR Spectrum of [10] in d_4-methanol 149

23. Computer Drawing of a Single Molecule of the Quaternary Ammonium Salt Derived from 9 bromomethylacridine and Chlorpromazine 150

24. Computer Drawing Showing the Acridine-acridine Antiparrallel Stacking About the Center Symmetry at 0, 1/2, 0. The Box Represents the Unit Cell Boundaries 151

25. 60 MHz PMR ($CDCl_3 + CD_3OD$) of the Chlorprothexene Quaternary [31] 160

26. IR Spectrum (KBr) of the Chlorprothixene Quaternary [31]. 161

27. 100 MHz PMR Spectrum (d_6-DMSO) of the Promazine Quaternary [32] 163

28. IR Spectrum (KBr) of the Promazine Quaternary [32] . . . 164

List of Figures, Continued

29. IR Spectrum (KBr) of 9-acridinylmethylpyridinium Perchlorate 166

30. 60 MHz PMR Spectrum ($CDCl_3$) of the Imipramine Quaternary [28] 167

31. 60 MHz PMR Spectrum ($CDCl_3$) of 9-(p-bromomethylphenyl) Acridine [33] 169

32. IR Spectrum (KBr) of 9-(p-bromomethylphenyl) Acridine [33] 170

I. MECHANISM OF PHOTOLYSIS OF (9-ACRIDINYLMETHYL) QUATERNARY AMMONIUM SALTS

CHAPTER 1

INTRODUCTION

Our interest in the photolysis of quaternary ammonium salts arose during the development of a fluorescence method for assaying tertiary amine drugs in biological fluids (1).

Scheme I

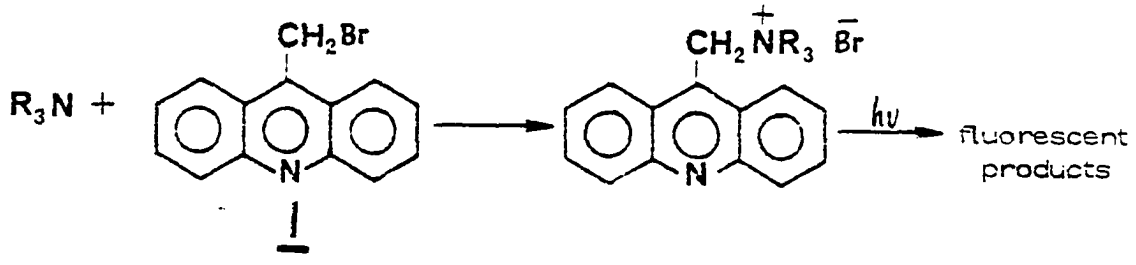

In the method, the tertiary amine drug is first quaternized via reaction with 9-bromomethylacridine [1](2). The quaternary ammonium adduct (itself nonfluorescent) is separated from other compounds by TLC and photolyzed on the TLC plate to generate fluorescence. The amount of fluorescence observed is proportional to the amount of

tertiary amine drug originally present, thereby enabling its quantitation. Recently reported results from our laboratory (3) indicated that the analytical photolysis reaction generates 9-methylacridine [2], 9-acridinylcarboxaldehyde [3] and 9-acridinylmethanol [4]. However,

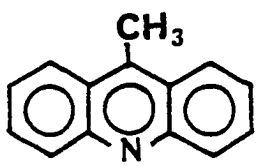

2

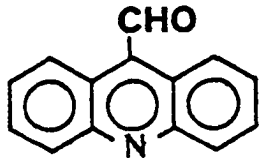

3

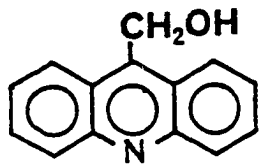

4

these products represent only ca. 25% of the theoretical yield of fluorescent products. We felt that a mechanistic study of the photolysis reaction might produce information that could be applied to increasing the yield of fluorescent products in the photolysis reaction, thereby improving the analytical methodology. Also, we were interested in making a mechanistic comparison of the photolysis reaction of (9-acridinylmethyl) quaternary salts with those of the structurally similar benzyl trialkyl ammonium salts. In 1971, Ratcliff and Kochi (4) first reported on the photolysis of a series of primary, secondary, tertiary and quaternary ammonium salts. Subsequently, Appleton et al. (5,6) proposed the following mechanism (scheme II) to account for the products observed in photolysis of benzyl trimethyl ammonium salts, which are analogous to the 9-acridinylmethyl quaternary ammonium salts used in this investigation.

Scheme II

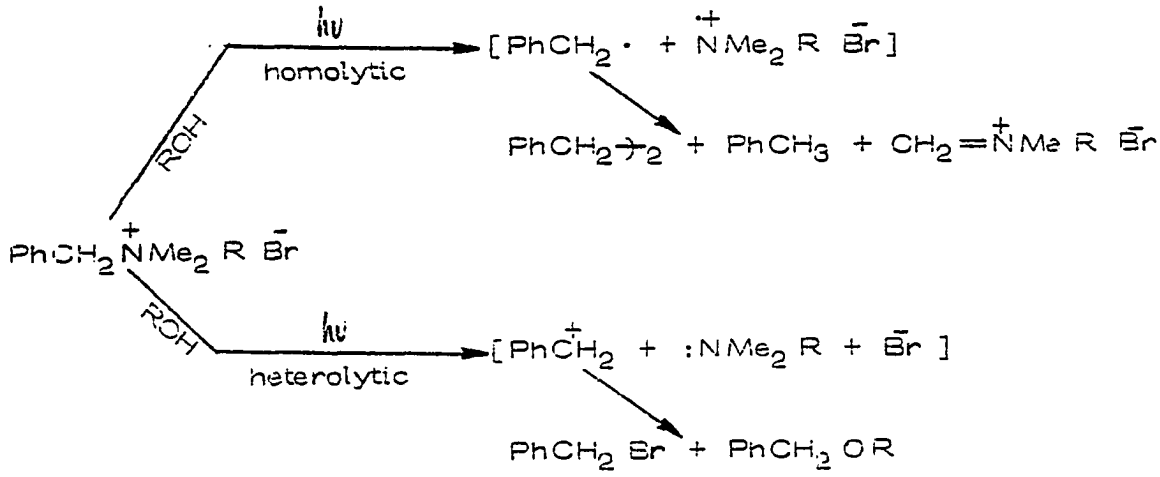

In their work, they suggest that the photoexcited molecule may either react as a singlet or undergo intersystem crossing to a triplet. They conclude that the triplet photoexcited state undergoes homolytic cleavage of the C-N bond to yield a geminate radical pair which may either disproportionate in a solvent cage reaction or escape the cage and primarily dimerize. The use of a triplet quencher piperylene showed that all the bibenzyl and ca. 60% of the toluene produced in the reaction came from the triplet state.

The solvent cage disproportionation reaction was suggested by the presence of dimethylamine in the reaction mixture following acidic hydrolysis (scheme III).

It was suggested that the singlet photoexcited state may undergo either heterolytic cleavage to finally yield an ether as the solvent

Scheme III

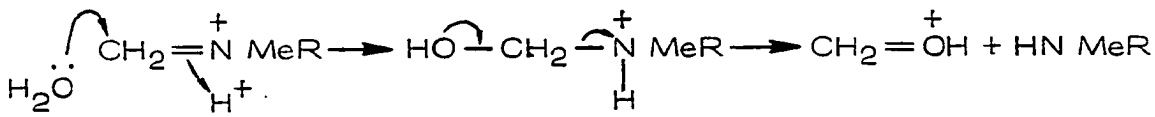

recombination product or homolytic cleavage to form a radical pair which then disproportionates in the solvent cage. Ratcliff and Kochi (4) had shown earlier that the singlet pathway predominates in the unsensitized reaction and that there is an almost equal probability of occurrence for both heterolytic and homolytic cleavage of the singlet excited state. In the photolysis of (9-acridinylmethyl) quaternary ammonium salts dissolved in methanol, the yield of 9-(methoxymethyl)-acridine [5] and/or 9-bromomethylacridine [1] would indicate the amount of heterolytic cleavage occuring in the reaction (scheme IV). On the other hand,

Scheme IV

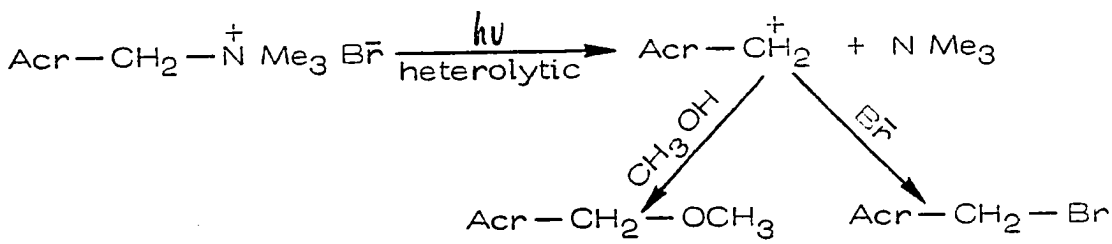

homolytic cleavage of the C-N bond would produce a geminate radical pair inside a solvent cage. The radical pair could disproportionate inside the solvent cage and produce 9-methylacridine and dimethylimmonium bromide. If, however, the radicals escape the cage, a variety of products could be produced such as a dimer, 1,2-bis

(9-acridinyl) ethane [6], 9-methylacridine [2] and 2-(9-acridinyl) ethanol [7] (scheme V).

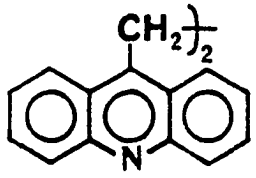

6

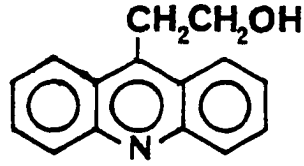

7

Scheme V

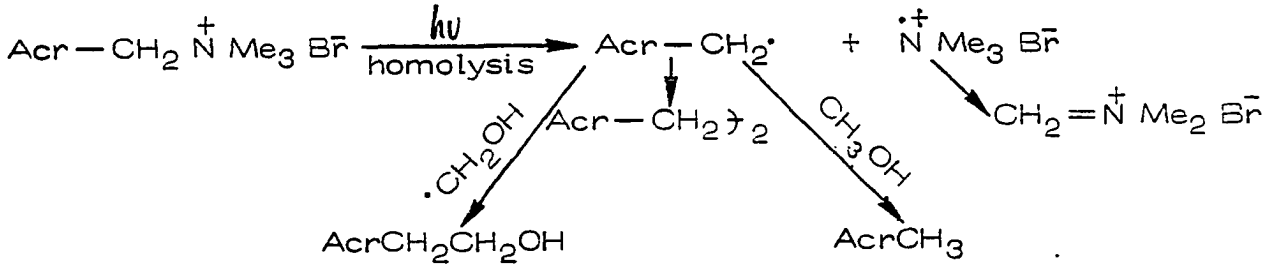

Furthermore, in the acridine system further photolysis of the primary acridine photoproducts is also possible. Acridine and 9-alkyl acridines undergo photoreduction (7) in deoxygenated alcohol solvents to yield various reduced acridans (scheme VI).

Scheme VI

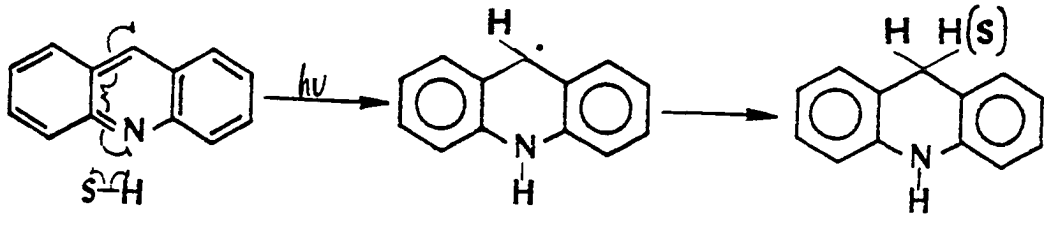

Early investigators felt that the reacting species in the acridine photoreduction was a triplet since the reaction was quenched by oxygen (8). However, the absence of photolysis in the triplet sensitized reaction using biphenyl as the sensitizing agent (10), and the observation that acridans are photo-oxidized to acridines in the presence of oxygen (9) led others to suggest that a singlet excited state was the reactive species (10). Subsequently, it was shown that photoreduction and fluorescence were simultaneously quenched by biacetyl, further confirming that the reactive species was indeed a singlet (11). However, later experimental evidence (12) suggested that the photoreductive singlet was different from the fluorescing singlet. This conclusion was obtained by comparing the effect of solvent composition on the quantum yield of both photoreduction and fluorescence. It was found that replacement of benzene by toluene enhanced photoreduction but had no effect on the fluorescence. The same result was observed for the addition of 2-propanol to tert-butanol. Therefore, these authors proposed that the initially formed $^1\pi,\pi^*$ singlet decays to a lower lying singlet, probably the $^1 n,\pi^*$ singlet which is the species undergoing photoreduction.

Therefore, in the case of 9-acridinylmethyl quaternary ammonium salts, various pathways and reactive species could be involved. The following study was undertaken to determine the mechanism of photolysis of quaternary ammonium salts.

CHAPTER 2

RESULTS AND DISCUSSION

Conditions of Photolysis

Since initial studies of the photolysis of chlorpromazine quaternary salts indicated a complex mixture of products, we chose to first study a case in which the amine was structurally simpler and in which fewer non-acridine containing products would be expected to be formed. Therefore, the mechanistic studies were performed with the quaternary salts produced by reacting 9-bromomethylacridine with trimethylamine and N,N-dimethyl-3-phenylpropylamine.

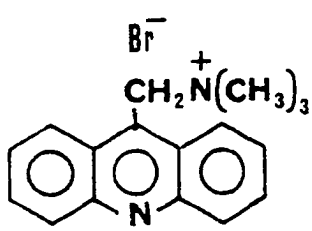

10

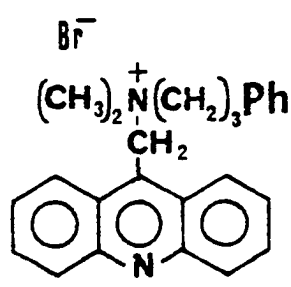

11

The limited solubility of the quaternary acridine salts restricted the solvent choice to polar solvents such as alcohols. Furthermore, other workers have previously investigated the

photolysis of both 9-alkylacridines (9-12) and benzyl ammonium salts (4) in alcoholic solvents. Anhydrous methanol was found to be the solvent of choice because the ether which might arise from solvent attack on the intermediate produced by heterolytic cleavage of the C-N bond (see scheme II) could be prepared and purified (scheme VII). The ethyl ether

Scheme VII

$$AcrCH_2Br \xrightarrow[0^\circ]{ROH/RO^-Na^+} AcrCH_2OR$$

was found to be far less stable and could not be successfully prepared and handled, at least under conditions similar to those which would be encountered in the photolysis reaction.

A possible explanation for the observed differences in stability can be drawn from results obtained with the analogous picolyl ethers (13). In that system, treatment of the ethyl ether but not the methyl ether, with strong base results in abstraction of the benzylic proton followed by alkyl migration (scheme VIII).

Scheme VIII

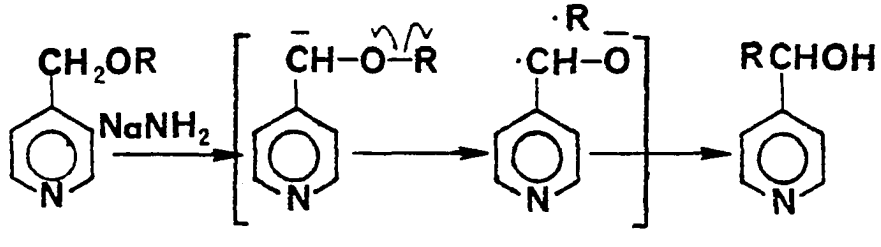

In our system, we feel that the benzylic protons are much more basic than those in the picolyl ethers and therefore would be much more susceptible to base catalyzed decomposition initiated by the alkoxide used to synthesize the ether. Furthermore, by analogy, the ethyl ether should be the least stable. Because of the observed differences in stability of the methyl and ethyl ethers derived from 9-bromomethylacridine, methanol was chosen as the primary alcoholic solvent to be used in the mechanistic studies of the photolysis reaction.

Considerable variations in product distribution were observed in our initial photolyses. Two major factors were responsible for these observations. First, in some instances (less concentrated solutions), further photolysis of the primary photoproducts resulted in a variety of secondary photoreduced products. Second, variable trace amounts of oxygen were evidently present in the solvent following an initial "degassing" procedure, which entailed bubbling prepurified nitrogen through the reaction mixture. This conclusion was suggested by the observation that variable amounts of oxygenated products such as acridone [8], 9-acridinylcarboxaldehyde [3], 9-acridinylmethanol [4] and 9-acridinecarboxylic acid [9] were formed under these conditions.

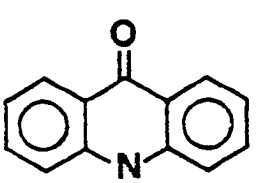

8

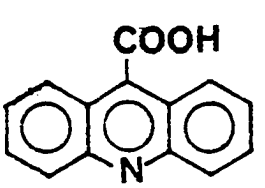

9

In order to achieve reproducible results and to prepare the large number of degassed samples necessary to perform the study, the following apparatus and procedure was employed.

Freeze-thaw procedures normally used to deoxygenate samples are not very applicable to a large number of small volume samples because each sample must have a vacuum stopcock with very little dead space between the liquid surface and vacuum source in order to prevent significant solvent losses. The need for these stopcocks can be negated, however, if the freezing point of the solvent is lower than the temperature at which its vapor pressure is 1 mm. Such is the case for methanol which has a 1 mm vapor pressure at -44° (14) and a freezing point of -94° (15). Therefore, by alternating the samples between a dry ice acetone bath and a liquid nitrogen bath, the freeze-thaw cycle can effectively be achieved without solvent loss. Furthermore, it was subsequently shown that subjecting a sample, cooled to -78°, to a vacuum of 0.05-0.01 Torr for approximately 12 hrs was sufficient to achieve deoxygenation. The samples for photolysis were prepared by placing ca. 0.5 mL of reaction mixture in 8 mm x 10 cm pyrex tubing sealed at one end, degassing by the above procedure, and sealing the tubes under vacuum. Large volume preparative photolysis samples were prepared by the normal freeze-thaw procedure.

The photolysis reaction was then investigated by irradiating the sample in the region of the acridine long-wavelength absorption (ca. 360 nm) and the products were quantified spectrophotometrically following TLC fractionation.

Photolysis Products and Stoichiometry

The photolysis of (9-acridinylmethyl) trimethylammonium bromide [10] (100 mg, 0.3 mmole) in 30 mL deoxygenated anhydrous methanol led to the separation of 26 mg (45%) of straw-colored crystalline product which was recrystallized from chloroform and identified as 1,2-bis-(9-acridinyl)ethane [6] on the basis of its NMR (Figure 1)

Scheme IX

$$\underset{[10]}{AcrCH_2\overset{+}{N}(CH_3)_3Br^-} \xrightarrow[CH_3OH]{h\nu} \underset{[2]}{AcrCH_3} + \underset{[6]}{(AcrCH_2)_2}$$

IR (Figure 2) and mass spectra (Figure 3). The NMR spectrum shows the characteristic acridine aromatic protons from 7.35 - 8.35 delta (16H) and the singlet methylene protons at 4.15 delta (4H). The mass spectrum shows a parent ion at m/e 384.

The filtrate obtained from the photolysis was evaporated, dried and shown by its NMR spectrum to contain [2] and [6] (ca. 4% and 8% of theory, respectively) and unreacted starting material. The presence of 9-methylacridine in the mixture was suggested by the

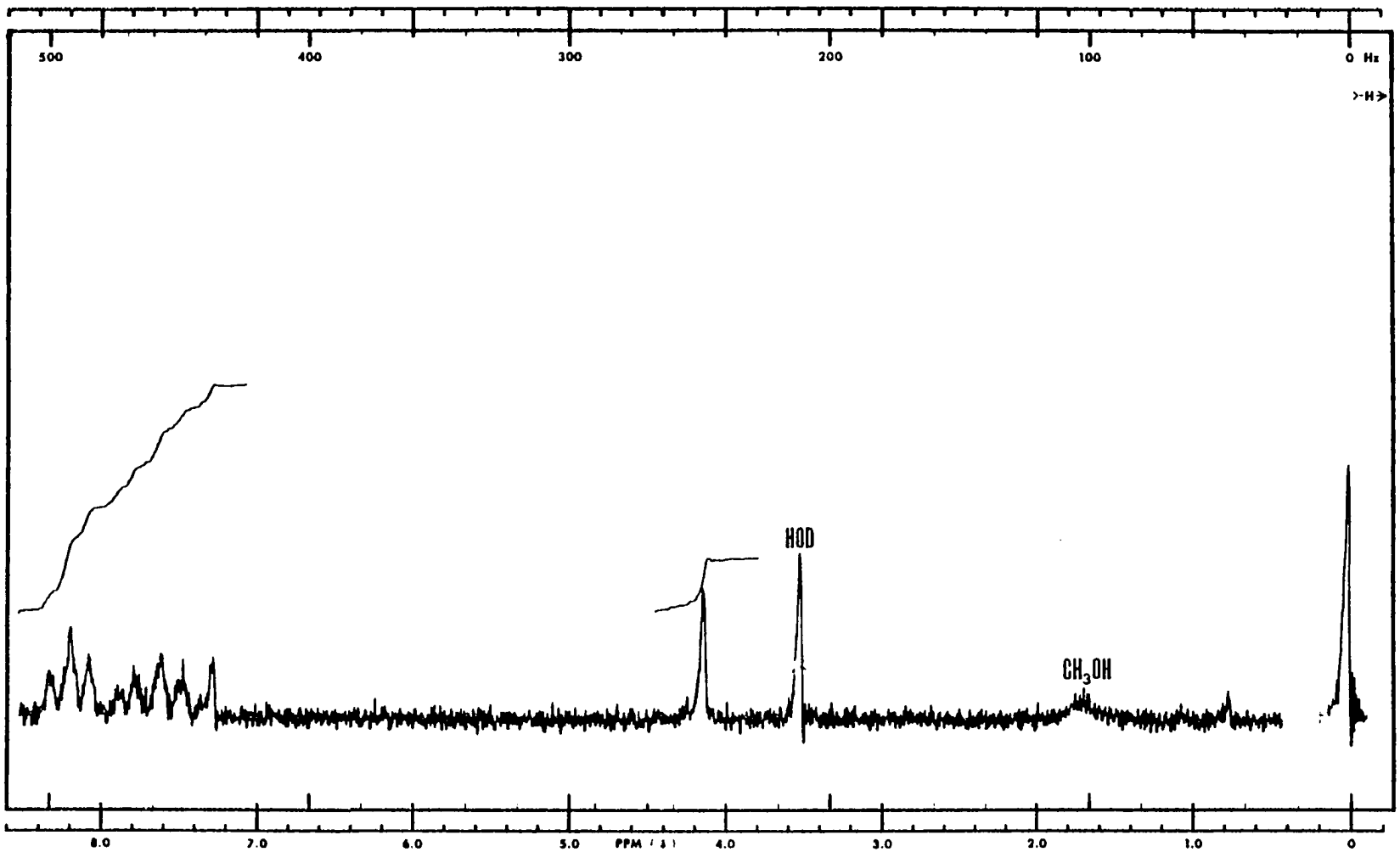

Figure 1. 60 MHz PMR spectrum ($CDCl_3$) of 1, 2-bis-(9-acridinyl)ethane [6].

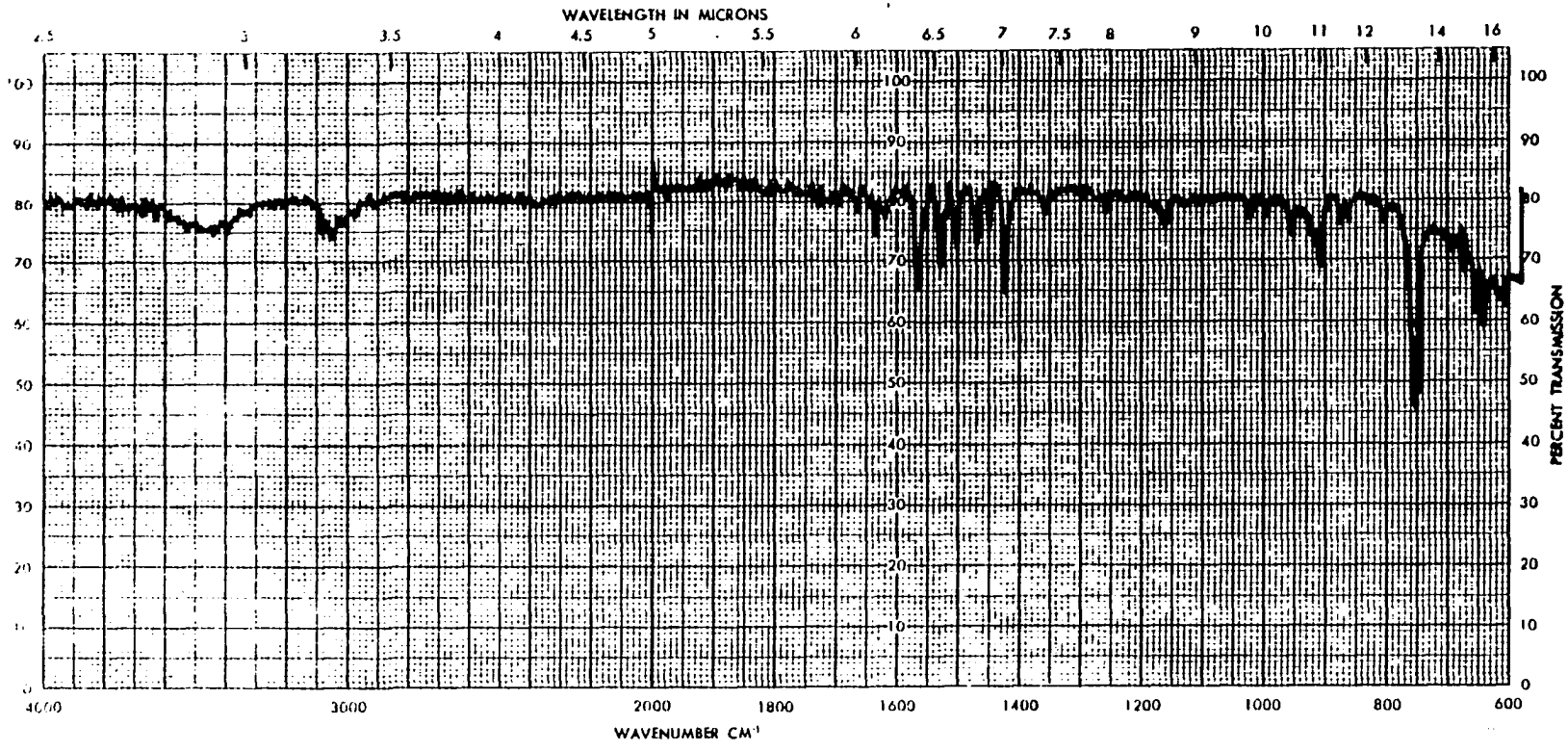

Figure 2. IR spectrum (KBr) of 1,2-bis-(9-acridinyl) ethane [6].

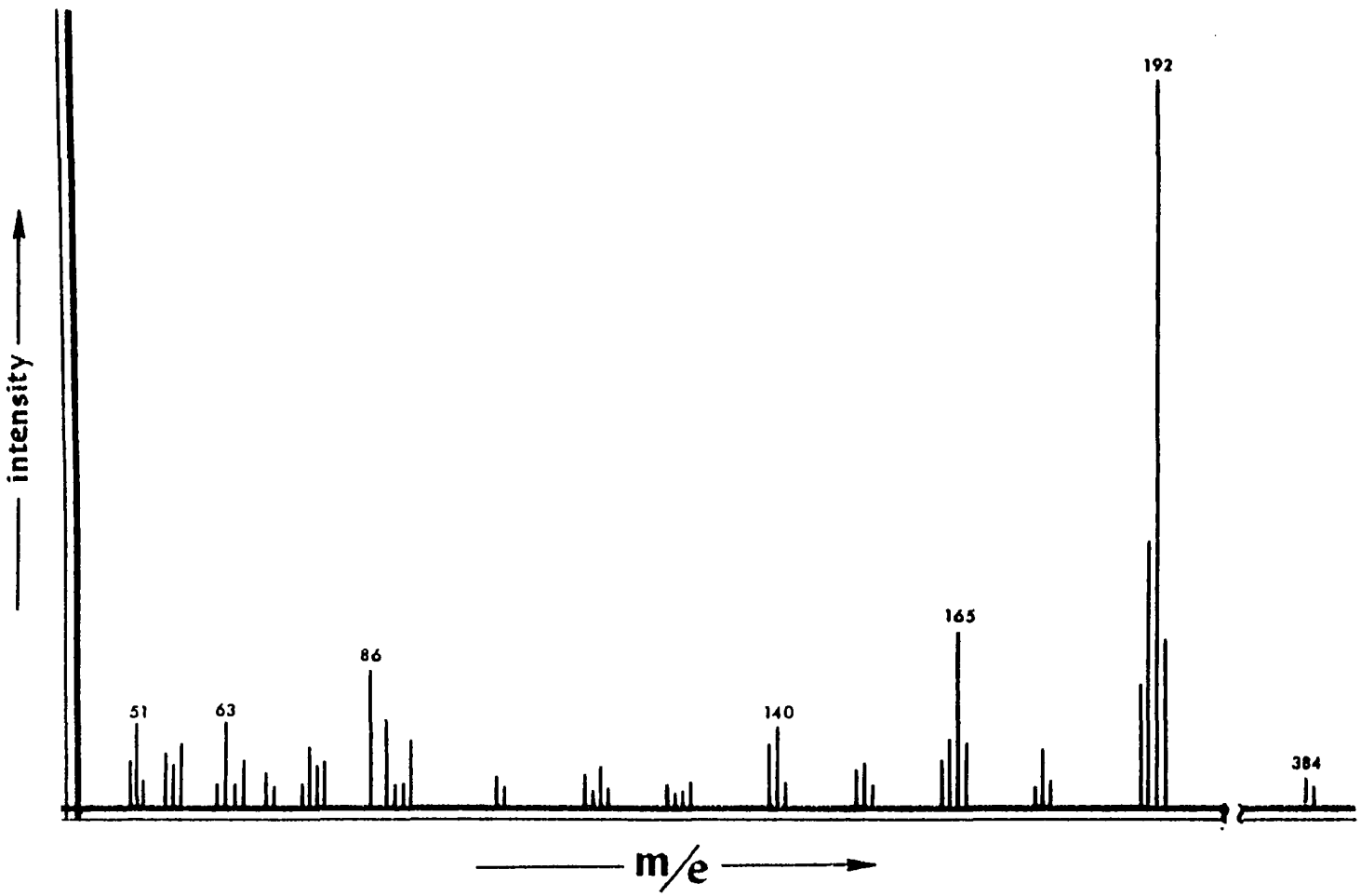

Figure 3. Mass spectrum (70 ev) of 1,2-bis-(9-acridinyl)ethane [6].

presence of a singlet methyl absorption at ca. 3.0 delta. The position of the NMR methyl absorption is concentration dependent and varies from 2.9-3.1 delta. Further, confirmation for this structural assignment was obtained by TLC comparison of the reaction mixture to authentic [2] and [6].

An additional NMR absorption (2.95 delta) present in the PMR spectrum of the photolysis reaction mixture was shown to be due to trimethylamine which was isolated from the reaction mixture after neutralization with Na_2CO_3 by vacuum distillation. No dimethylamine could be detected. Since the identity of the amine fragment produced during the photolysis can be used to determine whether or not a solvent cage disproportionation reaction (scheme X) is occuring, an accurate identification of all amines produced is needed. We felt confident in our NMR amine identification procedure which indicated dimethylamine was not present within the limits of detection. However, the implication of the somewhat surprising absence of a solvent cage disproportionation reaction prompted the further investigation of another quaternary salt to confirm this fact as a generalization for acridine quaternary salts. Therefore, the quaternary salt [11] derived from N,N-dimethyl-3-phenylpropylamine was prepared to further confirm the results obtained with the trimethylamine quaternary.

When a 10^{-2}M solution of the quaternary salt derived from N,N-dimethyl-3-phenylpropylamine was photolyzed in deoxygenated

methanol for thirty minutes, 92% of the quaternary was consumed. The reaction mixture was concentrated, subjected to dilute acid hydrolysis and the amine products were extracted into hexane after basification with Na_2CO_3. The only amine found was N,N-dimethyl-3-phenylpropylamine (76% yield by GLC). The absence of detectable amounts of N-methyl-3-phenylpropylamine (<10%) further confirmed that a solvent cage disproportionation (scheme X) is not a significant reaction pathway.

In order to further understand the photolysis reaction, time profiles for the disappearance of the trimethylamine quaternary [10] and the appearance of [2] and [6] were obtained from photolysis of 10^{-2} and 10^{-3} solutions in methanol and are shown in Figure 4. Under these conditions, all products remain in solution.

The concentration of the various components present in the photolysis reaction mixture was determined by a combination of TLC and of UV spectrophotometry. The components were fractionated on silica gel TLC plates using benzene:acetone (95:5) as the eluting solvent. The compounds were then extracted from the silica gel using 95% ethanol for the photoproducts and 2N H_2SO_4 in 95% ethanol for unreacted started material. Quantitation was achieved by measuring the intensity of their ultraviolet maxima relative to those of known quantities of the products processed in the same manner. In the early time intervals the unphotolyzed starting material, [2], and [6], account

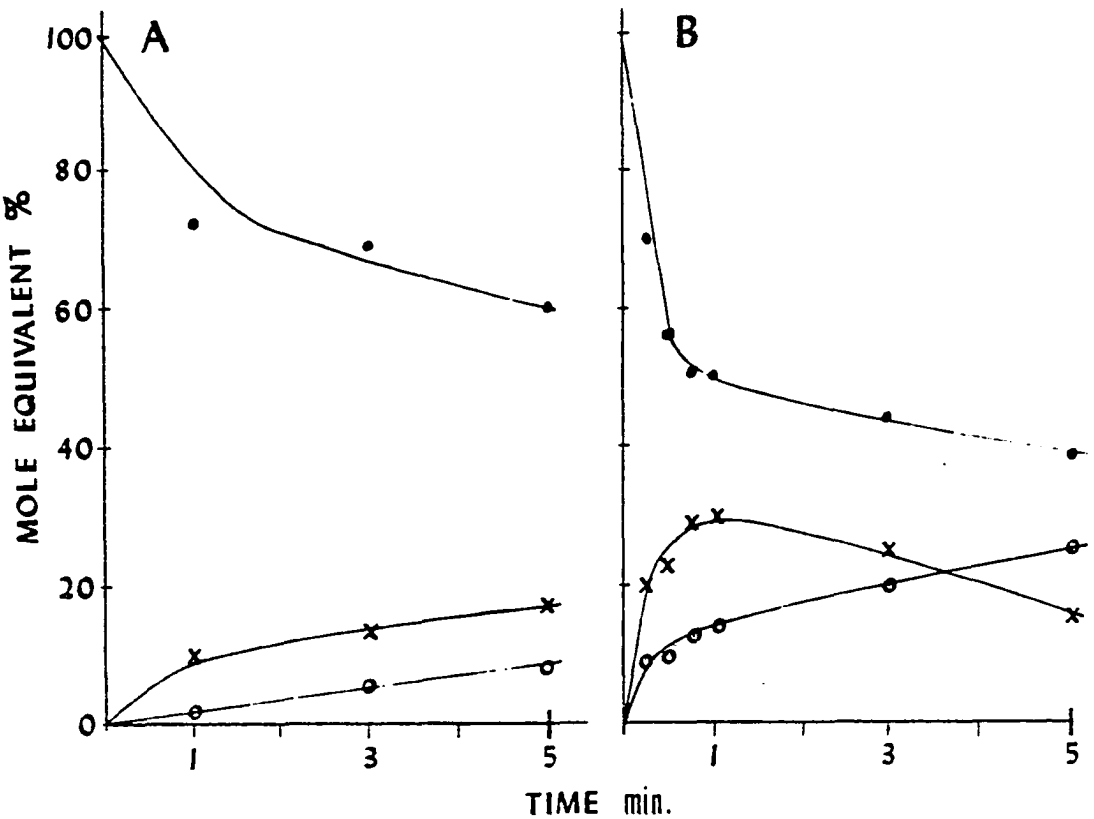

Figure 4. Time profiles for the photolyses of 10^{-2} (A) and 10^{-3}M (B) solutions of [10] in degassed methanol. Compounds measured are [10] ●—●—●; [6] x—x—x; [2] o—o—o.

for greater than 90% of the components in the reaction mixture. However, at later time intervals, the primary photolysis products appear to undergo secondary photolytic reactions. This phenomenum is most evident in the 10^{-3}M time profile. The quaternary concentration decreases very rapidly initially with most of it being converted to [6]. The level of [6], however, was subsequently reduced from a high of 30% of theoretical at 1 minute to 12% at 5 minutes. Secondary photolysis of the primary products was confirmed by irradiating 10^{-2}M degassed methanolic solutions of various 9-substituted acridine compounds.

The photolysis of 9-methylacridine [2] yields a series of photoreduced acridans [12-14]. Following a preparative scale

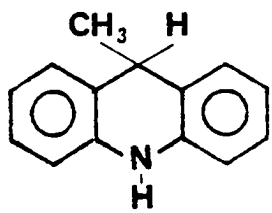

12

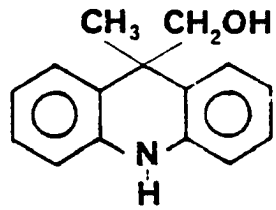

13

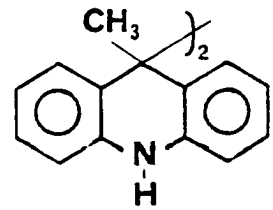

14

photolysis, the acridans were isolated by column chromatography and identified by their previously reported PMR spectra (7). The photolysis of pure samples of [6] indicates that it also undergoes secondary photoreductions to first yield [2] and then the photoreduced acridans. A probable mechanism is the rapid cleavage of the ethylenic C-C bond to yield two 9-acridinylmethyl radicals which abstract a hydrogen radical and form [2]. The 9-methylacridine thus produced is slowly photoreduced giving the same product profile obtained by photolysis of pure [2]. In deoxygenated methanol, the trimethylamine quaternary [10] yields [6], [2] and the various photoreduced acridans whereas under oxygenated conditions, the primary products are [2], [6] and various oxygenated products.

Another possible pathway for quaternary photolysis (scheme X) is heterolytic cleavage of the C-N bond yielding either a methyl ether [5] or the bromide [1] from reaction of the 9-acridinylmethyl carbonium ion with the nucleophiles present in the reaction mixture. Therefore, the

stability of these two compounds under reaction conditions was investigated to determine if they were stable enough to reaction conditions to be observed if formed. Although 9-(methoxymethyl) acridine [5] has the same TLC R_f value as does 9-methylacridine in all solvent systems investigated, NMR analysis of the reaction mixtures could be used to examine the fate of [5] under reaction conditions. Preparative scale photolysis of a 10^{-2}M solution in deoxygenated methanol revealed that [5] is only slowly consumed under reaction conditions. The products were not investigated in detail, but appeared by NMR and TLC analysis to be the acridans expected to result from photoreduction. Further, these products had R_f values slightly different from those produced in prolonged photolyses of [2] and [6]. Control photolysis of the other possible carbonium ion product, 9-bromomethylacridine [1] indicated that it was too unstable under reaction conditions to be observed. However, the primary product of photolysis of [1] in deoxygenated methanol, as shown by NMR analysis of a 10^{-2}M preparative scale photolysis, is [5]. Therefore, the ether, which only undergoes a slow photoreduction under control reaction conditions, would be indicative of heterolytic cleavage. However, this product was not observed by NMR analysis of a 10^{-2}M preparative scale photolysis of the quaternary acridine salt [10]. Therefore, heterolysis of the C-N bond is not a significant reaction pathway in the quaternary photolysis.

The results previously mentioned are consistent with the

Scheme X

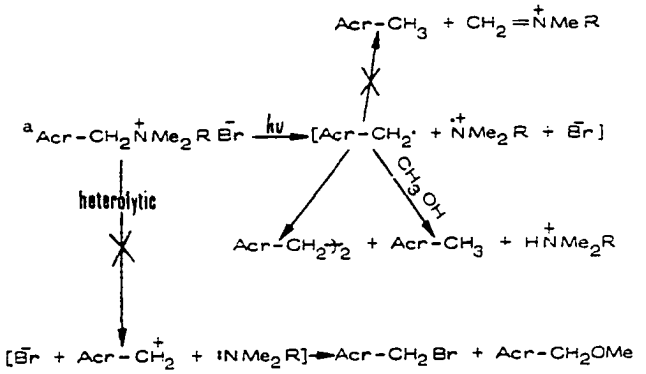

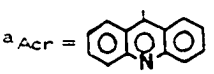

reaction pathway shown in scheme X. Homolytic cleavage of the C-N bond occurs to the apparent exclusion of heterolytic cleavage. Thus 9-bromomethylacridine [1], and 9-(methoxymethyl) acridine [5], expected products of heterolytic cleavage, are not observed as products, while 9-methylacridine [2] and 1,2-bis (9-acridinyl) ethane [6] are produced in good yield. Solvent cage disproportionation of the radical resulting from homolysis of the C-N bond does not occur in this system since the only amine products produced are tertiary amines.

This mechanism proposes that the hydrogen atom abstracted by the 9-acridinylmethyl radical originates from the solvent. An attempt to obtain further confirmation of this pathway, by analysis of the deuterium content of the 9-methylacridine resulting from photolysis of [10] in d_4-methanol, was unsuccessful. Control experiments established that 9-methylacridine containing three deuterium atoms

in the methyl group suffered extensive deuterium loss during the isolation procedure.

No secondary amine, which should be produced by hydrolysis of the immonium ion, could be observed. It is proposed that the amine cation radical produced by homolysis escapes the solvent cage and abstracts a hydrogen atom from solvent. Hydrogen abstraction from solvent by aminium ions is well documented (16). Further, support for the proposed fate of the aminium ion was provided by observing the NMR spectrum of the reaction mixture obtained by photolyzing [10] in d_4-methanol. A large singlet at 2.95 delta, the same as that observed for the hydrochloride salt of trimethylamine, was observed prior to workup of the reaction mixture. The lack of solvent cage disproportionation in this system, as opposed to that observed in photolyses of benzyl quaternary ammonium salts, may reflect a greater stability of 9-acridinylmethyl radical vs. benzyl radical, which enables escape of the radical from the solvent cage prior to reaction.

The deuterium isotope effects on the rate of production of 9-methylacridine [2] and 1,2-bis (9-acridinyl) ethane [6] in d_4-MeOH vs. MeOH have been examined. The reduced yield of [2] obtained during photolysis in d_4-MeOH relative to that obtained in MeOH (Table 1) is consistent both with the proposed mechanism (scheme X) and with an alternative mechansim for the production of 9-methylacridine via photoreduction (scheme XI). However, the latter mechanism

Table 1. The Effect of Deuterated Methanol on the Photolysis of [10][a]

Solvent	Percent Reactant Consumed	Percent Products Produced	
		2	6
Methanol	67.8	7.7	39.7
90% d_4-methanol	64.7	1.3	36.2

[a] [10] = 10^{-2}M in anhydrous deoxygenated solvent. 3 min photolysis using broad band irradiation at 350 nm.

Scheme XI

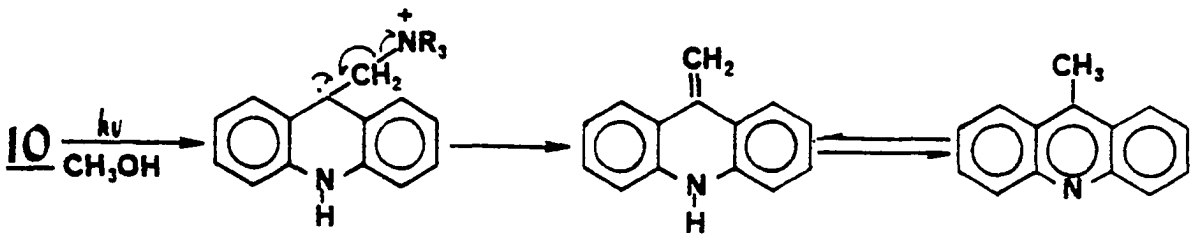

is unlikely based upon results obtained during photolysis of [10] in the presence of 10^{-2}M benzophenone. Previous results (10, 17) have established that a 5-6 fold increase in the rate of photoreduction of acridine occurs under these conditions, due to rapid hydrogen atom donation by the benzophenone ketyl radical. However, the yield of [2] produced from the photolysis of [10] is unchanged by the presence of 10^{-2}M benzophenone. Consequently, the photoreduction route to [2] is unlikely.

The proposed photolytic route in scheme X leaves unspecified the multiplicity and nature of the reactive excited state. In order to gain insight into the nature of the excited state involved, several experiments were devised. The effect of reaction medium on the rate

Table 3. The Effect of Reaction Medium on the Photolysis[a] and Fluorescence[b] of (9-acridinylmethyl) trimethylammonium bromide [X]

Reaction Medium	Photolysis P/P_o[c]	Fluorescence f/f_o[d]
Anhydrous methanol	1.0	0.1
Anhydrous methanol ($O_2 = 8.9 \times 10^{-3}$ M)	0.13[e]	0.1
33% aqueous methanol	0.49	0.2
66% aqueous methanol	0.33	0.5
90% aqueous methanol	----[f]	1.0
0.5 N aqueous H_2SO_4	ca. 0	---[g]

[a] X = 10^{-2} M in stated solvent. 3 min photolysis using broad band irradiation at 350 nm. Deoxygenated reaction medium unless otherwise stated.
[b] X = 2×10^{-6} M in stated solvent. Values obtained at peak height at excitation and emission maxima.
[c] P_o taken as the amount of X consumed in anhydrous deoxygenated methanol.
[d] f_o taken as the fluorescence intensity observed in 90% aqueous methanol.
[e] See [h] in Table II.
[f] The desired concentration of X could not be attained because of solubility problems.
[g] Under these conditions, the intense fluorescence of the dication is observed at a different emission maximum.

of photolysis and on the fluorescence of [10] (Table 3) makes the involvement of a $^1\pi,\pi^*$ state highly unlikely. Thus, as the hydrogen bonding ability of the solvent increases, fluorescence is enhanced, as expected (18) by anology in the acridine but the rate of photolysis decreases. The effect is especially pronounced in the case of strongly acidic medium, wherein the acridine nitrogen is protonated. Further, the quantum yield of fluorescence is unaffected when the methanol solution is saturated with O_2, although the rate of photolysis drops sharply under those conditions.

The effect of oxygen upon the rate of photolysis (Table 2) enables the calculation of an approximate lifetime of the photoreactive

Table 2. The Effect of Various Energy Transfer Agents on the Rate of Photolysis of (9-acridinylmethyl) trimethylammonium Bromide [x]

Agent	Concn, M	Energy levels of agents[a] E_T	E_S	Results[a] P^0/P
Sensitizers				
Benzophenone[b]	10^{-2}	69		1.0
Michler's ketone[c,d]	10^{-2}	61		0.11
Quenchers[e]				
Oxygen	1.8×10^{-3}[f]		22.5, 36.6[g]	2.9
	8.9×10^{-3}[f]			≥7.5[h]
NaI	10^{-3}–10^{-1}			~1[i]
Benzophenone	10^{-3}–10^{-2}	69[j]	76[j]	1.0
Biphenyl	10^{-3}–10^{-2}	65[j]	116[j]	0.875–1.05
Naphthalene	10^{-3}	61[j]	90[j]	0.91
Biacetyl	10^{-2}	55[k]	68	0.89
Benzil	10^{-3}–10^{-2}	53[j]	73[l]	0.875–1.0
Benzoquinone	10^{-3}	50[j]	60[m]	1.02
Azobenzene	10^{-3}[n]	~40[j]	64[o]	1.03

[a] Ratios of X consumed under control conditions (P_0) to the amount consumed in the presence of the energy transfer agent (P). [b] X (5×10^{-4} M) in anhydrous methanol, 10 min photolysis at 280 ± 5 nm. [c] 4,4'-Bis(dimethylamino)benzophenone. [d] X (1×10^{-3} M) in anhydrous methanol, 3 min photolysis using broad irradiation at 350 nm; >95% of light absorbed by sensitizer. [e] X (5×10^{-3} M) in anhydrous methanol, 3 min photolysis time using broad irradiation with a maximum of 350 nm. [f] Gmelins "Handbuch der Anorganischen Chemie", 8th ed, Verlag Chemie, Weinheim/Bergstr., Germany, 1958. [g] O. J. Guzeman, F. Kaufman, and G. Porter, *J. Chem. Soc., Faraday Trans. 2*, **69**, 708 (1973). [h] Higher ratios were also observed but the values obtained are subject to wide variations because of the small value of the denominator. [i] High concentrations of NaI interfere somewhat with the analytical chromatography and UV analysis and the results at high concentration are approximate. [j] O. L. Chapman, "Organic Photochemistry", Vol. 2, Marcel Dekker, New York, N.Y., 1969, pp. 10–13. [k] N. J. Turro, "Molecular Photochemistry", W. A. Benjamin, New York, N.Y., 1967, p 132. [l] B. S. Ault and B. S. Pimentel, *J. Phys. Chem.*, **79**, 626 (1975). [m] P. E. Stevenson, *J. Mol. Spectrosc.*, **17**, 58 (1965). [n] Higher concentrations absorbed significant amounts of the incident light and were not investigated. [o] E. D. Bergman and B. Pullman, Ed., "The Jerusalem Symposia on Quantum Chemistry and Biochemistry", Vol. 2, "Quantum Aspects of Heterocyclic Compounds in Chemistry and Biochemistry", The Israel Academy of Science and Humanities, 1970, p 204.

state (19). Assuming a Stern-Volmer relationship for the quenching,

$$P^o/P = 1 + k_q \tau [Q]$$

P^o/P = the ratio of reactant consumed under control conditions (P^o) to the amount consumed in the presence of the quencher (P)
k_q = quenching constant
τ = lifetime of the reactive state
[Q] = concentration of quencher

and quenching constants of $3.1 \times 10^{10}\ M^{-1}\ sec^{-1}$ and $3.4 \times 10^{9}\ M^{-1}\ sec^{-1}$ for singlets (20) and triplets (21) respectively, lifetimes of $\geq$215 nsec are calculated for a triplet and $\geq$25 nsec for a singlet. The effects of energy transfer agents on the photolysis reaction have been investigated, (Table 2), using concentrations dictated by the approximate lifetimes calculated. The lack of triplet sensitization requires that a triplet state, if involved, have E_T: ca. 60 kcal/mole. Since acridine is reported (17) to have energy levels at ca. 45 kcal/mole for the $^3\pi,\pi^*$ state and in the range of 61-67 kcal/mole for the $^3 n,\pi^*$ state, the involvement of the $^3\pi,\pi^*$ state is unlikely because of the large energy difference between it and the sensitizer. The involvement of the $^3 n,\pi^*$ state is also unlikely, based upon the quenching data cited in Table 2, since the lower energy quenchers do not retard the photolysis rate. Thus, triplet states do not make a major contribution to the reaction.

The involvement of a $^1 n,\pi^*$ excited state is a strong possibility. The lifetime calculated for the excited state in this reaction

($\geq$25 nsec), is somewhat longer than expected based upon the value (1-5 nsec) reported by Whitten and Lee (12) for the proposed $^1 n, \pi^*$ state involved in the photoreduction of acridine, but is not unreasonable for a typical $^1 n, \pi^*$ state which may have lifetimes from 10^{-6}-10^{-9} sec (22). The energy of the $^1 n, \pi^*$ state of [10] is difficult to estimate. The difficulties of estimating the energy of this state have been discussed in detail (10, 23) in the case of acridine and in that case is estimated to be 75 ± 5 kcal/mole. The concentrations of the lower energy singlet quenchers were limited because of their absorptivity to levels that are calculated to produce small effects on reaction rate. Therefore, the data in Table 2 are equivocal with respect to the involvement of the $^1 n, \pi^*$ state. Another possible excited state, involving charge transfer between the counterion (Br^-) and the acridine nucleus is unlikely, since replacement of Br^- with BF_4^- (24) had no effect on the reaction rate. The $^1 n, \pi^*$ state thus appears to be the most likely candidate for the photoreactive state.

Photolysis of Chlorpromazine Quaternary [15]

The information obtained about the photolysis of acridine quaternary salts using the model compounds [10] and [11] was then applied to the investigation of the photolysis of the quaternary salt of chlorpromazine [15]. The rate of photolysis of [15] was compared to that of the trimethylamine quaternary [10] in oxygenated and deoxygenated

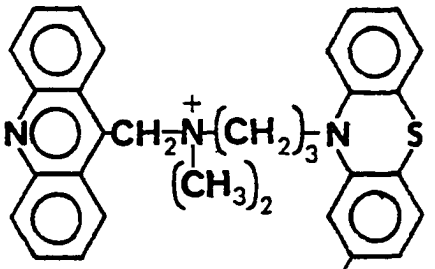

15

Table 4. Comparison of the Photolysis of Acridine Quaternary Salts Derived from Trimethylamine [10] and Chlorpromazine [15]

Reactant, Conditions	Reactant Consumed (%)	Yield (%)	
		[2]	[6]
[15], deoxygenated	17.4	5.9	2.7
[10], deoxygenated	54.6	7.0	22.6
[15], 100% O_2 atm	14.6	5.9	ca.0
[10], 100% O_2 atm	7.2	2.9	5.3

methanol (Table 4). The product distribution was also determined. The rate of photolysis of [15] is only ca. one third of that of [10]. This may well explain the differences in the product ratios observed since a lower steady-state concentration of the acridinylmethyl radical would be expected to result in the formation of a higher percentage of 9-methylacridine (see figure 4 for effect of concentration on product ratios).

The two most important differences observed in the photolysis of [15] compared to [10] are the apparent insensitivity of the rate of reaction of [15] to oxygen concentration and the constant yield of [2]. First, the unchanged yield of 9-methylacridine under oxygenated and deoxygenated conditions could have been indicative of a solvent cage

reaction which is immune to exogenous radical scavengers. A solvent cage reaction would produce desmethylchlorpromazine [17] as the amine product after acidic hydrolysis rather than chlorpromazine [16] (scheme XII). A TLC investigation of the amines produced in the

Scheme XII

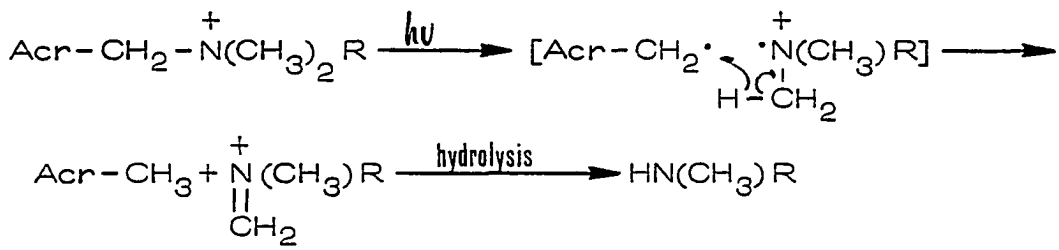

R = 3-[10-(2-chlorophenothiazinyl] propyl-

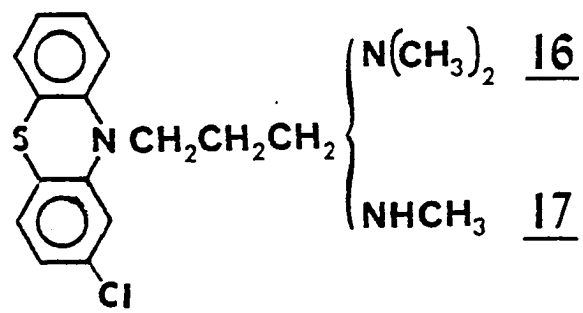

reaction showed that chlorpromazine [16] was the only amine produced, in analogy with the results obtained from photolysis of the model compounds [10] and [11]. It must therefore be concluded that the lack of effect of oxygen concentration on the rate of production of [2] is not a result of a change to a solvent cage mechanism.

The failure of a 100% oxygen atmosphere to significantly reduce the reaction rate implies a reduced lifetime of the reactive

photoexcited state of [15] relative to [10] and thus would rule out significant triplet involvement. A variety of possible explanations such as the formation of a charge transfer excited state, energy transfer from the acridine to the phenothiazine nucleus or the involvement of the shorter lived $^1\pi,\pi^*$ state were considered. Photoreactivity from the $^1\pi,\pi^*$ state cannot be unequivocally ruled out by presently available information. The fact that the photolysis of [15] proceeds, although slowly, in aqueous acid and is not quenched by oxygen tends to support involvement of a $^1\pi,\pi^*$ state. However, it is difficult to reconcile a $^1\pi,\pi^*$ photoreactive state in this reaction with the properties normally attributed to that state. It usually fluoresces; the chlorpromazine quaternary does so only weakly. The fluorescence does not increase in going to 12 N H^+ and the extremely low quantum yield of fluorescence observed for [15] relative to [10] and [11] would indicate that the phenothiazine nucleus functions to facilitate deactivation of the acridine singlet excited state. Since the fluorescent state of [10], which is not quenched by oxygen, does not appear to significantly participate in the photolysis of [10] reaction under oxygenated conditions, it seems unlikely that the $^1\pi,\pi^*$ of [15] could be involved in the photoreaction. Therefore, it is likely that the ^{1} n ,π^* state, whose properties have been modified by the presence of the phenothiazine nucleus, or a new charge transfer excited state is the photoreactive state.

The lifetime of the excited state, τ_o, (19) can be described

by the following equation where k_i represents the rates of the various pathways by which the excited state can be deactivated. The natural

$$\tau_o = \sum_{i=1}^{n} \frac{1}{k_i}$$

lifetime which is an intrinsic property of excited states can be calculated for the case where radiative emission is the only pathway: the average measured lifetime is usually shorter due to other competing intramolecular and intermolecular processes, such as internal conversion and intersystem crossing. The most reasonable process which could effectively contribute to a shortened photoreactive lifetime would involve energy transfer from the acridine excited state to the phenothiazine nucleus, a process that is likely to lead to deactivation of the photoreactive state. Alternatively, an exciplex excited state with different properties from that of the uncomplexed excited acridine molecule could account for the experimentally observed results.

Attempts were made to investigate the possibility of energy transfer to the phenothiazine nucleus by looking for luminescence from that nucleus. Previous reports indicate that the optimum fluorescence from chlorpromazine occurs in aqueous base (25). However, the fluorescence at 455 nm in 0.1 N NaOH is extremely weak. Although the observed fluorescence characteristics of acridines from [15] is ca. 30 times less than that observed for the trimethylamine quaternary [10] under these conditions, it is still sufficient to obscure the fluorescence

produced by an equimolar amount of chlorpromazine. Thus it does not appear possible at this time to account for the apparent reduced lifetime of photoreactive excited state by an energy transfer mechanism.

The possible role of a charge transfer ground state or an exciplex excited state was also investigated. Generally, a C-T ground state interaction should be detected as a new UV absorption band (26) or as a shift in the proton NMR spectrum (27), however, neither was observed. Similarly, exciplex emission which would be observed as a new longer wavelength emission band in the fluorescence spectrum (28) was not observed using the experimental techniques and equipment available for this study. The details of the spectroscopic study are presented in Part II. The fluorescence quenching observed for [15] relative to [10] could be attributed to an excited state charge transfer complex but also is consistent with other mechanisms such as enhanced radiationless decay rates or energy transfer. None of the proposed mechanisms could be confirmed under conditions similar to those used for the photolysis reaction. The apparent properties of the chlorpromazine quaternary salt [15] can be summarized as follows. The lifetime of the photoreactive excited state is much shorter than that observed for the trimethylamine quaternary salt [10] and the rate of photolysis is relatively independent of changing environmental conditions. The lack of appreciable fluorescence under all conditions tends to rule out the involvement of the $^1\pi,\pi^*$ state and the insensitivity of the rate of

photolysis to oxygen would rule out any triplet state involvement. An energy transfer mechanism would account for most of the observed properties as would exciplex formation.

As a final stage of our investigation of the photolysis of acridine quaternary ammonium salts, the solid state reaction under conditions similar to those used in the analytical procedure (1) was studied. The comparison of the solid state photolysis of [10] and [15] was made by adsorbing the quaternary salts on silica gel plates and the results are given in figure 5.

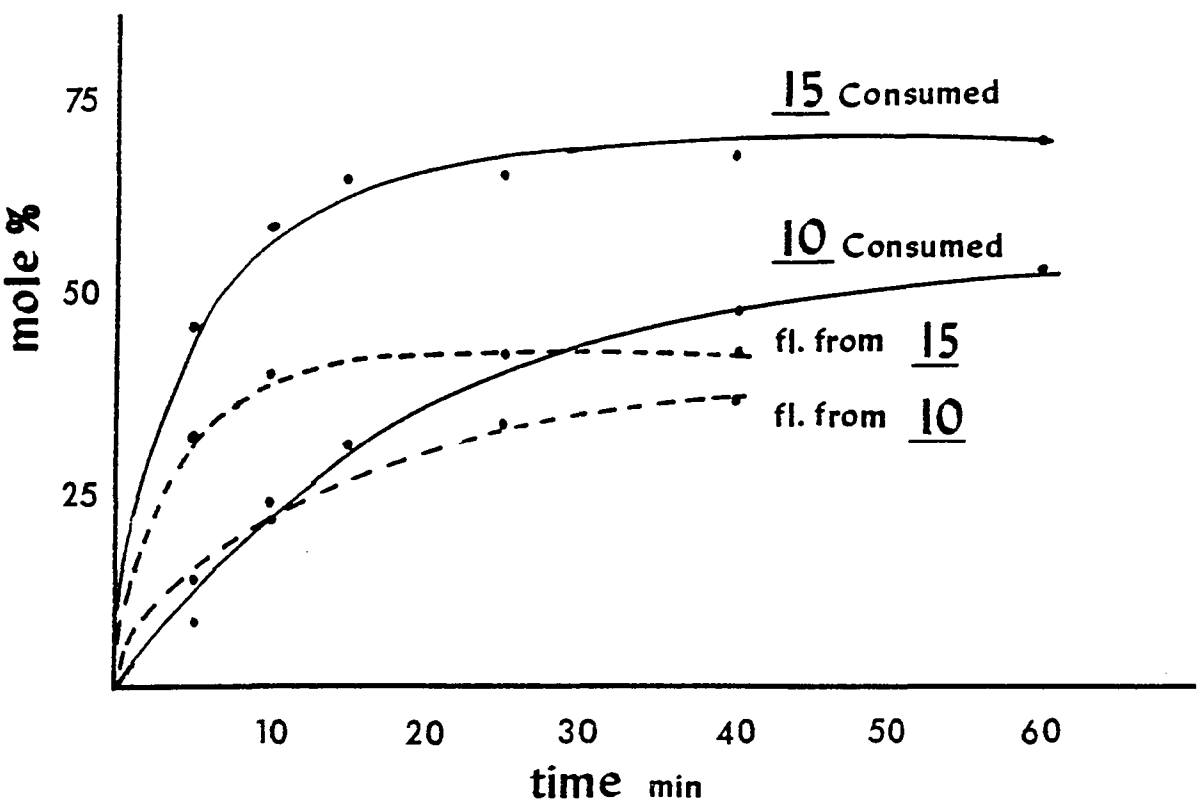

Figure 5. Time profile for the photolysis of [10] and [15] on a silica gel TLC plate using broad band irradiation at 350 nm. ·—— · represents amount of quaternary consumed during the reaction; ·------· represents the appearance of fluorescent products.

The percentage yield of fluorescent products based on the amount of quaternary consumed is apparently lower for [15]. The yield of "fluorescence" at 40 min was approximately the same, however, ca. 70% of [15] was consumed compared to ca. 50% of [10]. The amount of quaternary consumed was determined by the UV method described previously. The major products of the photolysis of [15] which include 9-methylacridine [2], 9-acridinylcarboxaldehyde [3] and 9-acridinylmethanol [4] have previously been reported (3). These products have similar quantum yields and hence the fluorescence data adequately reflects the yield of these identified products. The fluorescence values were converted to a molar basis by comparing the observed intensity to that obtained from a known amount of 9-methylacridine processed by the same procedure.

Figure 5 shows that the differences in photolysis rate observed for [10] and [15] are further exemplified in the solid state. The chlorpromazine quaternary, whose photolysis is not quenched in solution by acid or by oxygen, is photolyzed much faster than [10] on the TLC plate. The presence of acid on the silica gel plates is indicated by the fact that the visual fluorescence observed is that of the cation and hence the differing results on the TLC plate are consistent with the previous results where the photolysis of [10] in solution is quenched completely by 0.5 N H^+ and the photolysis of [15] still proceeds slowly in 12 N H^+.

Chromatographic examination of the quaternary spot after

photolysis revealed a number of additional minor products such as acridone [8] and 9-acridinecarboxylic acid [9] which were identified by their R_f values whereas others could not be identified by R_f values and were not investigated further. No major non-fluorescent product(s) and no dimer [6] could be found to account for the remaining ca. 30% of unaccounted for products. The photolysis of quaternary salts on silica gel plates always results in the deposition of non-elutable acridine-containing fluorescent materials on the silica. This observation was further confirmed by depositing the quaternary on silicic acid and performing the photolysis in a transparent cyclohexane slurry. The major amount of visible fluorescence remained on the silicic acid after exhaustive elution with acidic alcohol and therefore, it must be concluded that these products are covalently bound to the silica, probably through silyl ether linkages.

Qualitative TLC analysis of the amine products produced by co-chromatography with authentic samples indicated that chlorpromazine was the major amine produced. Visual examination of the TLC plate indicated that only a small percentage of desmethylchlorpromazine [16] was produced. Other minor phenothiazine containing products were also present but since they also appeared in the control photolysis of chlor-promazine, they were not investigated in detail. The very small yield of secondary amine product indicates that geminate pair disproportion-ation is still a minor pathway even under conditions that should favor that pathway.

A question still remained regarding the mechanistic pathway(s) responsible for the solid state photolysis reaction. The results in solution had indicated that the photolysis proceeds almost exclusively by a homolytic route with only radical derived products being observed under deoxygenated conditions. As the percent water in the reaction mixture was increased, 9-acridinylmethanol [4], an expected heterolytic cleavage product, was not observed. It was, however, observed under oxygenated reaction conditions. Since the solution photolysis of 9-bromomethylacridine [1] had indicated that it proceeded by a heterolytic mechanism, the solid state photolysis of (9-acridinylmethyl) trimethylammonium bromide [10], 9-bromomethylacridine [1] and 9-methylacridine [2] was compared for possible mechanistic information. A qualitative examination of products produced during photolysis on silica gel plates indicated that all the observed products could arise from each of the compounds. This observation yielded no conclusive mechanistic information about the involvement of a heterolytic pathway since heterolytic cleavage of [2] is highly unlikely. However, all the observed products could arise from an initial homolytic cleavage by analogy to the results gained from previous investigations of reactions of organic radicals (29). The major product of the solid state photolysis is 9-methylacridine [2] which arises from a straight forward hydrogen abstraction reaction from silica gel or the organic binders present on the plate. All the other products are produced in very low yields and can come

from secondary reactions of the 9-acridinylmethyl radical with the oxygen, water and acid present on the plate (Figure 6).

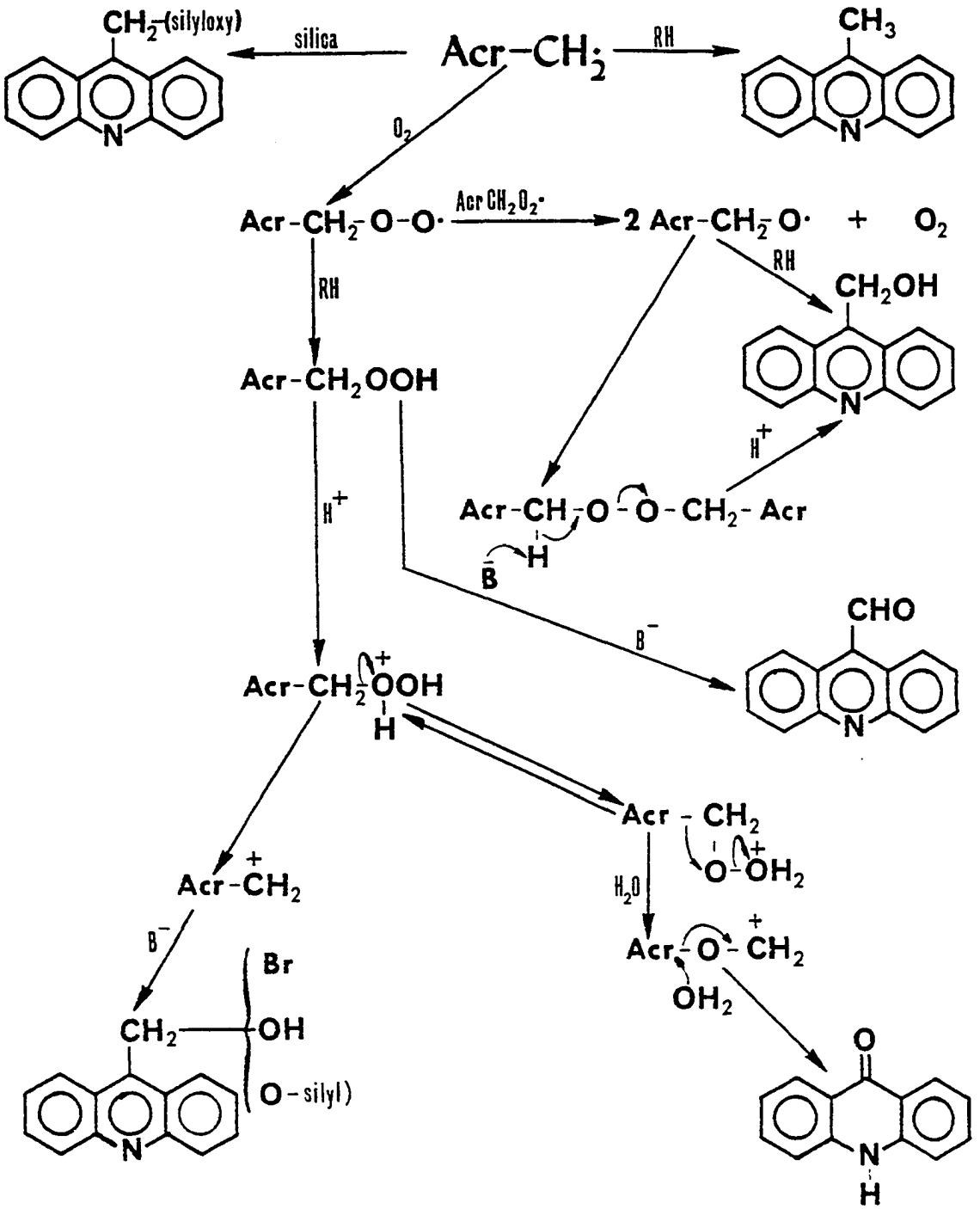

Figure 6. Potential reaction pathways for 9-acridinylmethyl radical on silica gel TLC plates.

Although the intermediate 9-acridinylmethyl carbonium ion could be produced by heterolytic cleavage of the quaternary, its generation from a protonated hydroperoxide intermediate is more consistent with the results observed. The significant yield of acridone under oxygenated conditions further supports the presence of the hydroperoxide intermediate. Thus, it is concluded that the mechanistic description of the photolysis reaction gained from the solution studies where the parameters can be better controlled, is also applicable to the solid state reaction.

CHAPTER 3

EXPERIMENTAL

Ultraviolet spectra were obtained on a Cary 14 spectrophotometer. NMR spectra were obtained on a Varian Associates T-60 or XL-100 spectrometer. Mass spectra were obtained on a Hitachi-Perkin Elmer RMU-7 spectrometer. Fluorescence spectra were obtained on either an Aminco Bowman or a Perkin Elmer MPF-3L spectrofluorometer. IR spectra were recorded on a Beckmann IR-8. Intensities of absorptions are referred to as strong (s), moderate (m) and weak (w). Melting points were determined on a Gallenkampf MF370 capillary melting point apparatus and are uncorrected. Merck $PF_{254+366}$ silica gel was used for column and general thin layer chromatography (TLC) while 100 μ terephthalate backed silica gel plates without indicator, Eastman Kodak, were used for the quantitative analyses. Microanalyses were performed by Galbraith Laboratories, Inc., Knoxville, Tenn. Anhydrous methanol refers to Nanograde methanol which is dried by distillation over $Mg(OMe)_2$(30). Degassed methanol refers to methanol that was degassed by at least four freeze-thaw cycles under a vacuum of 0.05-0.01 Torr by alternating between liquid N_2

and dry ice-acetone baths or by pumping on the sample for 12 hrs in a dry ice-acetone bath.

Photolyses were effected with a Rayonet RPR-100 Photochemical Reactor. The photolysis results cited in Figure 4 and Tables 1-4 were obtained by the following procedure. To a 8 mm x 10 cm Pyrex tube sealed at one end was placed 0.5 mL of a 10^{-2} or 10^{-3} M solution of [10], [11] or [15] in anhydrous methanol. The samples were degassed by the procedure cited above, were flame sealed under vacuum and were photolyzed for periods of time from 10 sec to 10 min in a Rayonet reactor equipped with eight 3500 Å lamps. Following photolysis, the tubes were opened and 10 μL aliquots were spotted on two silica gel TLC plates. One was developed with benzene:acetone (95:5) to isolate the dimer [6], and methylacridine [2] and the other was developed in acetonitrile:water (9:1) to isolate the quaternary salts [10], [11] or [15]. The products were visualized under UV light, and the spots were cut out with scissors and added to 50 mL centrifuge tubes. Products [2] and [6] were eluted with 5 mL of ethanol and the quaternaries with 2 N ethanolic H_2SO_4. The tubes were shaken for 15 min, the solvent decanted and analyzed spectrophotometrically at 252 nm for [2] and [6] and 262 nm for [10], [11] and [15]. Yields were determined by comparing the extinction coefficients of the products at the cited wavelengths with those of known quantities of authentic compounds processed in the same manner. For benzophenone, a 5 x 10^{-3} M solution of [10] containing 10^{-2} M

benzophenone was irradiated at 280 ± 10 nm for 10 min. Quenching experiments were performed by dissolving the indicated concentration of quencher in a 5×10^{-3} M solution of [10] and exposing the deoxygenated solution to UV light (350 nm) for 3 min.

Oxygenation experiments were performed as above except that a stopcock was sealed to the photolysis tube to permit introduction of the desired quantity of oxygen. Air or 100% oxygen was bubbled through the sample for 10 min, the stopcock closed and the rate of photolysis determined by the above procedure.

Control photolyses of the "dimer" [6], 9-methylacridine [2], 9-bromomethylacridine [1] and the ether [5] were also performed under the above conditions.

Preparation of (9-acridinylmethyl) trimethylammonium bromide [10]

Into a saturated solution of 9-bromomethylacridine [1] 200 mg, 0.735 mmoles) in acetonitrile (ca. 20 mL) was bubbled approximately a five-fold molar excess of trimethylamine (generated from the hydrochloride salt by addition of 40% KOH). The reaction mixture was allowed to stand at room temperature for 24 hr and deposited crystals of [10] (208 mg, 85% yield), which were recrystallized from a 9:1 mixture of acetonitrile:methanol as light yellow plates that decomposed upon heating above 175° without melting. The spectral data for [10] are: 60 MHz NMR (CD_3OD, TMS, delta)(Figure 7): 3.23 (9H,s), 5.76 (2H,s),

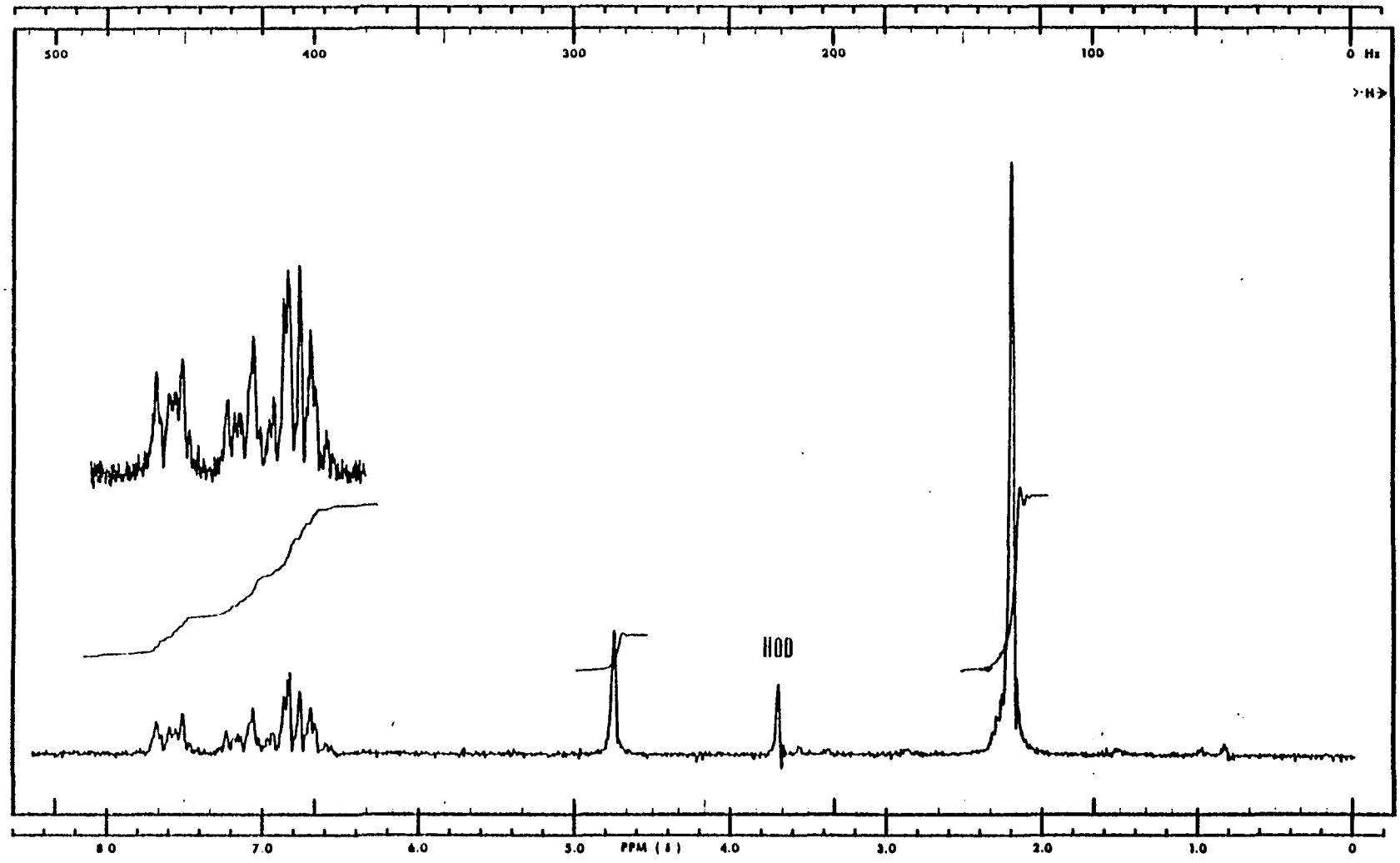

Figure 7. 60 MHz PMR spectrum (CD_3OD) of (9-acridinylmethyl) trimethylammonium bromide [10].

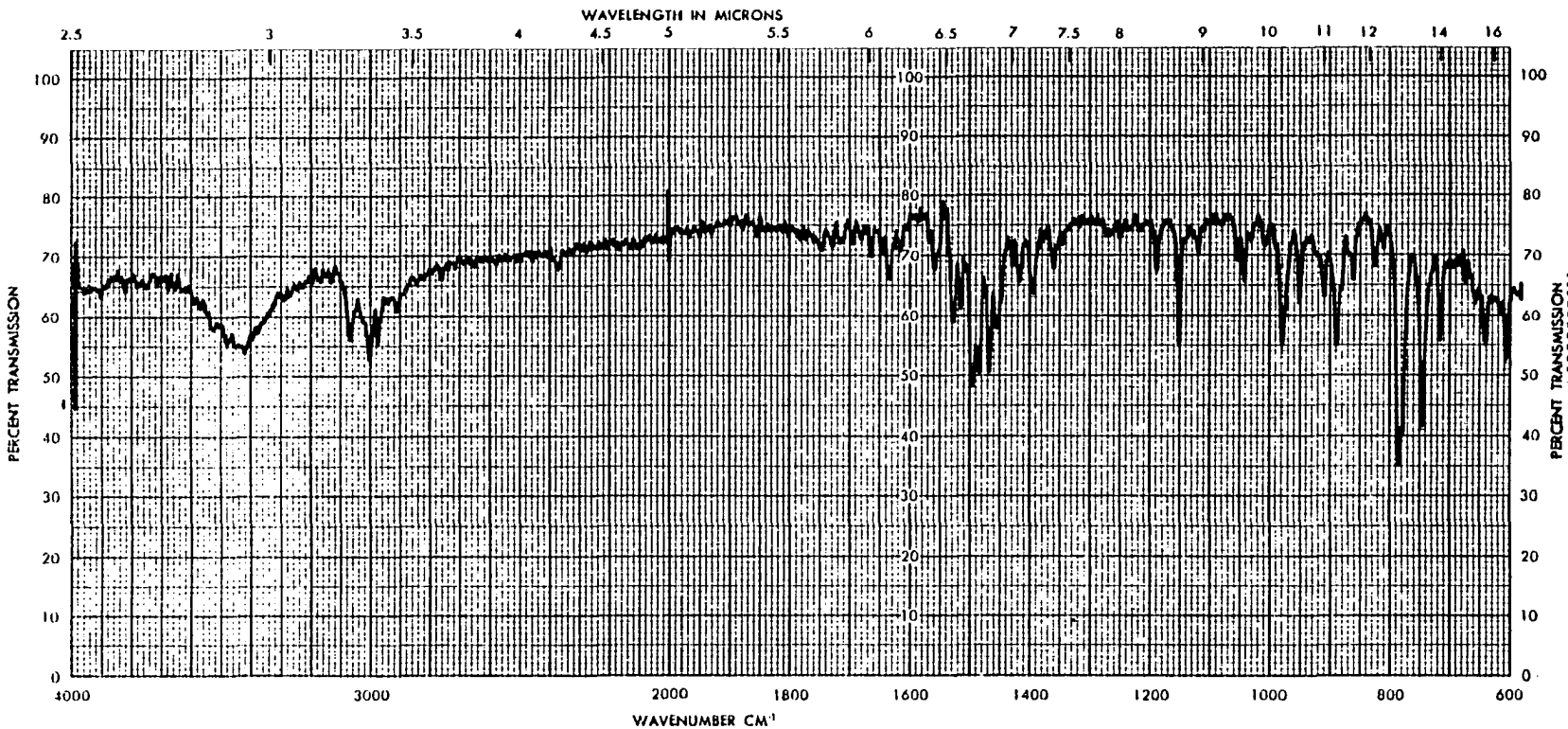

Figure 8. IR spectrum (KBr) of (9-acridinylmethyl) trimethylammonium bromide [10].

8.74-7.66 (8H,m); UV: 95% EtOH; λ_{max}nm, (ϵ_{max}): 252 (1.25×10^5), 366 (7.2×10^3), 390 (3.1×10^3); IR: (cm^{-1}, KBr)(Figure 8): 3405 (m), 3340 (w), 3050 (w), 2995 (m), 2985 (m), 1660 (w), 1620 (m), 1540 (w), 1480 (s), 1470 (s), 1450 (s), 1440 (s), 1130 (m), 1025 (w), 960 (m), 930 (w), 865 (m), 840 (w), 760 (s), 725 (s). Analysis for $C_{17}H_{19}N_2Br$: calculated, C 61.64, H 5.78, N 8.45; found, C 61.50, H 5.71, N 8.47.

Preparation of (9-acridinylmethyl) (3-phenylpropyl) dimethylammonium bromide [11]

N,N-dimethyl-3-phenyl-propylamine (31) (0.3 g, 1.83 mmole) was added to a solution of [1] (0.5 g, 1.8 mmole) in ca. 50 mL CH_3CN. The reaction mixture was allowed to stand at room temperature for 72 hr, the CH_3CN was removed under reduced pressure, and the solid residue was titurated with three 5 mL portions of acetone, which gave [11] (417 mg, 87% yield) which was then recrystallized twice from CH_3CN at -20°. The pale orangish yellow plates of [11] melted with decomposition at 160-164°. Spectral data for [11] are: 60 MHz NMR ($CDCl_3$, TMS, delta)(Figure 9): 2.06 (2H,m), 2.58 (2H,t), 3.33 (6H,s), 3.98 (2H,m), 6.68 (2H,s), 6.86-7.26 (5H,m), 7.58-8.16 (8H,m); UV: 95% EtOH; λ_{max}nm, (ϵ_{max}): 252 (1.14×10^5), 365 (9.4×10^3), 390 (3.4×10^3); IR: (cm^{-1},KBr)(Figure 10): 3450 (s), 3410 (s), 3050 (m), 2980 (w), 1625 (w), 1600 (w), 1550 (w), 1515 (m), 1495 (m), 1450 (s), 1135 (w), 1120 (w), 1020 (w), 975 (w), 940 (w), 835 (m), 760 (s).

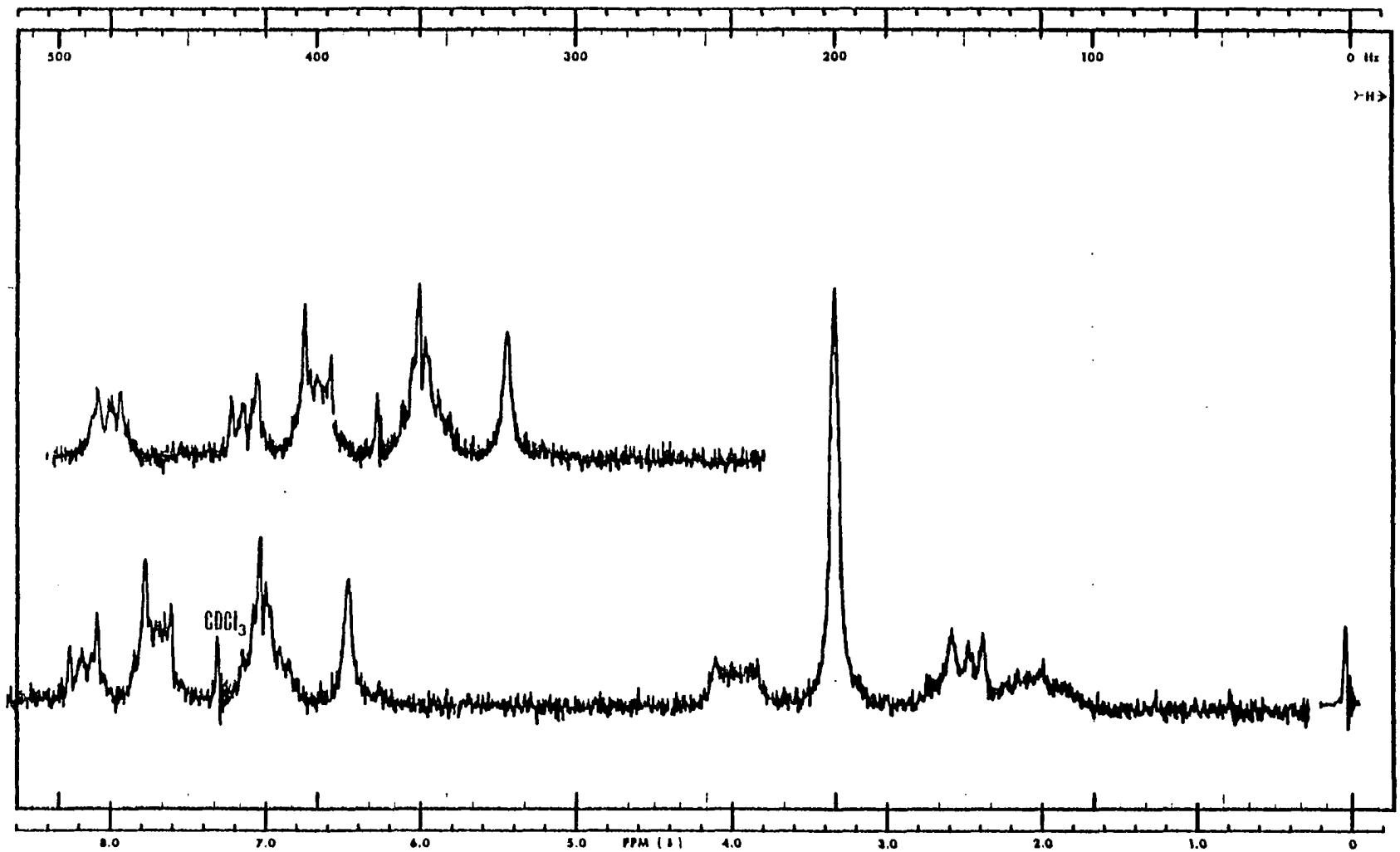

Figure 9. 60 MHz PMR spectrum ($CDCl_3$) of (9-acridinylmethyl)(3-phenylpropyl) dimethylammonium bromide [11].

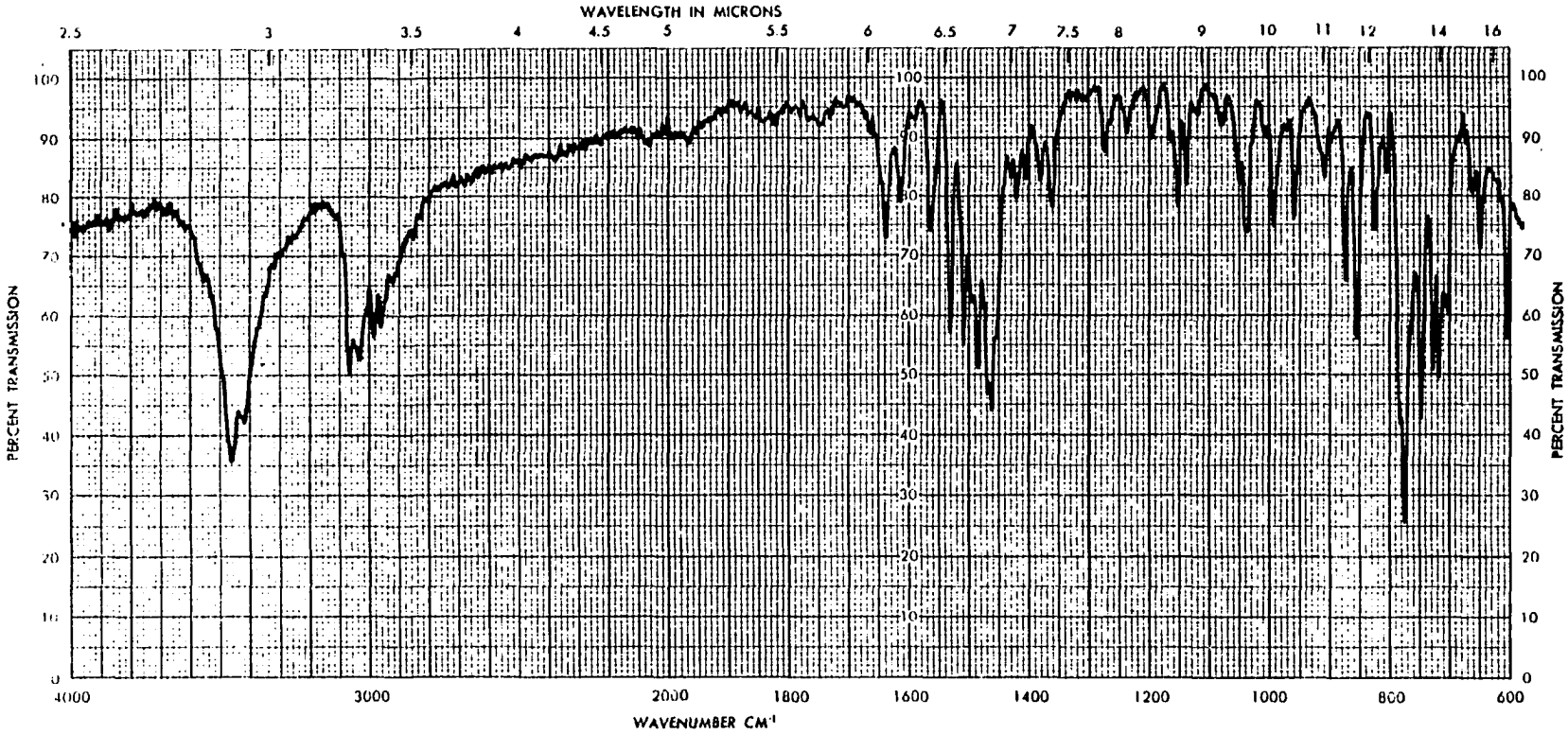

Figure 10. IR spectrum (KBr) of (9-acridinylmethyl)(3-phenylpropyl) dimethylammonium bromide [11].

Analysis for $C_{25}H_{27}N_2Br$: calculated, C 68.96, H 6.25, N 6.43; found, C 68.85, H 6.28, N 6.28.

Preparation of (9-acridinylmethyl)[3-(2-chlorophenothiazin-10-yl) propyl] dimethylammonium bromide [15]

The preparation and properties of [15] have previously been reported by Lehr and Kaul (3). Samples of [15] used in this study were prepared by that method.

Preparation of 9-(methoxymethyl)-acridine [5]

Sodium methoxide (6 mL, 0.4 M) in methanol was added dropwise over a two hr period to a solution of 9-bromomethylacridine [1] (273 mg, 1.0 mmole) in anhydrous methanol (5 mL). The reaction mixture was allowed to stand at -20° for twelve hrs, then it was added to ether (ca. 100 mL) and the solution was washed with saturated aqueous $NaHCO_3$ (20 mL) once and with water (20 mL) three times. Removal of the ether layer and evaporation afforded the crude product (210 mg, 94%) as a straw colored powder. It was recrystallized twice from ether at -20° and was further purified by column chromatography using TLC grade silica gel (10 gm) and using CH_2Cl_2 to first flush the more non-polar components and CH_2Cl_2 plus 5% acetone to elute the desired product. In retrospect, a more gradual polarity gradient would have been desirable. The [5] isolated in this manner was recrystallized twice from Et_2O to afford light straw-colored needles of

mp 113.5-114°. Spectral data for [5] are: 60 MHz NMR ($CDCl_3$, TMS, delta)(Figure 11): 3.4 (3H,s), 5.36 (2H,s), 7.3-8.4 (8H,m); UV: 95% EtOH; λ_{max}nm, (ϵ_{max}): 252 (1.47×10^5), 343 (6.8×10^3), 359 (1.0×10^4), 384 (3.9×10^3); IR: (cm^{-1}, KBr)(Figure 12): 3060 (w), 2990 (w), 2880 (w), 1620 (w), 1605 (w), 1550 (w), 1450 (w), 1090 (s). Mass spectrum (70 ev, relative abundance) (Figure 13): 223 (M^+, base peak), 208 (18), 192 (86), 180 (47), 178 (10). Analysis for $C_{15}H_{13}NO$: Calculated, C 80.69, H 5.87; found, C 80.49, H 5.90.

Preparation of d_3-9-methylacridine

A solution containing equimolar amounts of [2] and triethylamine in 0.5 mL d_4-methanol was prepared. The reaction mixture was allowed to stand at room temperature for two weeks. Direct mass spectral analysis of the solid obtained by evaporating the sample to dryness indicated that the mixture contained the following distribution of label: d_0 = 5.4%; d_1 = 19.3%; d_2 = 41.0%; d_3 = 34.3%, for a total of 68.0% (d ave = 2.04) deuteriation. When the compounds were isolated by TLC, developed in benzene:acetone (95:5) and were eluted from the plate with methanol, the mass spectral results indicated: d_0 = 47.5%, d_1 = 33.2%; d_2 = 15.5%; d_3 = 3.8%, for a total of 21.5% (d ave = 0.65) deuterium content. Thus, the high degree of isotope exchange observed under TLC conditions precludes any meaningful mechanistic studies using isotopic labeling.

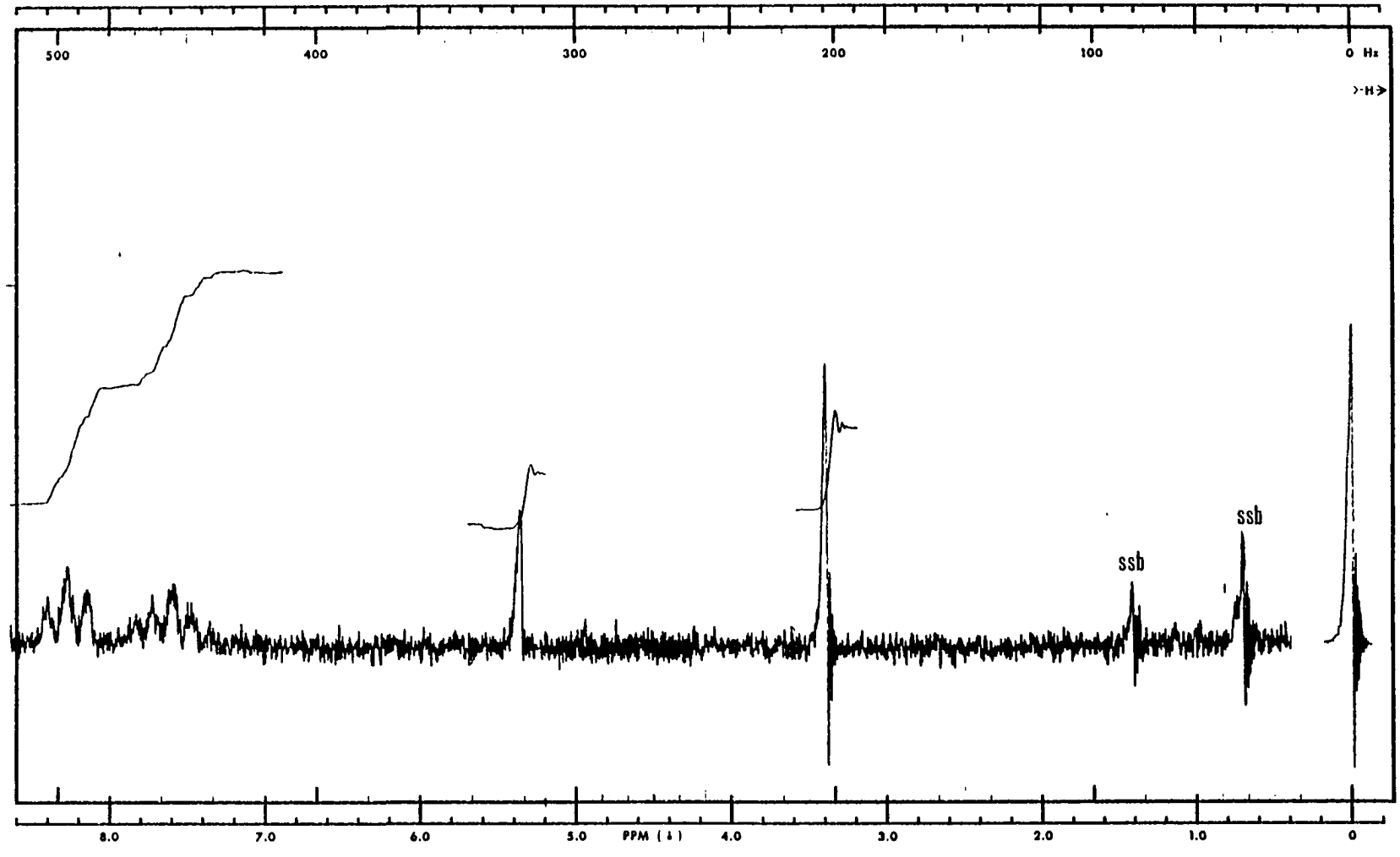

Figure 11. 60 MHz spectrum ($CDCl_3$) of 9-(methoxymethyl)-acridine [5].

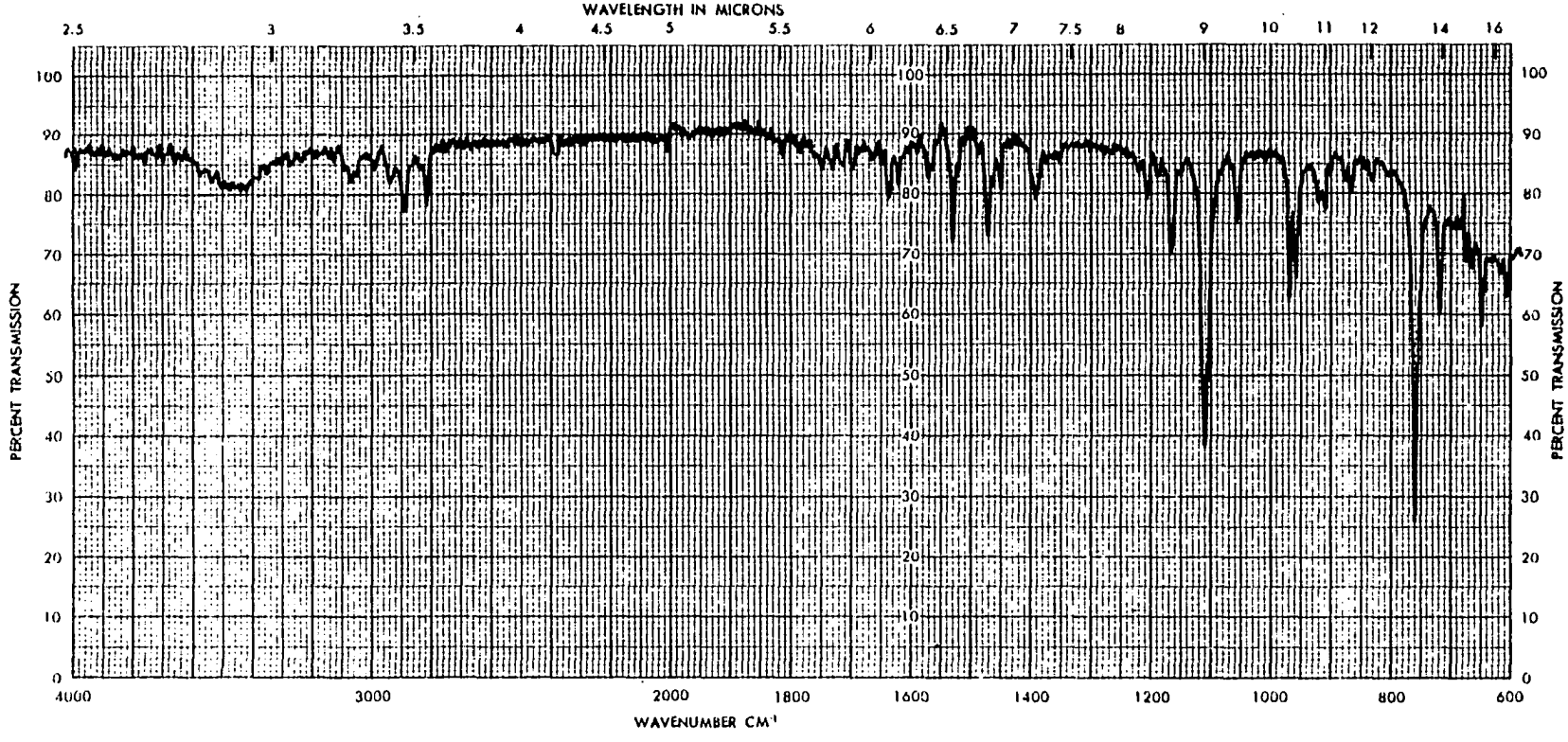

Figure 12. IR spectrum (KBr) of 9-(methoxymethyl)-acridine [5].

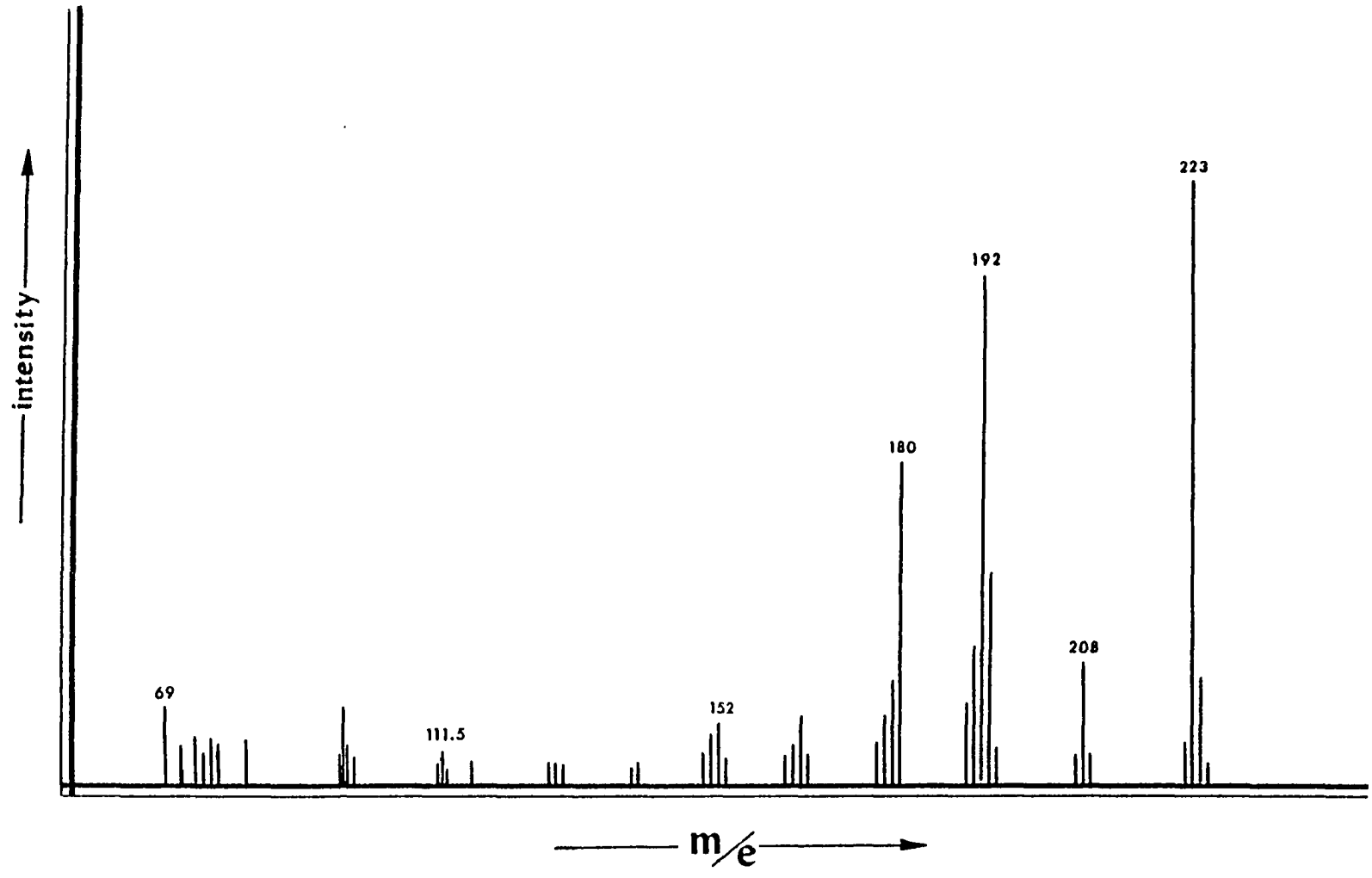

Figure 13. Mass spectrum (70 ev) of 9-(methoxymethyl) acridine [5].

Preparative scale photolysis of [10]

A 50 mL pear-shaped pyrex flask containing [10](100 mg, 0.3 mmoles) in a 30 mL anhydrous methanol was fitted with a vacuum stopcock and deoxygenated by freeze-thawing under a vacuum of 0.01 Torr. The mixture was photolyzed one hr in a Rayonet reactor using eight 3500 Å lamps. A straw-colored product [6] (26 mg, 45%) crystallized out of the reaction mixture. It was collected and recrystallized from $CHCl_3$ at -20° as clear straw-colored needles that melted at 257-259° with decomposition when the melting point chamber was preheated to that temperature. Attempts to obtain a melting point by the normal procedure of slowly raising the temperature results in a slow time-dependent decomposition from 240-255° resulting in a brown amorphous mass which will not melt ($< 300°$). However, if the sample is put in the preheated melting point apparatus at any temperature at or above 257-259°, melting occurs while temperatures of 255° and less result in decomposition with no melting. Spectral data for [6] are: 60MHz NMR ($CDCl_3$ TMS, delta)(Figure 1): 4.15 (4H,s), 7.35-8.35 (16H,m); UV: 95% EtOH; λ_{max}nm, (ϵ_{max}): 342 (1.26×10^4), 359 (1.94×10^4) and 393 (9.41×10^3); IR: (cm^{-1}), KBr)(Figure 2): 3480 (w-br), 3050 (m), 1620 (w), 1605 (w), 1548 (m), 1510 (w), 1485 (w), 1435 (w), 1405 (m), 732 (s); Mass spectrum (70 ev, relative abundance)(Figure 3): 384 (M^+,4), 192 (base peak). Analysis for $C_{28}H_{20}N_2 \cdot 2H_2O$: Calculated, C 79.98, H 5.75, N 6.66; found C 80.23, H 5.67, N 6.69.

The filtrate was concentrated and analyzed by NMR, which indicated the presence of unreacted starting material, [2] (ca. 8%) and [6] (ca. 4%). The presence of [2] in the mixture was suggested by the presence of its characteristic methyl absorption (ca. 3.0 delta) and further confirmation was obtained by TLC comparison of the reaction mixture with authentic [2], using benzene:acetone (95:5) as the eluting solvent. An additional NMR absorption (2.95 delta) was ascribed to trimethylammonium bromide. The assignment was confirmed in a subsequent experiment in which a deoxygenated 1.9×10^{-1} M d_4-methanol solution of [10] was photolyzed for 90 min. The photolysis tube was opened while frozen in liquid N_2, solid K_2CO_3 was added and the tube was resealed under vacuum with a NMR tube attached as a side arm. The mixture was allowed to warm to room temperature and the volatile components were transferred to the NMR tube by cooling it in liquid N_2. The only absorption observed was a singlet at 2.2 delta units, which is identical to the chemical shift of authentic trimethylamine in the same solvent. Also, acidification of the solution with HCl shifted the absorption to 2.95 delta, the same absorption observed for authentic trimethylamine acidified with HCl.

Identification of the amine produced in photolysis of [11]

A 50 mL flask containing [11] (43.5 mg, 0.1 mmole) in 10 mL anhydrous CH_3OH was deoxygenated and photolyzed for 30 min. An aliquct of the reaction mixture was removed and analyzed by TLC-UV,

which indicated that the reaction was 92% complete. The remaining solution was concentrated to ca. 1 mL, and 4 mL 0.2N H_2SO_4 was added (4, 5). The solution was allowed to stand at room temperature for 30 min. The reaction mixture was neutralized with Na_2CO_3 and extracted with hexane. This procedure extracts the amine products relatively free of acridine products. The hexane extract was concentrated to 0.5 mL and was examined by GLC (6'x1/8", 5% apiezon L on 3% KOH treated Chromsorb W 100/120, 175°). These conditions separate N,N-dimethyl-3-phenylpropylamine and N-methyl-3-phenylpropylamine. Only N,N-dimethyl-3-phenylpropylamine could be detected. Its yield was estimated at 76%, based upon comparison of peak areas resulting from three, one μL injections of the hexane solution with three, one μL injections of a standard hexane solution of the amine (11.7 mg/0.5 mL).

Identification of the amine produced in photolysis of [15]

A 5×10^{-3} M solution of [15] in methanol (5 mL) was placed in a 15 mm O.D. pyrex tube, deoxygenated and sealed under vacuum. The reaction mixture was photolyzed as previously described, for 30 min, concentrated to ca. 0.5 mL and 4 mL 0.2N H_2SO_4 added (4, 5). After 1 hr, the mixture was neutralized with Na_2CO_3 and extracted three times with 10 mL portions of hexane. The hexane extract was dried over anhydrous Na_2SO_4 and concentrated to 0.1 mL. A 10 μL aliquot

was spotted on a silica gel TLC plate and developed in benzene:dioxane: diethylamine (95:5:2). The phenothiazine containing amines were visualized by spraying with 2N H_2SO_4 containing ca. 1% $FeCl_3$. The only amine produced was identified as chlorpromazine by co-spotting with authentic material. No desmethylchlorpromazine, which has a lower R_f value, was found.

Solid state photolysis of [10]

Preparative scale reaction: A 50 mL round bottomed flask containing 2 gm 100 mesh silicic acid, 40 mg [10] and 10 mL anhydrous methanol was placed on a rotary evaporator and the solvent was slowly removed to deposit [10] on the silicic acid. Samples of 200 mg $\pm$ 5 mg were weighed and 1 mL cyclohexane added to form transparent slurries. Deoxygenation was attempted by 3-5 freeze-thaw cycles and the samples were photolyzed for 10 min. The samples were treated with 10 mL methanol followed by 5 mL ethanolic 2N H_2SO_4. The extracts were concentrated, the acidic extract neutralized with Na_2CO_3, and analyzed by TLC. The primary products found were 9-methylacridine and unreacted [10]. Variable amounts of 9-acridinylmethanol [9] were observed and since the yield was highest under conditions where deoxygenation was not complete, it appeared likely that the yield of [4] was correlated with the degree of deoxygenation. However, the presence of [4], although much reduced by extended deoxygenation, could not be completely eliminated indicating that complete deoxygenation was not

achieved under experimental conditions. The extracted silicic acid still had a very intense fluorescence. Further confirmation of this observation was obtained by spotting ca. 20 μL of the cyclohexane slurry on a TLC plate and developing in acetonitrile:water (9:1). A very large fluorescent spot remained at the origin indicating that a significant amount of the fluorescent products are covalently bound to the silicic acid.

TLC photolysis: Duplicate 10 mL aliquots of a 10^{-2} M stock solution of [10] and [15] were spotted on 2-100 μ silica gel plates. The plates were suspended in the Rayonet reactor and exposed to UV light for periods up to 1 hr. The spots on one plate were cut out and placed in 50 mL centrifuge tubes and eluted with 5 mL 0.1 N H_2SO_4 containing 10% methanol and the fluorescence determined. The molar equivalence of the fluorescence intensity was determined by processing various concentrations of [2] through the same procedure.

The other plate was developed in acetonitrile:H_2O (9:1) and the quaternary spot was eluted with ethanolic 2 N H_2SO_4 and quantified by the normal UV method.

Photoreduction of 9-methylacridine [2]

The procedure used was essentially that of Goth et al. (7) to isolate the photoreduced acridan products needed as TLC reference samples. Since the yield of 9,9'-dimethyl-9,9' biacridan [14] from the photolysis of [2] is concentration dependent, a concentrated

photolysis reaction mixture was used to isolate that product while a dilute solution was used for the other products.

A solution of 9-methylacridine [2] (200 mg, 1.03 mmoles) in anhydrous methanol (15 mL) in a 50 mL pear shaped pyrex flask was degassed and photolyzed (as described under preparative photolysis of [10]) for 15 hr. At the end of the reaction, 95 mg (46% crude yield) of [14] had crystallized out and was isolated and washed repeatedly with acetone to give 50 mg (25% yield) of a powder. The PMR spectrum was obtained in CF_3COOH and was identical to that reported (7): 3.52 ppm (6H s) and 7.8-8.4 ppm (16H m); except that the aromatic protons had an additional component from 8.65-8.9 ppm which was required to obtain the proper integral area (Figure 14). This compound is extremely insoluble in normal solvents and readily exidizes when exposed to air and disproportionates when under nitrogen in the dark (7). Therefore, it was not possible to obtain a reference TLC R_f value for this compound because no new R_f value could be observed. The monomeric photoreduced products were obtained from the preparative photolysis (under identical conditions as above) of 9-methylacridine (100 mg, 0.52 mmoles) in anhydrous methanol (125 mL). The reaction mixture was filtered to remove the solid precipitate of [14] and taken to dryness. Short column chromatography using dichloromethane as the eluting solveny gave 9-methylacridan [12] (11.5 mg, 11% yield) and 9-methyl-9-hydroxymethyl acridan [13] (34 mg, 26% yield) which were identified by their PMR spectra (7).

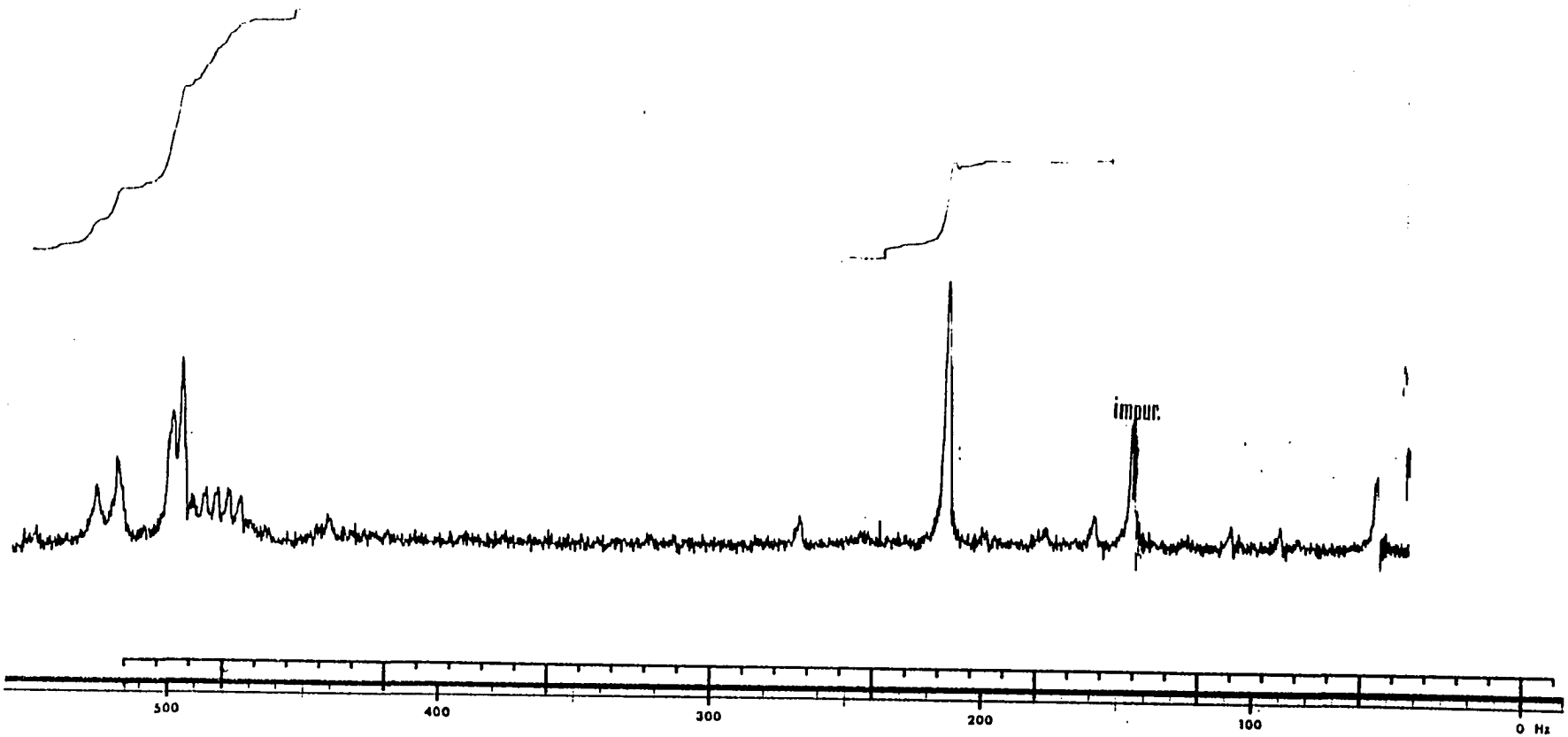

Figure 14. 60 MHz PMR (CF_3COOH) of [14].

Photolyses of 9-bromomethylacridine [1] and 9-(methoxymethyl)-acridine [5]

Photolyses were effected under the conditions described for preparative scale photolysis of [10]. The reaction mixtures were analyzed by TLC and NMR. The NMR spectra of the mixtures produced in the photolyses of [1] and [5] were almost identical. In each instance, 9-(methoxymethyl)-acridine was identified as the major constituent by its characteristic NMR absorptions at 3.40 (3H s) and 5.36 (2H s) delta and by its TLC R_f value of 0.51 in benzene:acetone (95:5). The spectrum of the photolysis mixture in both cases contained a single peak at ca. 5.35 delta but the addition of [1] produced a new signal with approximately the same chemical shift indicating that [5] is the major product. Furthermore, no absorption characteristic of the methyl group in 9-methylacridine (ca. 3.0 delta) was observed. Additionally, each mixture contained minor products tentatively identified as acridans derived from [5] by their characteristic TLC behavior. Namely, their spots are initially nonfluorescent but, upon standing, exhibit the fluorescence characteristic of acridines.

LITERATURE CITED

1. P. N. Kaul, R. E. Lehr, M. W. Conway and L. R. Whitfield, IRCS Biomed. Tech.; Pharmacol., 2, 1343, (1974).

2. A. Campbell, C. S. Franklin, E. H. Morgan and D. J. Tivey, J. Chem. Soc., 1145, (1958).

3. R. E. Lehr and P. N. Kaul, J. Pharm. Sci., 64, 950, (1975).

4. M. A. Ratcliff, Jr. and J. K. Kochi, J. Org. Chem., 36, 3112, (1971).

5. D. C. Appleton, D. C. Bull, R. S. Givens, V. Lillis, J. McKenna, J. M. McKenna and A. R. Walley, J. Chem. Soc. Chem. Commun., 473, (1974).

6. R. S. Givens, personal communication.

7. von H. Goth, P. Cerutti and H. Schmid, Helv. Chim. Acta., 48, 1395, (1965).

8. A. Kira, Y. Ikeda and M. Koizumi, Bull. Chem. Soc. Jpn., 39, 1673, (1966).

9. A. Kira and M. Koizumi, Bull. Chem. Soc. Jpn., 42, 625, (1969).

10. E. Vander Donckt and G. Porter, J. Chem. Phys., 42, 1173, (1967).

11. M. Koizumi, Y. Ikeda and H. Yamashita, Bull. Chem. Soc. Jpn., 41, 1056, (1968).

12. D. G. Whitten and Y. J. Lee, J. Am. Chem. Soc., 93, 961, (1971).

13. I. Suzuki, Pharm. Bull.,4, 211, (1956), (Chem. Abst., 51: 7372h).

14. D. R. Stull, Ind. Engin. Chem., 39, 517, (1947).

15. R. C. Weast ed., "Handbook of Chemistry and Physics", 53rd ed., Chemical Rubber Co., Cleveland, Oh., (1972), p. C 370.

16. N. C. Deno, W. E. Billups, R. Fishbein, C. Pierson, R. Whalen and J. C. Wyckoff, J. Am. Chem. Soc., 93, 438, (1971).

17. A. Kellmann and J. T. Dubois, J. Chem. Phys., 42, 2518, (1965).

18. E. J. Bowen, N. J. Holder and G. B. Woodger, J. Phys. Chem., 66, 2491, (1962).

19. I. B. Berlman, "Handbook of Fluorescence Spectra of Aromatic Molecules", Academic Press, N. Y., (1965), p.35.

20. W. R. Ware, J. Phys. Chem., 66, 455, (1962).

21. O. L. J. Guzeman, F. Kaufman and G. Porter, J. Chem. Soc., Faraday Trans. II, 69, 708, (1973).

22. D. M. Hercules ed., "Fluorescence and Phosphorescence Analysis", Wiley-Interscience, N. Y., (1966), p. 24.

23. K. Tokumura, K. Kikuchi and M. Koizumi, Bull.Chem. Soc. Jpn., 46, 1309, (1973).

24. T. D. Walsh and R. C. Long, J. Am. Chem. Soc., 89, 3943, (1967).

25. J. B. Ragland and V. J. Kinross-Wright, Anal. Chem., 36, 1356, (1964).

26. N. Mataga and T. Kubot, "Molecular Interactions and Electronic Spectra", Marcel Dekker, Inc., N. Y., (1970), chapter 6.

27. R. Foster and C. A. Fyte, in "Progress in NMR Spectroscopy", 4, J. N. Ensley, J. Feeney and L. H. Sutcliffe ed., Pergamon Press, N. Y., (1969), p. 1.

28. Reference 26, chapter 9.

29. R. Hiatt in "Organic Peroxides", 2, D. Swern ed., Wiley Interscience, N. Y., (1971), chapter 1.

30. H. Lund and J. Bjerrum, Ber., 64B, 210, (1931).

31. F. N. Jones, M. F. Zinn and C. R. Hauser, J. Org. Chem., 28, 663, (1963).

II. LUMINESCENCE CHARACTERISTICS OF 9-SUBSTITUTED ACRIDINE DERIVATIVES

CHAPTER 1

INTRODUCTION

Prior experience in using fluorescent tagging reagents as the basis for the development of an analytical method for the quantitation of chlorpromazine metabolites (1-3) stimulated our interest in the luminescence characteristics of acridine derivatives. We were looking for a fluorescent molecule which, when suitably derivatized, would react with tertiary amine drugs thus enabling their quantification by fluorometry.

Alkyl and benzyl halides react quantitatively with tertiary amines to yield quaternary salts (4). More specifically, ^{14}C-methyl iodide has been shown to react with chlorpromazine to yield a radioactive quaternary salt which is the basis for a radioassay procedure (5). Therefore, the introduction of a substituted methyl halide functionality appeared to be the preferential coupling mode for a fluorophore.

In screening the potential compounds which might be useful as tagging reagents, it very quickly became evident that acridine derivatives

should be suitable for this purpose for a number of reasons. First, the quantum yield, and more importantly, the relative fluorescence yield of most acridine derivatives is sufficiently intense to allow quantification of the picomole quantities of tertiary amine drugs present in biological samples. Secondly, the chemistry of acridine derivatives has been extensively studied (7,33,54) with over 3,000 derivatives prepared and their chemical properties investigated. Furthermore, the synthesis of one potentially useful tagging agent, 9-bromomethylacridine, had previously been reported (6).

These facts all supported the choice of acridine derivatives as the basic fluorophore. Table 1 (7) shows the state-of-the-art of much of the acridine fluorescence characterization data. The data shows that a detailed fluorometric characterization is not available for most acridine derivatives; however, enough information is available to develop a preliminary list of potentially useful tagging reagents, several of which are shown in Figure 1.

The tagging reagent, 9-bromomethylacridine, was prepared and reacted with chlorpromazine [16]. The product was isolated, purified and found to be nonfluorescent. However, exposure to UV light on a TLC plate resulted in the appearance of fluorescent products via a photolysis reaction. That reaction has been characterized in detail in Part I. The quantitation procedure for chlorpromazine using 9-bromomethylacridine was developed and standardized and is presently being

Table 1

Colour of Fluorescence of various Acridines in Ultra-violet Light (?).
(The fluorescence in daylight is weaker but similar in colour except where otherwise indicated.)

Substance.	Neutral molecule.*	Kation.*	Anion.	Reference.
Acridine	Violet-blue	Green	—	—
1-, 2-, 3- and 4-Methylacridines	Violet-blue	Green	—	Reed (1944
3-Methoxy-5: 8-dichloroacridine	Violet-blue $\lambda_{max.}$ = 4500 A., in amyl alcohol)	—	—	Butler (1944)
2-Hydroxyacridine	—	Yellow †	Yellow †	—
3-Hydroxyacridine	—	(Faint orange)	Orange ‡	—
4-Hydroxyacridine	—	Nil	Nil	—
1-Aminoacridine	Nil	Nil	—	—
2-Aminoacridine	(Faint green)	Yellow †	—	—
3-Aminoacridine	Greenish-yellow	(Faint orange)	—	—
4-Aminoacridine	(Faint orange)	Nil	—	—
5-Aminoacridine	Green	Violet-blue (yellow † when concentrated)	—	—
1 : 8-Diaminoacridine	Nil	Yellow ‡	—	—
2 : 5-Diaminoacridine	(Faint yellow)	Yellow-green (violet in strong acid)	—	—
2 : 6-Diaminoacridine	(Faint yellow)	(Faint yellow)	—	—
2 : 7-Diaminoacridine	Greenish-yellow	Orange ‡	—	—
2 : 8-Diaminoacridine	(Faint yellow)	Yellow - green yellow in strong acid)	—	—
2 : 8-Diamino-*N*-methyl-acridinium chloride	—	Green ($\lambda_{max.}$ = 5275 & 5360 A.)	—	Twarowska (1935)
2 : 8-*bis*Dimethylaminoacridine	Yellow-green	Yellow †	—	—
2 : 8-Diamino-3 : 7-dimethyl-acridine	Orange-yellow ‡	Yellow-green	—	Twarowska (1935)
2 : 8-Diamino-5-phenyl-3 : 7-di-methylacridine	—	Green ($\lambda_{max.}$ = 5360 A.)	—	—
2 : 5-Diamino-7-ethoxyacridine	Green	Yellow-green	—	—
5-Amino-3-methoxy-8-chloro-acridine	—	Blue ($\lambda_{max.}$ = 4800 A.)	—	Butler (1944)
Atebrin	Green	Green ($\lambda_{max.}$ = 5000–5100 A. depending on solvent; another peak at 4000)	—	Butler (1944); Brodie & Udenfriend (1943)
2-Acetamidoacridine	Violet-blue	Yellow-green	—	—
Acridine-3-carboxylic acid	Violet	Green	Blue	—
Acridan	Nil	—	—	—
Acridone	Violet	Greenish-blue	Blue-green	—
N-Methylacridone	—	Green	Blue	—
3-Methoxy-8-chloroacridone	Violet ($\lambda_{max.}$ = 4200 A.)	—	—	Butler (1944)
2-Aminoacridone	Violet	Green	—	—
3-Aminoacridone	Green	Nil	—	—
2: 7-Diaminoacridone	Green	Nil	—	—
2 : 8-Diaminoacridone	Violet	Green	—	—

* Neutral molecule in 0·1N-alcoholic sodium hydroxide; katien as hydrochloride in water.
† Green in daylight.
‡ Nil in daylight.

Reed, J. Chem. Soc., 679, (1944)
Butler, J. Pharmacol., 80, 70, (1944)
Twarowska, Acta Phys. Polon., 4, 369, (1935)
Brodie and Udenfriend, J. Biol. Chem., 151, 299, (1943).

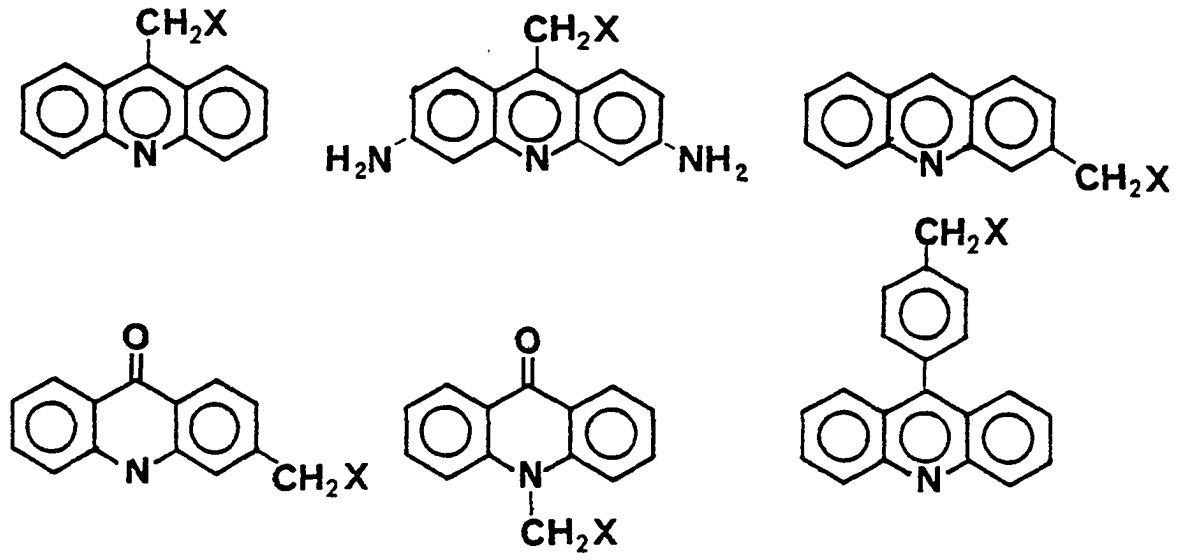

Figure 1. Potentially useful acridine fluorescence tagging reagents.

applied to blood samples obtained from schizophrenic patients (8). However, we still had an interest in developing a suitable tagging reagent for preparing fluorescent quaternary salt derivatives of tertiary amine drugs and felt that a basic study of the chemical and luminescent properties of acridine derivatives should lead to a viable approach to a solution of this problem.

The luminescence characteristics which might be exhibited by a compound can best be understood by discussing the mechanistic pathways of excited state population and deactivation and then looking at the general rules for fluorescence and phophorescence which have been developed in light of these factors.

The understanding of the radiative processes in organic

molecules has been advanced significantly in the last two decades. The total integrated absorption over a band for a given transition is a constant characteristic of a molecule and is relatively independent of the temperature, state of the molecule and other variables (9). However, the distribution of intensities between the various structured bands within the absorption region can alter with conditions.

The absorption of light results in the promotion of an electron from the lowest vibrational level of the highest occupied molecular orbital of the ground state to an unoccupied antibonding molecular orbital (Figure 2) of a singlet excited state. The equilibrium internuclear distances in excited states are often greater than those in the ground state because of the reduced bonding character. The probability for an electronic transition from the lowest vibrational level of the ground state, $S_o(o)$, to the kth vibronic level of an excited state, S_1, is given by the oscillator strength $f_{S_o(o),\, S_1(k)}$. In symmetry allowed transitions, the most probable vibronic transitions, according to the Franck-Condon principle, are those in which the potential energy surface boundary of the $S_{1(k)}$ vibronic level is at the same internuclear distance as the starting point of the transition. Thus, the $7 \longleftarrow O$, $8 \longleftarrow O$ and $9 \longleftarrow O$ (ν' given first) for the example given in Figure 2 are the most intense bands. In such a vertical transition, the nuclear configuration and the kinetic energy of the vibrational motion remains almost unchanged during the transition, thus satisfying the requirements of the Franck-Condon principle.

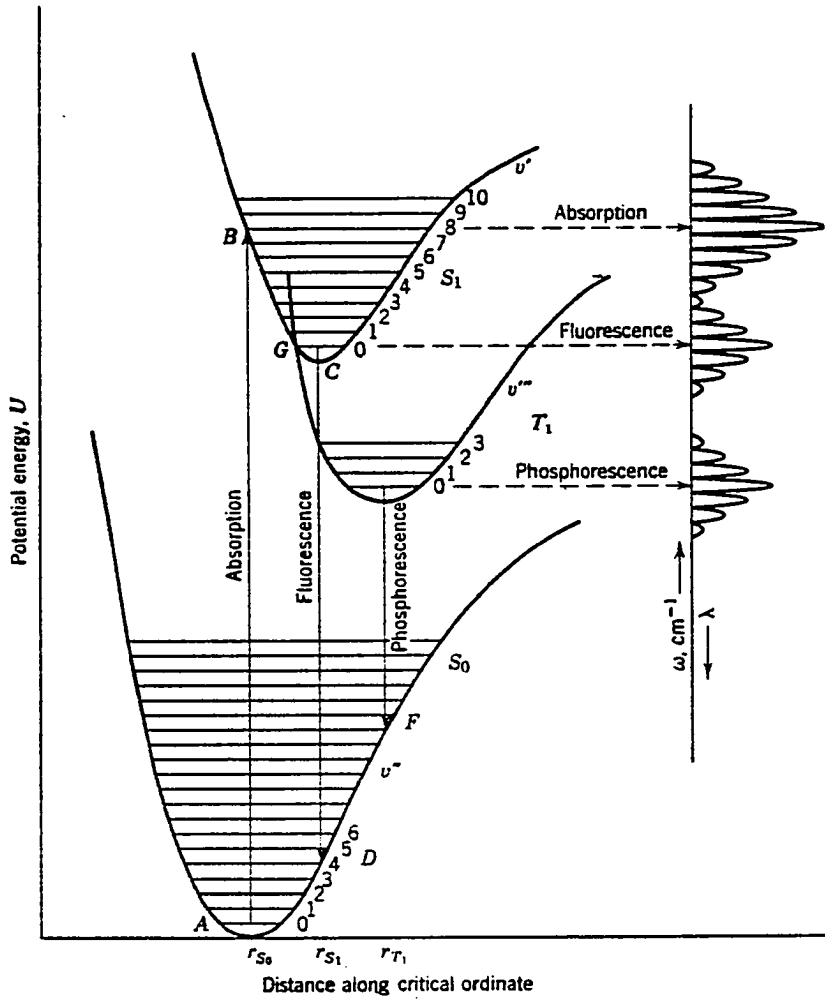

Fig. 2 Potential energy diagram, giving the shape of the hypersurface along a critical coordinate for the ground state S_0 and the first excited singlet S_1 and triplet T_1 states of a representative organic molecule in solution. G is a point of intersystem crossing, $S_1 \rightarrow T_1$. For convenience in representation the distances r were chosen $r_{S_0} < r_{S_1} < r_{T_1}$ so the spectra are spread out. Actually, in complex, fairly symmetrical molecules $r_{S_0} \cong r_{S_1} < r_{T_1}$ and the 0—0 absorption and fluorescence bands almost coincide, but phosphorescence bands are significantly displaced to the longer wavelengths. (10)

The calculation of f_{S_0, S_1} is quite fundamental to our understanding of radiative processes in that the reverse transition from the excited state (fluorescence) depends, subject to certain limitations, on the same parameters. Therefore, any factors which reduce the transition probability to the excited state will also reduce the rate of luminescence from that state.

The derivation of the relationship between the molar extinction coefficient and the natural lifetime, τ_o, was done by Strickler and Berg (11) and is given by the following equation:

$$1/\tau_o = 2.88 \times 10^{-9} n^2 \left\langle \nu_f^{-3} \right\rangle_{av}^{-1} \, gl/gu \int \epsilon \, d \ln \nu$$

n = refractive index of the solvent

$$\left\langle \nu_f^{-3} \right\rangle_{av}^{-1} = \frac{\int I(\nu) \, d\nu}{\int \nu^{-3} I(\nu) \, d\nu}$$

$I(\nu)$ = intensity of a vibrational band

ν = frequency of the transition in cm^{-1}

gu, gl = the degeneracies of the upper and lower states, respectively

ϵ = molar extinction coefficient

The natural lifetime, τ_o, represents the lifetime of the excited state that would be observed if fluorescence were the only excited state deactivation process.

The above relationship holds because it is often observed that the fluorescence spectrum of a large molecule in solution will very closely resemble a mirror image of the absorption spectrum. In these cases, the frequencies of vibrational excitation in the lowest excited singlet are within 10-20% of those in the ground state, which is responsible for the mirror image relationship. The absence of such a relationship between the two spectra may be taken to indicate a large change in the excited state configuration, and in these cases, the correlation between the radiative transition probabilities for absorption and fluorescence may not be observed.

Kasha (12) has proposed an interesting empirical relationship between the observed molar absorption coefficient (ϵ), the oscillator strength (f) and the natural lifetime (τ_o) (Figure 3). In this analysis,

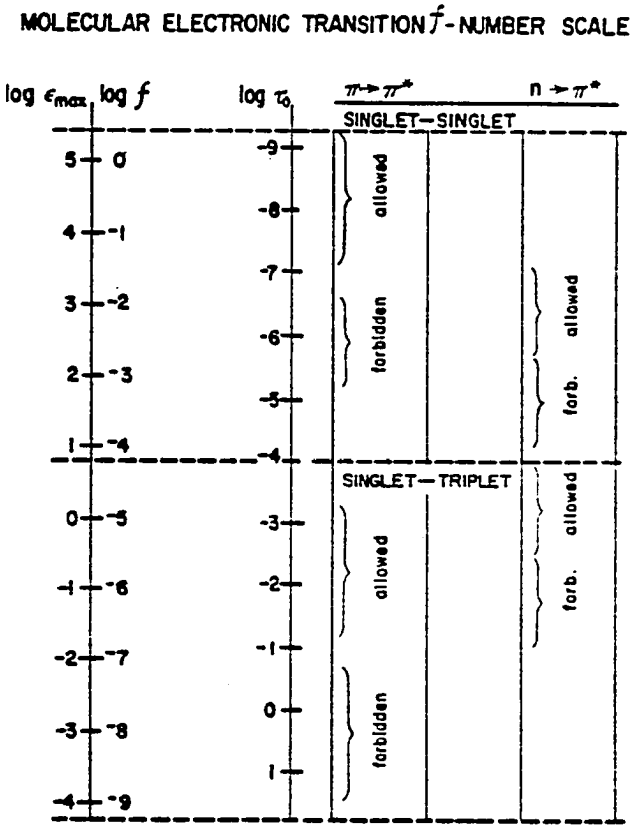

Figure 3. Classification of molecular electronic transitions by approximate correlation with molar absorption coefficient (ϵ), oscillator strength (f), and intrinsic luminescence lifetime (τ_o).

the spin allowed singlet-singlet transitions and spin forbidden singlet-triplet transitions are classified as "allowed" or "forbidden" based on symmetry considerations. Spin forbidden transitions occur through spin-orbit and spin-spin interactions while symmetry forbidden

transitions occur through vibronic coupling. However, the total symmetry of a vibronic state is specified by the direct product of the representation to which the electronic and vibrational wave functions belong and thus the symmetry selection rules are modified according to the total symmetry of the higher vibronic levels of the excited state. This fact generally reduces the differences observed between the transition probabilities for symmetry allowed and symmetry forbidden transitions.

Thus having identified the fundamental relationship between the natural lifetime and the absorption extinction coefficient, which is only strictly valid in cases where good mirror symmetry exists, we are now ready to proceed in our analysis. If the natural lifetime, τ_o, is equal to the observed lifetime, then the fluorescence quantum yield ϕ_f must be equal to unity by definition. Using the relationship between the experimentally measurable parameters, namely molar extinction coefficient and fluorescence intensity, certain assumptions can now be made. In a series of structurally related compounds having similar absorption characteristics, changes in fluorescence intensity must be related to changes in radiationless pathway transition probabilities and not fluorescence transition probability. Similarly, when changes in environment for a given compound do not alter the absorption characteristics, then changes in fluorescence intensity must also be indicative of changes in radiationless rather than fluorescence pathways.

The observed luminescence characteristics of a molecule are

therefore determined by the relative rates of various excited state deactivation pathways. The major radiative and nonradiative pathways and the order of magnitude estimates of their rates can best be discussed by examining a modified Jablonski diagram (Figure 4).

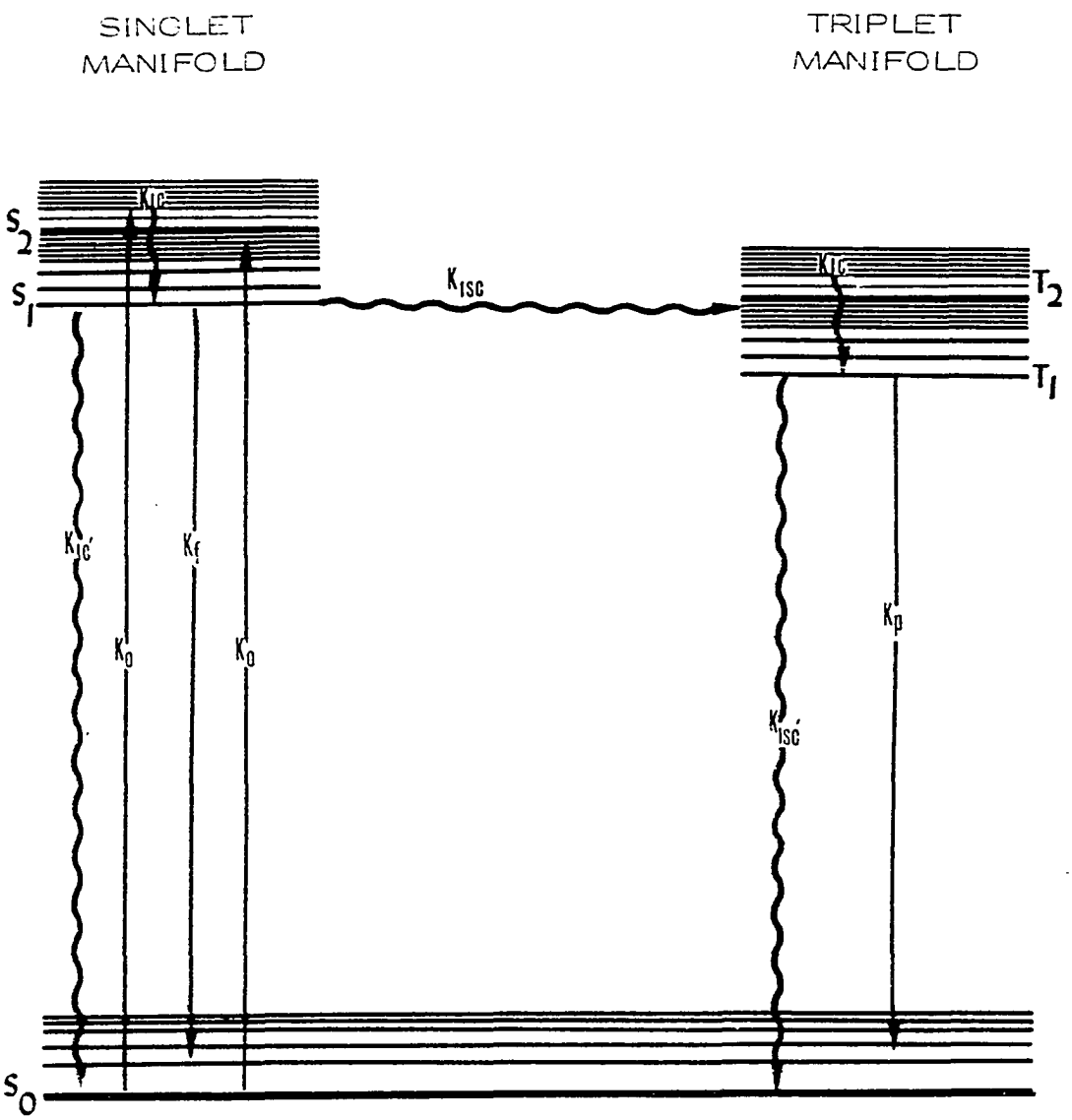

Figure 4. A modified Jablonski diagram showing various radiative (solid lines) and nonradiative (wiggly lines) pathways. See text for definition of the various rate constants (13, 14, 15).

Light is absorbed by a molecule at a rate (k_o) which is very fast (ca. 10^{15} sec^{-1}) with respect to the time constant for intramolecular vibrational motion. Nonradiative internal conversion occurs very rapidly ($k_{ic} = 10^{10}-10^{13}$ sec^{-1}) between higher excited states or vibronically excited levels to the lowest excited level (S_1) of the singlet manifold. Fluorescence then results from the S_1 state at a rate (k_f) which is $\leq 10^9$ sec^{-1}. The rate of the competitive internal conversion pathway (k_{ic}'), ranges widely ($0 < k_{ic}' < 10^{10}$ sec^{-1}). As a first approximation, this process is usually considered nonsignificant for most aromatic compounds. The rate of intersystem crossing (k_{isc}) must be $\geq k_f$ in order of magnitude to permit population of the triplet manifold. Although the reasons are not understood, it is interesting to note that the "spin-forbidden" intersystem crossing process and the "allowed" fluorescence process have comparable transition probabilities.

The rate (k_p) for the "forbidden" radiative process from the triplet state (phosphorescence) is quite slow ($k_p = 10^2-10^{-2}$ sec^{-1}). The phosphorescence decay time τ_p which is the observed lifetime of the triplet state is given by:

$$\tau_p = 1/(k_p + k_{isc}')$$

Since, for a given molecule, k_p should be fairly constant, any variations in the observed lifetime that occur due to changes in the external environment must be related to changes in k_{isc}'. Experimental observations have confirmed that the rate for the competitive "forbidden"

nonradiative process (k_{isc}') varies widely. Even in the same molecule, the observed rate depends primarily on parameters such as temperature and the physical state of the molecule. The lifetime of the lowest triplet state of naphthalene in n-hexane at room temperature is ca. 10^{-5} sec whereas it is ca. 2 sec in a rigid organic solvent at 77°K (16) which would suggest that in this case, k_{isc}' varies from 0.484 to 9.84×10^4 sec^{-1}. Therefore, phosphorescence is rarely observed for molecules in liquid solution because of the fast nonradiative pathway although the vibronically deficient molecule biacetyl is one of the notable exceptions (17).

The first real question that must be addressed deals with how a radiationless process such as intersystem crossing which involves a change in spin state can effectively compete with a spin allowed radiative process (fluorescence). Since the radiationless pathways involve transition between states of differing spin and symmetry elements, the perturbations that allow for forbidden radiative transitions must also be operating in the case of radiationless transitions. Henry and Siebrand (18) observed that spin allowed transitions, all other things being equal, tend to be about 10^8 times faster than the corresponding spin forbidden transitions. This finite number (rather than infinity) is due mainly to spin-orbit coupling. Furthermore, these authors noted that for aromatic hydrocarbons, orbitally allowed and orbitally forbidden transitions actually occur at roughly the same rates.

Various models have been proposed to calculate and describe

the transition probability for radiationless transitions. However, there is a certain attractiveness in looking at the early model of Robinson and Frosch (19, 20) because of the consolidated manner in which energy transfer, vibronic deactivation, solvent effects and the temperature dependence can be treated. In their model, electronic relaxation is simply a result of radiationless transitions among nearly degenerate nonstationary states of the overall system. This definition of the system as the solute molecule of interest plus the surrounding solvent molecules is fundamental to their argument. The so called electronic states of the free solute molecule are not free stationary states but are mixed through electronic and vibronic interactions with the solvent. One of the most important empirical relationships drawn from their study is the dependence of the square of the overlap integral on ΔE which is shown in Figure 5.

> These authors concluded "...certainly one important general conclusion can be drawn from these crude estimates. One expects nonradiative singlet-triplet transitions among excited states to be much faster, because of small energy gaps, and probably larger matrix elements, than those which occur between the lowest triplet and the ground state. Thus $S_1 \longrightarrow T_1$ transitions either directly or through intermediate triplet states are fast, while $T_1 \longrightarrow S_o$ transitions are generally slow."

One of the basic premises of the Robinson and Frosch model was that in the simplest case, the solvent plays no role in the radiationless transition other than to act as a collection of phonon oscillators into which energy in the form of lattice vibrations may ultimately flow.

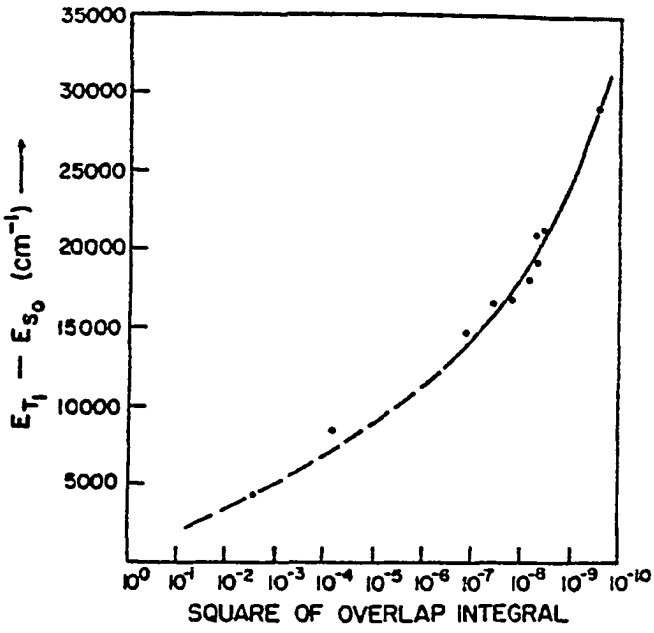

Figure 5. The dependence of vibrational overlap integral on the energy separation between the lowest triplet and ground states, as calculated by Robinson and Frosch (19).

Gouterman (21) developed a semiclassical model for radiationless transitions by noting that the problem of the radiationless transition is not very different from that of radiative transitions. In the latter case, a molecular system interacts with the harmonic oscillators of a photon field, while in the former case, with the phonon field. This model successfully described:

(a) the fast rates of radiationless transitions,

(b) the observed temperature dependence,

(c) the cut-off frequency for radiationless transitions,

(d) the existence of the Franck-Condon principle and,

(e) the lack of selection rules.

The study of radiationless transitions is currently one of the most active areas of investigation. Furthermore, this is an area where the combined expertise of the theorist and experimentalist is needed to attack the problem. Basically, sophisticated quantum mechanical models must be used to describe the experimental results since the primary event, the radiationless transition, is nonspectroscopic. However, photoacoustic spectroscopy (22) shows some promise in observing some of these transitions directly. The major difficulty in applying the theoretical models and experience gained from investigations of radiative transitions to the study of radiationless transitions is the following: the energy differences between interacting states for radiative processes is from 1,000 to 10,000 cm^{-1} and hence the Born-Oppenheimer approximation which is required to solve the mathmatical descriptions is valid. However, in the case of radiationless transitions, the energy differences are on the order of 1 - 100 cm^{-1} and the magnitude of the uncertainties introduced by the Born-Oppenheimer approximation and many of the other commonly used simplifying approximations are greater than the possible range of values for the rate determining parameters. Thus, the theoretical descriptions for radiationless processes have lagged behind those for radiative transitions for the reasons mentioned above.

Years of experimental investigations have generated a set of empirical rules which are useful in making preliminary predictions about the luminescence characteristics which might be observed for a given compound. Among the large number of known organic compounds, only a small fraction exhibit intense luminescence. The fluorescence (or lack thereof) of a molecule is dependent upon the structure of that molecule and the environment in which the spectrum is measured. There are only a limited number of generalizations which can be made about the structural factors which tend to enhance or repress luminescence and the chemist usually has little opportunity to chemically manipulate the structure to alter luminescence characteristics. On the other hand, the investigator usually has available a wide choice of media in which to examine the fluorescence of a compound. Although "structural" and "environmental" factors are treated separately, it is clearly impossible to completely separate these two topics which are so intimately related.

Analytically useful photoluminescence is restricted to compounds possessing large conjugated systems and for most aromatic hydrocarbons both fluorescence and phosphorescence is observed. The most intensely fluorescent aromatic compounds are characterized by rigid planar structures. For example, fluorescein [18] exhibits very intense fluorescence in liquid solution whereas phenolphthalein [19] does not, despite the structural similarity (17).

Table 2 (17) shows the effect of various substituents upon

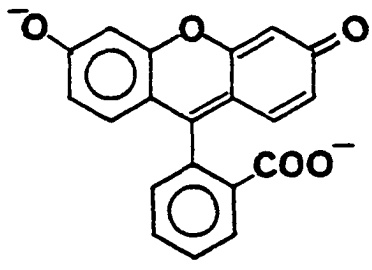

18

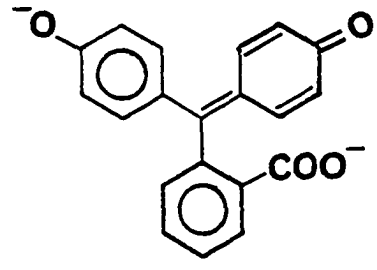

19

Table 2. Effects of Substituents upon the Fluorescence of Aromatics (17).

Substituent	Effect on frequency of emission	Effect on Intensity
Alkyl	None	Very slight increase or decrease
OH, OCH_3, OC_2H_5	Decrease	Increase
CO_2H	Decrease	Large decrease
NH_2, NHR, NR_2	Decrease	Increase
NO_2, NO	---	Total quenching
CN	None	Increase
F Cl Br I	Decrease	Decrease
SO_3H	None	None

fluorescence of aromatics. Though useful, such generalizations must be applied to practical work with care, for exceptions are not uncommon. Substituents which act as conjugated electron donors often increase the total luminescence yield of an aromatic system. The principal effect is to increase radiative transition probability. However, the list of substituents which can cause this effect is usually limited to amino and hydroxy functionalities. On the other hand, most strongly electronic accepting substituents or heavy atom substituents produce a very significant decrease in fluorescence yields. Heavy atom substituents increase spin-orbit coupling thus enhancing the rate of intersystem crossing. This may or may not affect the yield of phosphorescence.

The introduction of a heteroatom into an aromatic ring usually profoundly alters the luminescence characteristics compared to those of the parent aromatic. Most common heteroatoms possess at least one lone pair of nonbonding electrons which may be excited into the π^* ring orbital resulting in an n, π^* transition. If that state is the lowest excited singlet state, then fluorescence may be significantly quenched due to its very low radiative transition probability ($\epsilon < 1000$). Fluorescence is further diminished because singlet-triplet energy gaps are commonly smaller for n, π^* than for π, π^* excited states which leads to a greater rate constant for intersystem crossing.

The changes in fluorescence characteristics which may be ascribed to structural factors can only be explained relative to some

reference compound. Furthermore, the structural effects noted above are only valid under experimental conditions where optimum fluorescence intensity is observed. Although a wide range of solvent types are available, the fluorescence characteristics for most compounds have only been investigated for the "normal" solvents used for fluorescence characterization. The importance of this observation in trying to make general observations is best supported by a recent investigation of the fluorescent characteristics of halogen substituted anthracenes (23). The fluorescence of the reference compound, anthracene, is quite low (0.02) when measured in bromobenzene compared to 0.30 in hexane which is consistent with the previous description of "heavy atom" quenching of fluorescence. On the other hand, 9, 10-dibromoanthracene which has a low quantum yield, 0.087, in hexane actually has a higher quantum yield of 0.29 when measured in bromobenzene.

The effect of the solvent environment on fluorescence generally occurs because of two distinct mechanisms. Specific solute-solvent interactions such as hydrogen bonding, energy transfer, charge transfer complexation and protonation produce dramatic effects on the observed fluorescence. The potential existence of these interactions can usually be predicted by a knowledge of the fundamental chemical properties of the solvent and solute molecules. There is, however, a more general effect of the solvent environment on the fluorescence process which can be observed as changes in the emission wavelength and the variation in quantum yield.

The Franck-Condon principle of light absorption asserts that molecular transitions occur in a time interval, ca. 10^{-15} sec, that produces a transitory "Franck-Condon excited state", possessing an altered electron distribution but with the ground-state geometry. Rapid changes in molecular geometry and resolvation by the solvent cage produce a new equilibrium excited state. It is commonly observed that the fluorescence maximum of polyatomic molecules is shifted to lower energy (red shift) by solvation and the magnitude of the shift depends on the specific nature of the solvent-solute interaction, several important types of which are (17):

1. Dipole-dipole interactions between solute and solvent, in the case where both are polar.
2. Interactions between solute permanent dipoles and dipoles induced in the solvent by them.
3. Interactions between solvent permanent dipoles and dipoles induced in the solute by them.
4. Dispersive interactions between the transition dipole of the solute and the dipoles induced in the solvent by them; this interaction is present in all solute-solvent systems.

Veljkovic (24) was able to correlate the red shift in fluorescence in many meso substituted anthracenes with solvent polarizability. He attributed this effect to dispersion forces since the energy of this interaction, U, is related to polarizability

$$U = 3/2h \frac{I_a I_b}{I_a + I_b} \frac{(\alpha_a \alpha_b)}{R^6}$$

where the I's represent ionization potentials and the α's are polarizabilities of the interacting molecules at a distance R. Also, the red shift in polar molecules such as 9-CN anthracene could be correlated with the solvent dielectric constant and may well represent an enhanced dipole-dipole interaction.

Solvent effects on the quantum yield of fluorescence are generally more difficult to explain. The effect of purely electrostatic (dipolar) solvent-solute interactions are often due to the solvent shifts themselves if one accepts the hypothesis of Kearvell and Wilkinson (23). They propose that the rate of intersystem crossing is highly dependent on the relative levels of S_1, T_2 and T_3 as demonstrated by the temperature dependence. Changes in solvent usually affect singlet levels much more than triplet levels and will significantly alter the energy differences between these levels, thereby affecting the radiative quantum yield.

Specific short-range interactions such as hydrogen bonding, charge transfer complexation, energy transfer, etc., which were previously mentioned may also occur in addition to the general solvent effects. The influence on fluorescence of these specific interactions, if present, will usually predominate over generalized dipolar interactions (17).

Previous investigations of the acridine fluorescence characteristics exemplify many of the effects of the specific solvent-solute

interactions. Many nitrogen heterocycles are relatively nonfluorescent, even when the fluorescence yields of the parent hydrocarbon are quite large (25). The presence of one or more nonbonding orbitals which give rise to n ,π^* transitions are usually considered to be primarily responsible for the differences in the luminescence behavior. Furthermore, in the case of acridines and other heteroatom containing aromatics, hydrogen bond formation and acid-base reactions may lead to more than one fluorescing moiety. For example, acridine fluoresces very weakly ($\phi_f < 0.001$) in cyclohexane and benzene (25) and it is reported that many workers have failed to detect any fluorescence (26). In hydrogen bonding solvents such as alcohol and water, a more intense fluorescence is observed (25). The acridinium ion, on the other hand, has a quantum yield of 0.54 in water, and shows little solvent dependence (27). Various fluorescing species of acridine exists in protonating and hydrogen bonding solvents (scheme I) and the emission maxima for [20], [21] and [22] are 400, 415 and 474 nm respectively (25, 26).

Scheme I

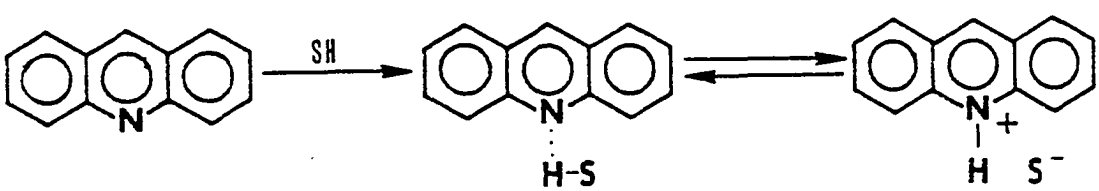

20 21 22

SH = hydrogen bonding, ionizing solvent

The variations in fluorescence yield most probably represent the percentage of [21] present in the solvent since the observed fluorescence of [21] is much greater than [20]. This conclusion is based on the fact that no further bathochromic (red) shifts are observed in luminescence in going from alcohol to water but the quantum yield increases (Table 3).

Table 3. Effect of Water on the Fluorescence of Acridine (27)

Volume % of water	ϕ_f Ethanol
100	0.37
90	0.34
80	0.28
70	0.18
60	0.11
50	0.079
40	0.062
30	0.048
20	0.036
10	0.034
0	0.032

Furthermore, Bowen (27) has pointed out that since the absorption spectra of acridine are remarkably similar in water, alcohol and benzene and the water solubility of acridine is very low (ca. 2×10^{-4} moles/L), there is probably negligible hydrogen bonding in the ground state. Following light absorption by [20], the more basic singlet excited state (28) rapidly hydrogen bonds with solvent to form [21] which either fluoresces or dissociates with energy degradation.

Acridines (27) as well as the parent hydrocarbon anthracene (23) show variations in quantum yield with temperature (Table 4). These data support the hypothesis that the primary processes which determine

Table 4. Effect of Temperature on Observed Quantum Yield of Fluorescence (23, 27)

Temp. (°C)	ϕ_f[a]-acridine	ϕ_f[a]-anthracene
0	0.49	---
10	---	0.283
20	0.33	0.275
60	---	0.243
70	0.09	---

[a]90% aqueous ethanol as solvent.

quantum yield are the nonradiative ones. Temperature dependent intersystem crossing from S_1 to a triplet state slightly above S_1 would be consistent with the experimental observations. With acridine, the relative energy levels of higher triplets such as the $^3 n, \pi^*$ state which may be close to the fluorescing $^1 \pi, \pi^*$ singlet are particularly important based on the studies of El-Sayed (29), who concluded that the nonradiative singlet-triplet transitions between states of different types ($^1 n, \pi^* \longrightarrow {}^3 \pi, \pi^*$ or $^1 \pi, \pi^* \longrightarrow {}^3 n, \pi^*$) should be two orders of magnitude more probable than those involving singlet and triplet states of the same type. The primary factor of importance is the presence of one-center spin-orbit interaction terms for transitions between states of different types which vanish for states of the same type. The observed magnitude of the spin-orbit coupling factor then depends on the ΔE between the states and, therefore, small changes in the relative energy levels of interacting states can profoundly alter the luminescence yield.

Because of a number of apparently anomolous fluorescence characteristics that have been observed for a variety of heteroaromatic and substituted aromatic compounds, a selected sample of data will be

presented to demonstrate some of the parameters that have been investigated in attempting to explain the experimental results. In most instances, definitive mechanistic confirmation was not found, but certain trends were observed. In all cases, it is important to remember that the results for a particular compound should be considered relative to some reference compound such as the analogous hydrocarbon. The spectrum must also be run under experimental conditions that consider the most obvious potential specific solvent effects such as hydrogen bonding and acid-base reactions. Also, aromatic and ketonic solvents which are capable of energy transfer or charge transfer complexation are best avoided. When these factors are taken into consideration, it is possible to summarize the fluorescence characteristics of acridine as follows:

> the fluorescence of the neutral molecule acridine is comparable to the analogous hydrocarbon, anthracene, while fluorescence from the protonated acridinum ion is much more intense.

Acid-base reactions have significant effects on the observed fluorescence of most compounds which contain acidic or basic functionalities. Table 5 shows the fluorescence observed from selected derivatives as a function of the state of ionization of the solute. Although there are no clear trends for predicting pH effects, the variations in quantum yield clearly show the need for investigating this effect for all

Table 5. Effect of Acid-base Properties on Fluorescence

Compound	ϕ_f (or rel. fluor.)
benzene[a]	0.07
toulene[a]	0.17
phenol[a]	0.21
phenol, anion[d]	NF[c]
aniline[b]	0.08
aniline, cation[b]	0.003
aniline, anion[b]	0.0015
benzoic acid[d]	NF
benzoic acid, anion[d]	NF
pyridine[e]	NF
2 amino pyridine[e]	0.71[f]
2 amino pyridine, cation[e]	1.20[f]

[a] I.B. Berlman, Handbook of Fluorescence Spectra of Aromatic Molecules, Academic Press, N.Y., (1965).

[b] J.W. Bridges and R. T. Williams, Biochem. J., 107, 225, (1968).

[c] NF = practically non-fluorescent

[d] B.L. Van Duuren, Chem. Rev., 63, 525, (1963).

[e] A. Weisstuch, Fluorescence of Pyridine Derivatives, Ph. D. Dissertation, St. Johns University, (1969).

[f] relative to dl-tryptophan, $\phi_f = 0.09$

compounds which possess significant acid-base properties. Furthermore, a variety of pH values should be investigated because excited state pKa's are often different from ground state pKa's and complete protonation/deprotonation is desired to accurately assess the effect of ionization on fluorescence.

Another important parameter to be considered is the substitution pattern for isomeric compounds. The extensive study of pyridine derivatives by Weisstuch (30) provides a clear indication of the significance of this parameter (Table 6).

Table 6. Effect of Isomeric Substitution on the Fluorescence of Pyridine Derivatives (30)

Compound	ϕ_f[a]
2-amino pyridine	0.71
3-amino pyridine	0.32
4-amino pyridine	0.001

[a] relative to dl-tryptophan, $\phi_f = 0.09$

This phenomenum has been extensively studied (see ref. 30, chapter 2 for a detailed discussion) and is termed the "proximity effect" which relates to the progressive increase in the extent of n ,π^* character of the lowest excited singlet as the position of the substituent is varied from the 2- to the 4- position. Albert (32) has also observed different fluorescence characteristics for isomeric monoaminoacridines (Table 7).

Table 7. Fluorescence Characteristics of Isomeric Aminoacridines (32)

Acridine	Fluorescence in solution	
	base in alcohol	salts in H_2O
unsubstituted	violet	green
4-amino-	none	none
3-amino-	green	intense yellow
2-amino-	green	none
1-amino-	orange	none
9-amino-	green	intense bluish violet

These results, however, clearly indicate that the trend observed for the pyridine derivatives cannot be extended to the acridine series because 4-aminoacridine should be fluorescent by analogy.

In a recent study of the effect of molecular geometry on the spin-orbit coupling of aromatic amines, Adams, et al. (31) concluded

that the excited state behavior of aromatic amines is dominated by the influence of molecular geometry. The fluorescence quantum yield, phosphorescence quantum yield and lifetimes (Table 8) of a series of

Table 8. Fluorescence Characteristics of Selected Aromatic Amines (31)

Compound	ϕ_f [a]	K_f [b] $\times 10^7$ sec^{-1}	ϕ_p [c]	K_p [d] sec^{-1}	Kisc [e] $\times 10^7$ sec^{-1}
diphenylamine [23]	0.11	4.6	0.73	0.41	36
iminobibenzyl [24]	0.24	4.5	0.51	0.27	10
acridan [25]	0.32	3.1	0.51	0.24	5.2
carbazole [26]	0.42	2.7	0.24	0.056	3.7

[a] quantum yield of fluorescence

[b] $K_f = \phi_f / \tau_f$ = rate of fluorescence

[c] quantum yield of phosphorescence

[d] $K_p = \phi_p / \tau_p (1 - \phi_f)$ = rate of phosphorescence

[e] $\text{Kisc} = \frac{1 - \phi_f}{\tau_f}$ = rate of $S^* \longrightarrow T$ intersystem crossing

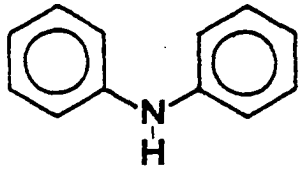

23

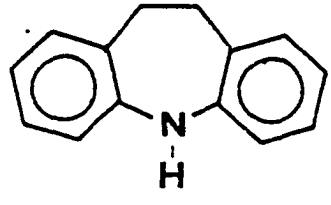

24

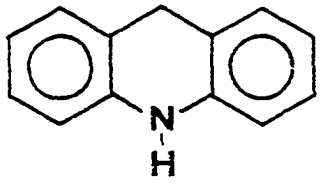

25

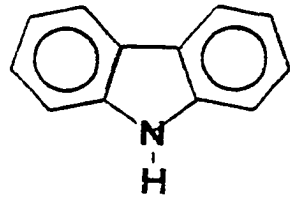

26

aromatic amines whose molecular configurations vary from nonplanar to a planar geometry were investigated in order to study the influence of the geometry of the lone pair orbital on spin-orbit coupling. The compounds studied varied from the distinctly non-planar diphenylamine to the progressively more planar compounds, iminobibenzyl, acridan and carbazole.

Comparison of these data reveals a particularly striking fact: the rate of intersystem crossing and the phosphorescence rate constant decrease dramatically in going from diphenylamine to carbazole while the rate of fluorescence varies only slightly. Since the phosphorescence and intersystem crossing processes between the singlet and triplet manifolds are spin forbidden and are allowed only through spin-orbit coupling of electronic motion in the presence of the nuclear fields, the authors concluded that the observed luminescence behavior is dominated by the dependence of the spin-orbit coupling factors on molecular geometry. However, even though these data seem to explain the effect of spin-orbit coupling for this series of compounds, the same discussion does not explain the high quantum yield of acridan, $\phi_f = 0.32$ compared to acridine $\phi_f = 0.37$ since planarity is usually considered to be one of the primary requirements for intense fluorescence.

The effects of structural and environmental factors on fluorescence are best summarized as tco complex to allow the development of simple predictive models for describing luminescence

behavior. This prediction is born out in a recent report by Sinsheimer et al. (100) who were evaluating the use of 9-acridinylisothiocyanate as a fluorescent labeling reagent for amines. The analomous fluorescence characteristics observed for various derivatives are shown in Table 9. Although the synthesis and luminescence characterization of all compounds of interest is quite time consuming, there does not appear to be a good alternative to this type of experimental approach at this time.

Table 9. Fluorescence Characteristics of Various (9-acridinyl) thiourea Derivatives (100)

Thiourea Derivatives [b] R_1	R_2	Relative Fluorescence [a]
-H	$-C_4H_9$	0.013
-H	$-C_6H_5$	0.030
-H	$-CH_2COOH$	0.084
$-C_2H_5$	$-C_2H_5$	0.0069
Reference Compounds [c]		
$-NH_2$		2.64
-Cl		0.088
-NCS		0.67

[a] Relative fluorescence is relative to a 1.60×10^{-6} M solution of fluorescein isothiocyanate at pH 10.

b.

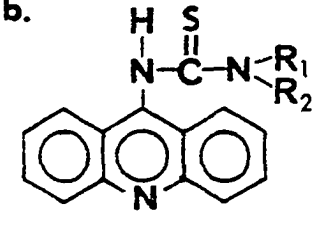

c.

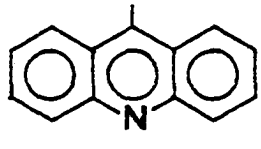

CHAPTER 2

RESULTS AND DISCUSSION: GENERAL PROPERTIES OF ACRIDINE DERIVATIVES

From the discovery of acridine in 1870 to the present day, the acridines have been extensively studied, not only because of their interesting chemical and physical properties, but also because of the many useful applications which have been found for them. Many noted investigators such as Acheson, Albert, Bernthsen, Zanker and Ullman, to name a few, have spent many years investigating the properties of acridines. For this reason, the preparation of many of the compounds needed for this study has previously been reported. In fact, many of the basic synthetic procedures have been independently reviewed by Albert (7, 33) in much the same manner as are the synthetic procedures reported in the Organic Synthesis series. In this chapter, the basic synthetic approach to the desired compounds and their general chemical and physical characteristics will be discussed.

A number of synthetic approaches exist for the preparation of 9-methylacridine which was the desired starting material for many of the derivatives needed for this investigation. The following (scheme II)

are the most common approaches to 9-alkylacridines:

Scheme II

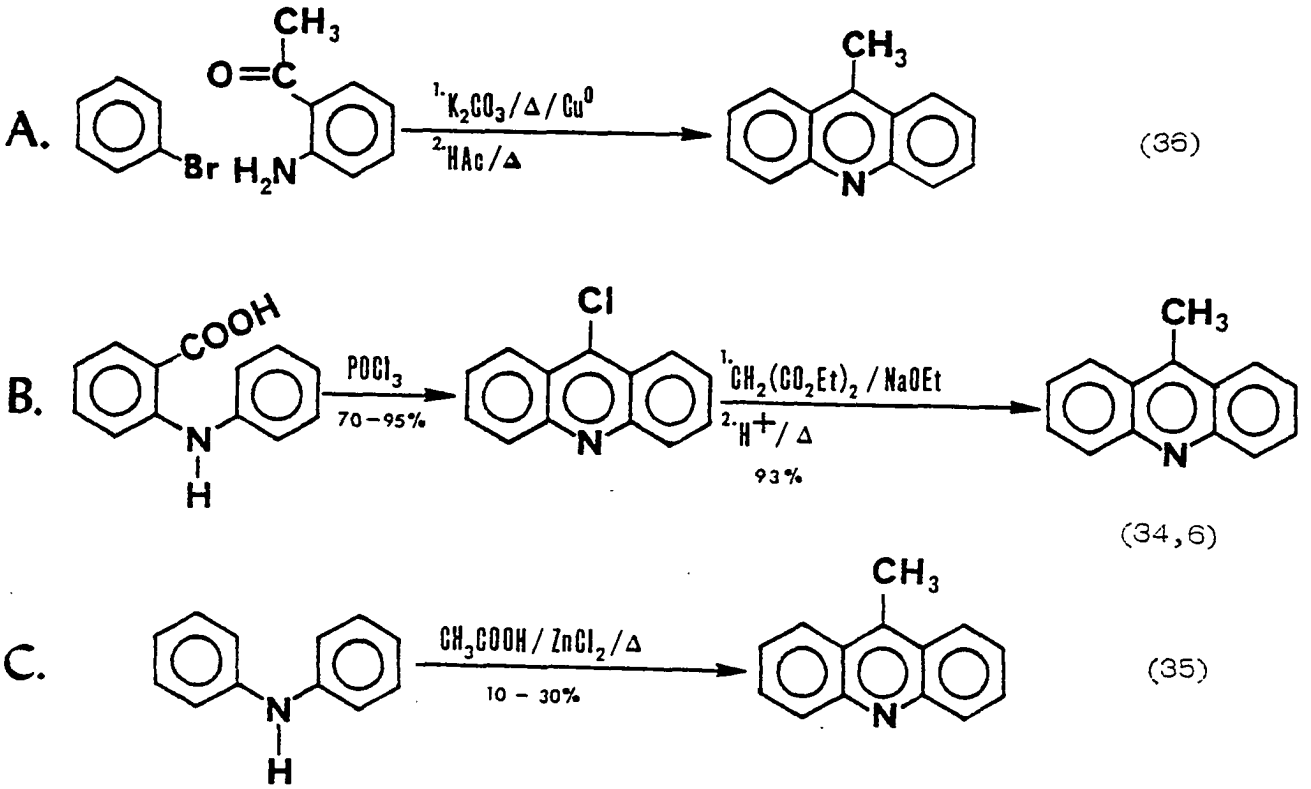

All methods offer certain advantages and disadvantages for the bulk preparation of starting materials. The Bernthsen synthesis (scheme II-C) offers the most direct route to 9-methylacridine and thus avoids the disadvantages of dealing with 9-chloroacridine [27]. Although the route involving [27] gives the highest yields, the tremendous dyeing capacity and lachrymator properties of [27] makes this approach very

undesirable for bulk chemical synthesis. On the other hand, the Bernthsen synthesis presents two major technical difficulties. First, the temperature required for the reaction (ca. 220°) is difficult to attain and secondly, the recommended workup procedure which included extraction of the cooled solid mass with dilute sulfuric acid, proved impractical. Pressure bomb reactions were suitable for the preparation of small quantities of [2] but a more general procedure was developed that was much more practical for large scale preparations. Following the recommendations of Porai-Koshits and Kharkharov (37), diphenylamine, dry zinc chloride and acetic anhydride were refluxed at ca. 180° for 5 - 10 hrs with mechanical stirring and then the temperature was slowly raised by distillation of the acetic acid to ca. 240° for ca. 1/2 hr. As the mass was allowed to cool to ca. 150°, 80% glacial acetic acid was cautiously added to the melt in a sufficient quantity to maintain a pourable mixture as the temperature was further cooled. As the temperature reached ca. 60 - 80°, the melt was slowly added to a large quantity of vigorously stirred ethyl acetate. This step is the key to the successful workup of the reaction mixture because the soluble tar components, diphenylamine and diphenylamine derivatives are removed in the ethyl acetate layer which is discarded. The acid layer was filtered to remove the zinc salts, neutralized with ammonium hydroxide and the product was extracted into chloroform. The crude product was then purified by recrystallization from toluene and column chromatography on TLC

grade silica gel using dichloromethane to elute off diphenylamine and diphenylamine derivatives and dichloromethane–acetone (1–5%) as the eluent for [2]. Recrystallization from hexane was then used to finally complete the purification procedure.

A variety of approaches to the Bernthsen synthesis were used in our laboratory at various times with yields from 5 – 40%. In retrospect, the use of the modified workup procedure described above could be used with any of these approaches with less problems and giving a product of better purity. These reactions, although somewhat low yielding, can be easily scaled up to give the 5 – 10 gm of pure [2] needed for this study.

The 9–bromomethylacridine [1] alkylating reagent which was used to prepare many of the desired derivatives was prepared from [2] by the method of Campbell et al. (6) (scheme III).

Scheme III

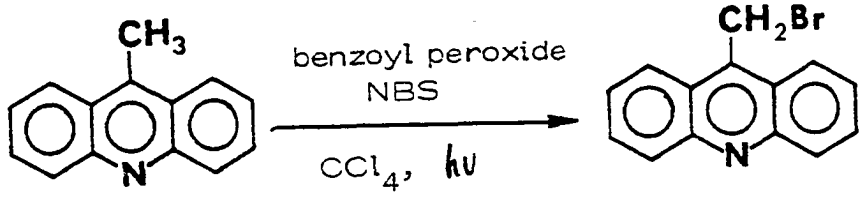

Attempts to prepare 9–acridinylmethanol [4] from [1] using potassium hydroxide in tetrahydrofuran were unsuccessful. However, the alcohol can be prepared in good yield (ca. 65%) from 9–acridinylmethyl acetate (scheme IV).

Scheme IV

$$Acr-CH_2-Br \xrightarrow[\text{acetate}]{\text{sodium}} Acr-CH_2-OOCCH_3 \xrightarrow{NaOH} Acr-CH_2-OH$$

The methyl and ethyl ethers were prepared from [1] by slowly adding the sodium alkoxide to a solution of [1] in alcohol over a 2 hr period. The presence of excess base, as shown by adding [1] to the alkoxide, results in decomposition of the product. Furthermore, the differences in stability of the methyl and ethyl ethers were described in Part I. The fact that the ether(s) could be prepared by using a strong base as a nucleophile whereas the alcohol could not, may be due to two factors. Because of the insolubility of [1] in basic water, only a limited quantity of water could be added to the tetrahydrofuran solution of [1] and hence the differences in the solvent characteristics for the reaction may be responsible for the failure of hydroxide to give a product whereas the alkoxides do. On the other hand, the facile reaction of sodium acetate with [1] would suggest that there is a competition between the displacement reaction and proton abstraction when strong bases are used and the alkoxides give products because, although they are slightly stronger bases than hydroxide, they are also better nucleophiles and displacement reaction proceeds much faster than proton extraction.

The difficulties of using strong bases with 9-methylacridine derivatives was further exemplified during attempts to prepare a

tosylate from [4]. Attempts to pre-form the alkoxide of [4] by NaH, n-BuLi or sodium metal followed by reaction with tosyl chloride resulted in decomposition of the starting material with very little desired tosylate being formed. The tosylate was evident by TLC examination throughout the course of the reaction, however, it appeared that decomposition prevented any significant accumulation of product. Since base catalyzed decomposition was a real possibility, other approaches that did not involve strong bases were attempted (scheme V).

Scheme V

A. $Acr-CH_2-OH \xrightarrow[\text{tosyl chloride}]{\text{lutadine}} Acr-CH_2-O\,Ts$ (38)

B. $Acr-CH_2-OH \xrightarrow[AgOTs]{CH_3CN} Acr-CH_2-O\,Ts$ (39)

These approaches generated small amounts of product which decomposed during the workup procedure. The instability of the tosylate, which has also been demonstrated for many analogous benzyl derivatives (39), indicated that it would not be a desirable alternative to the bromide [1] as an alkylating reagent. An attempt was made to prepare the sulfinate ester, which has proved useful as an alternative to tosylates in other cases where the tosylate is unstable (40). However, initial efforts in this area were not productive and this area of investigation was terminated.

The analytical (41, 42) as well as the preparative quaternization reaction (scheme VI) is quite sensitive to the reaction conditions

Scheme VI

$$Acr-CH_2-Br + \dot{N}R_3 \longrightarrow Acr-CH_2-\overset{+}{N}R_3\ Br^-$$

employed. Previous results (43) from our laboratory had indicated that acetonitrile was the solvent of choice for the quaternization reaction. The major differences observed for various solvents were the yield of quaternary from the reaction and the presence of polar side products which made purification of the quaternary difficult. A general procedure was adopted for the preparative quaternization reaction. The tertiary amine was added to a hot, nearly saturated solution of 9-bromomethyl-acridine [1] in acetonitrile. A 50% molar excess of [1] is used to ensure complete reaction of the tertiary amine since the presence of unreacted amine makes purification of the product very difficult in many instances. The reaction mixture is set in the dark at room temperature for 24 hr and then in the freezer (-20°) for 24 hr. Under these conditions, most quaternary salts crystallize out of the reaction mixture and after washing with a minimum volume of ether–acetone (1:1) are sufficiently pure for most uses. The quaternaries could be further purified by recrystallization from acetonitrile–methanol (ca. 10:1).

A number of quaternary salts of tertiary amine drugs were prepared. The structures of the tertiary amines are shown in Figure 6. Although the chemical and spectral properties of the quaternary salts derived from [1] were generally quite similar, certain notable exceptions were found. For example, only the quaternary salt derived from

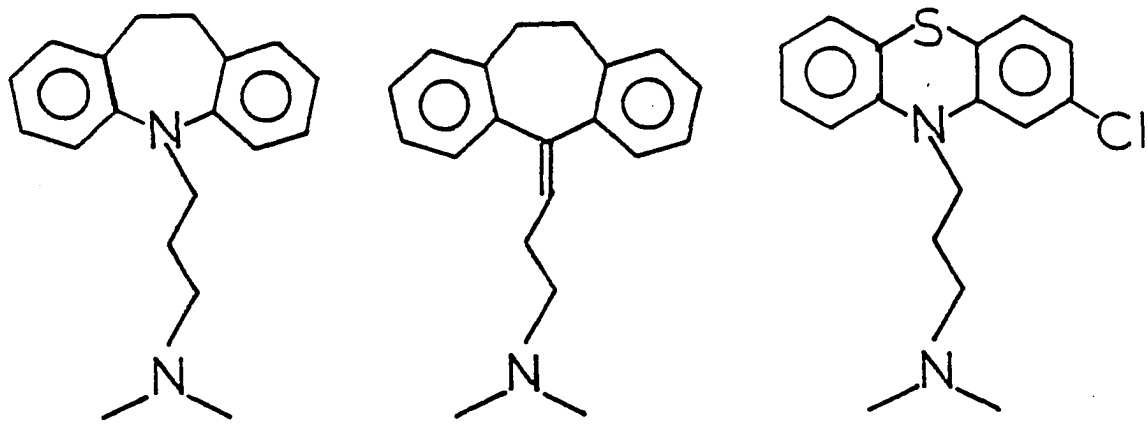

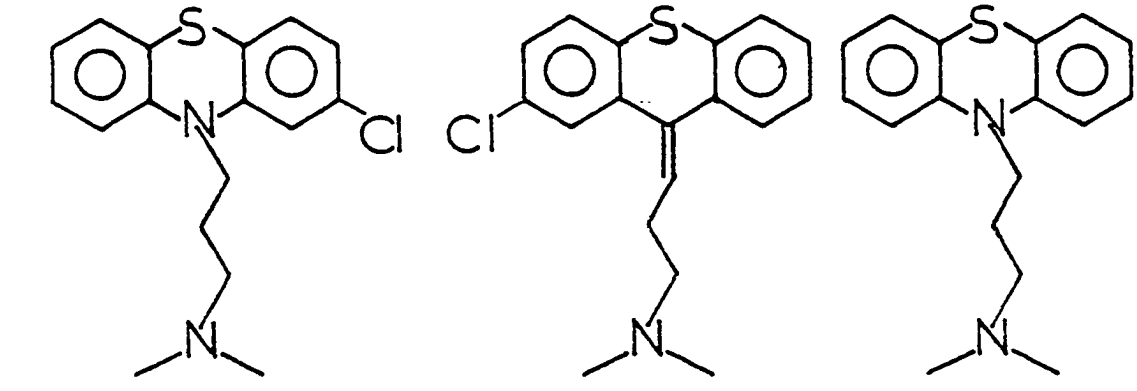

Figure 6. Tertiary amine drugs used to prepare quaternary salts for chemical and spectral characterization.

imipramine [28] was found to possess significant fluorescence in 12 N H_2SO_4 (see Part II, Table 12). The fluorescence characterization of the quaternary salts will be discussed in detail in the next chapter.

The NMR spectrum of the amitriptyline quaternary [29] proved to be unique among the derivatives investigated. The NMR spectrum of the chlorpromazine quaternary [15] (Figure 7) was typical of all of the other derivatives investigated in that the N,N-dimethyl signal at ca. 3.2 delta was a sharp singlet. On the other hand, the N,N-dimethyl

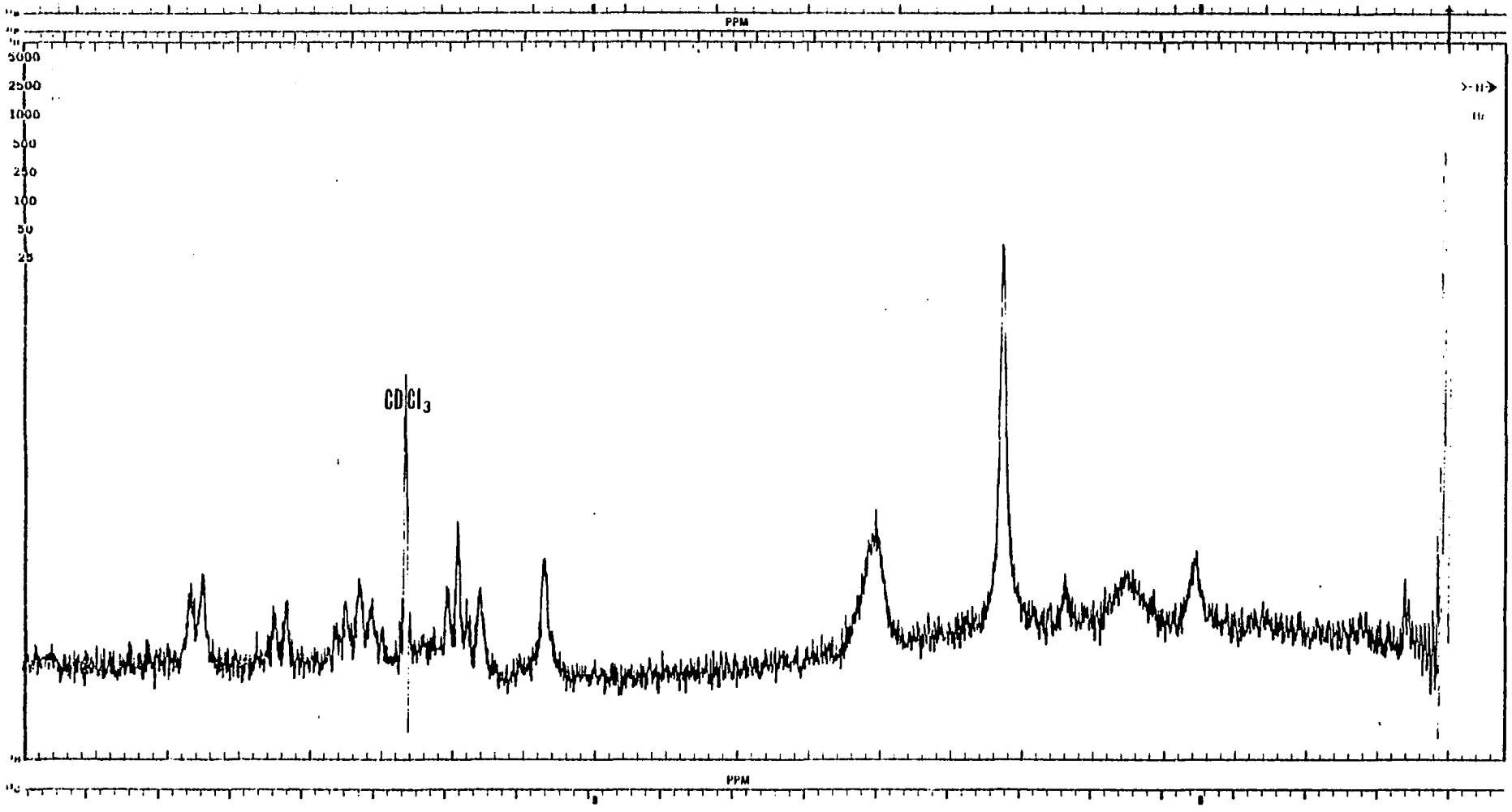

Figure 7. 100 MHz PMR ($CDCl_3$) of the chlorpromazine quaternary salt [15].

signal for the amitriptyline quaternary [29] was a broad doublet centered at ca. 3.2 delta at room temperature (Figure 8). As the temperature was raised (Figure 9), the doublet collapsed to a sharp singlet at 80° which reverted back to a doublet as the temperature was lowered back to room temperature. These data indicated that a barrier to conformational equilibration exists at room temperature. That barrier can be estimated at ca. 16.5 Kcal by using the following equation (102):

$$\Delta G_c^{\pm} = 2.3\ RT_c\ [10.32 + \log\ T_c/k_c]$$

where T_c is the coalescence temperature and the rate of interconversion, $k_c = \pi\ \delta\nu/\sqrt{2}$ (103). The most plausible explanation for this observation is a pseudo chair–boat interconversion in the dibenzocycloheptenyl ring which results in the N,N-dimethyl groups being in different magnetic environments in each conformation. The failure of the methylene protons in the cycloheptene ring to give a singlet signal (which is observed for the analogous imipramine quaternary (Figure 30) further supports this explanation for the NMR results.

One aspect which created considerable difficulty in dealing with the quaternary salts was their chromatographic behavior. These salts are mobile on silica gel plates when using a number of solvents such as n-butanol–acetic acid–water (5:1:4), chloroform–methanol–benzene–ammonium hydroxide (8:17.5:5:2.5) and acetonitrile–water (9:1). However, an assumably pure quaternary salt sample may give

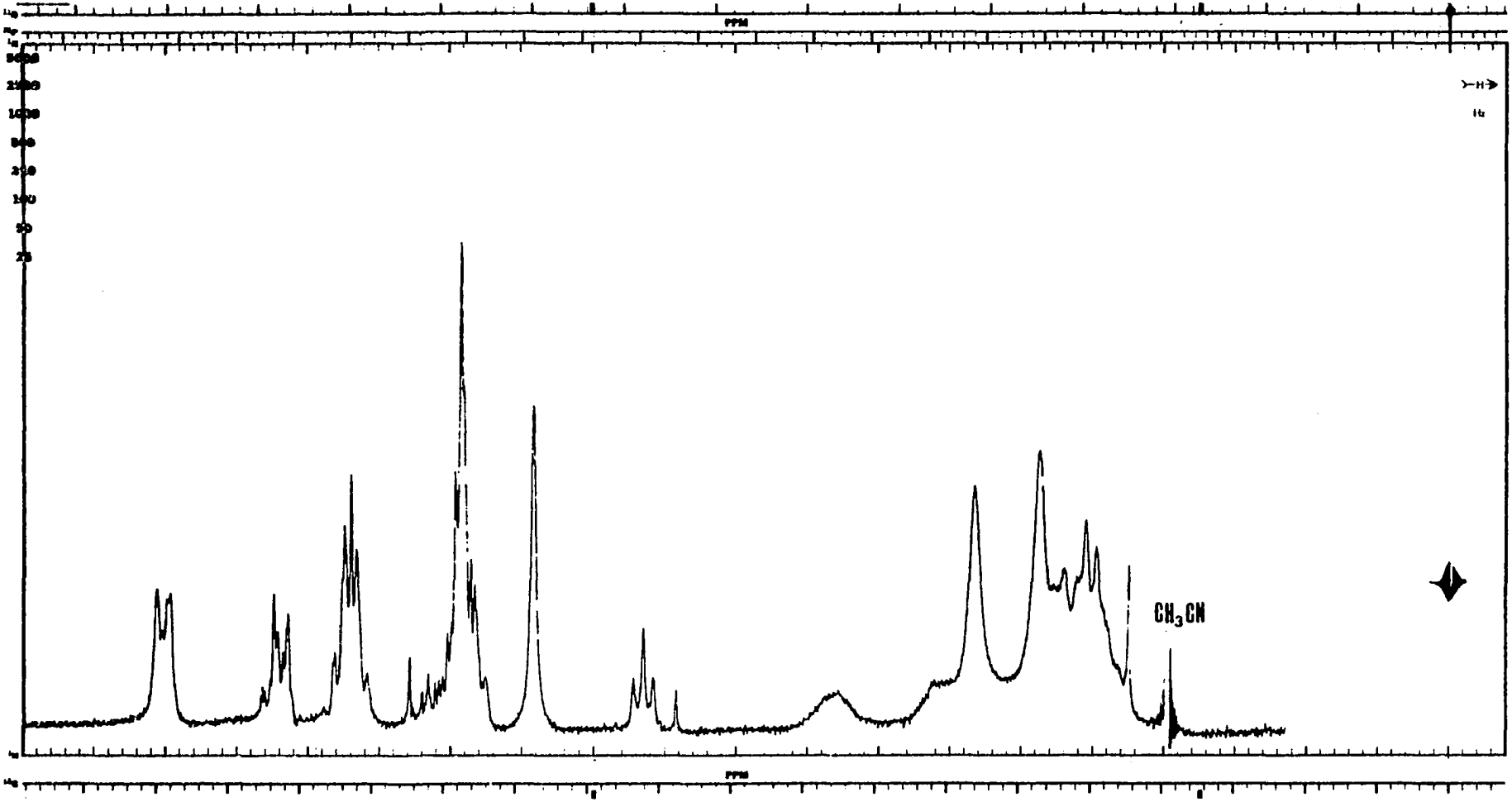

Figure 8. 100 MHz PMR ($CDCl_3$) of the amitriptyline quaternary [29] at room temperature.

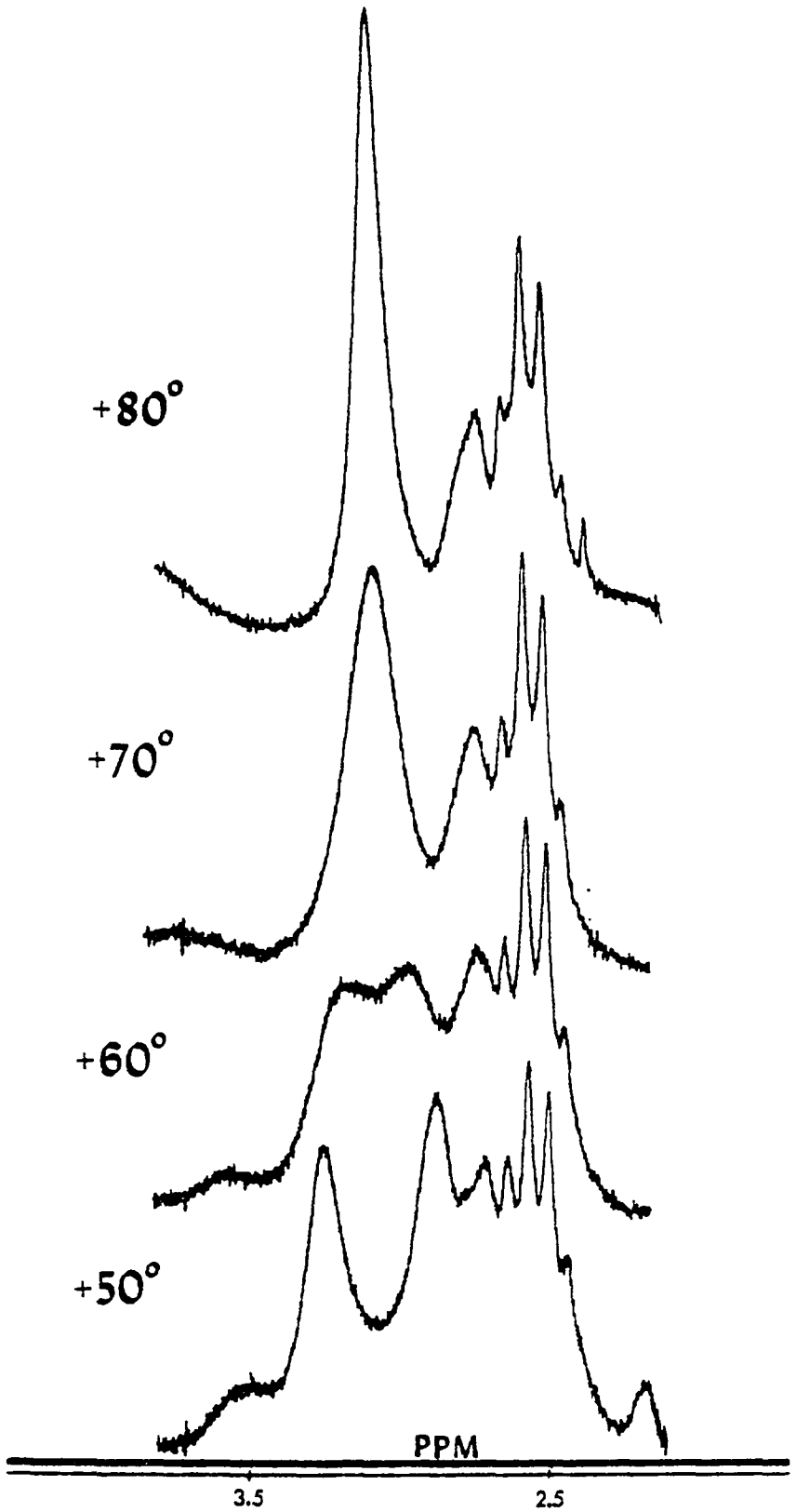

Figure 9. The effect of temperature on the N,N-dimethyl PMR signal of [29].

from 1 to 3 distinct TLC spots depending upon the manner in which the TLC plate was handled during spotting, drying and development. At the present time, although the application to the TLC plate may be responsible for certain amounts of degradation, the cause of multiple spots appears to be relative to parameters such as the solvent used for spotting and the manner in which that plate was dried. Furthermore, two dimensional chromatography indicated that even when a quaternary produces multiple spots, each of those can in turn generate all of the other observed spots. The variability of the chromatographic behavior has also been confirmed during the standardization of the analytical procedure. Even under apparently identical conditions, various spotted samples behaved differently. Work in this area is continuing in attempts to understand this phenomenum.

Another area of general concern was the development of good criteria for purity of the samples to be used for the fluorometric and photochemical studies. The problem of assuming compound purity based on literature reports is best exemplified in the case of 9-methylacridine prepared by Bernthsen synthesis. Certain reports (37) indicated that up to a 70% yield was obtained. However, the product obtained which melted at 94-96° is now known to be a 1:1 complex of 9-methylacridine and diphenylamine (35). TLC of the complex gives spots for both diphenylamine and 9-methylacridine. For this study, the TLC behavior of the products prepared was a primary criterion of

product purity. This was important because fluorescent impurities which could be the most damaging to the fluorescent characterization studies could be easily identified even in cases where other spectroscopic or physical evidence such as NMR, MS or IR spectra or melting point would not be particularly sensitive to low levels of fluorescent impurities.

One particularly difficult compound to prepare and purify according to reported methods was 9-acridinecarboxylic acid [9]. A number of routes leading to this product were available:

Scheme VII(44)

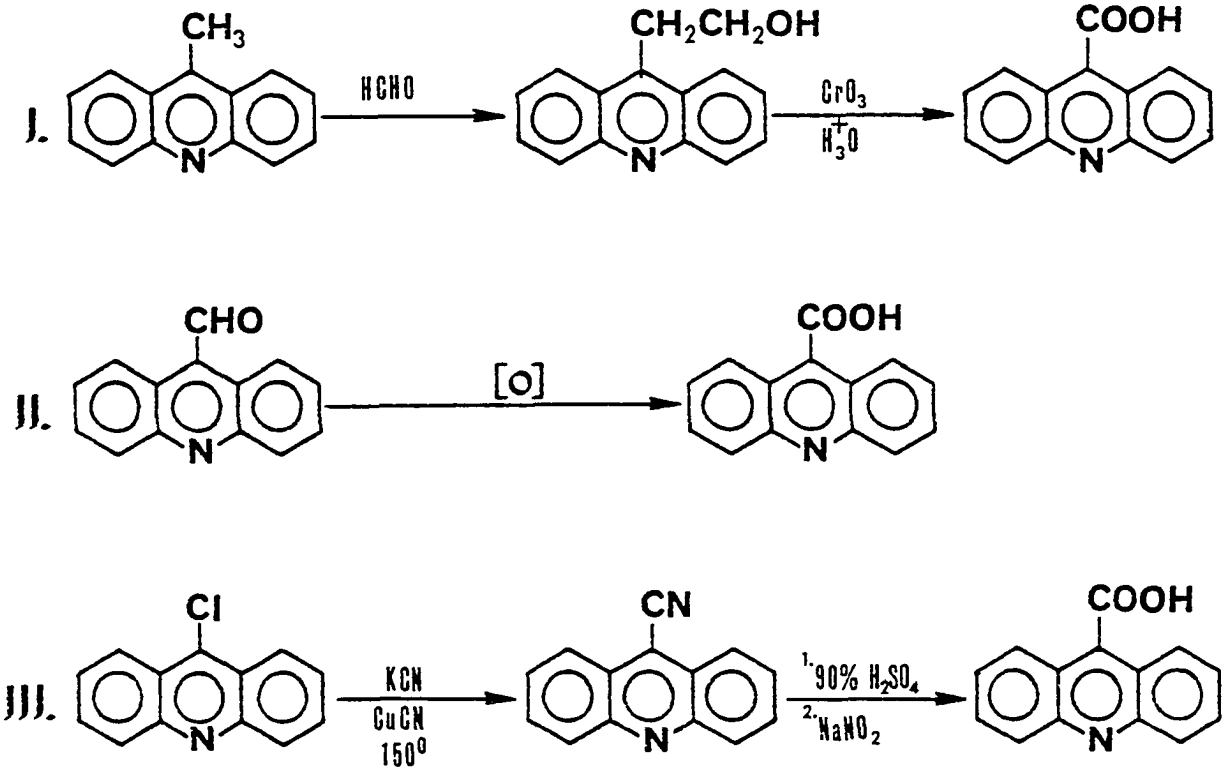

The route via 9(β -hydroxyethyl) acridine (route I) yielded crude acid [9]; however, repeated attempts by recrystallization to obtain a sample uncontaminated by acridine byproducts having R_f values less than [9] in acetonitrile-H_2O (9:1) were unsuccessful. In fact, the crude product obtained by route III appeared cleaner by TLC than the previously obtained recrystallized product. However, even this sample could not be purified to a point where only a single spot was observed in TLC.

In general, purification of acridine compounds poses an interesting problem. Many derivatives such as 9-acridinylmethanol [4], acridone [8], 9-acridinylcarboxylic acid [9] and the quaternary salts are sparingly soluble in common laboratory solvents and are very difficult to handle and purify by crystallization. Recrystallization of some acridine derivatives is an ineffective method of purification because of co-crystallization of complexes between the desired product and impurities. For this reason, preliminary separations such as short column chromatography, sublimation or controlled pH extraction can prove quite useful in removing significant amounts of impurities leaving a semi-purified sample that can then be purified by crystallization. These observations also explain why changing to a different synthetic approach can give samples that are easier to purify. In most cases, the key to a successful synthetic approach was the development of satisfactory purification procedures. Specific procedures for individual compounds are described in the Experimental Section.

CHAPTER 3

RESULTS AND DISCUSSION: SPECTRAL CHARACTERISTICS OF ACRIDINE DERIVATIVES

The initial observation that led to the study of the spectral characteristics of 9-substituted acridines was the apparent non-fluorescence of the quaternary ammonium adduct derived from chlorpromazine [16] and 9-bromomethylacridine [1]. The first step chosen for investigating the mechanism of quenching of the acridine fluorescence was to determine the luminescence characteristics of various 9-substituted compounds. Such studies have been often used to investigate the mechanistic aspects of certain chemical and spectral observations.

The dependence of acridine fluorescence quantum yield on the environment has previously been documented (25, 26, 27). Using these studies as a guide, an examination of the effect of solvent, pH and other environmental factors on fluorescence was undertaken for selected derivatives. Based on these results, standard conditions were established for the fluorescence characterization of the other derivatives. Acridine [20], 9-methylacridine [2] and (9-acridinylmethyl)

trimethylammonium bromide [10] were used for the initial standardization experiments.

The fluorescence characteristics of acridines, and particularly the observed quantum yield, strongly depend on the solvent medium. Figure 10 shows the relationship between the relative fluorescence

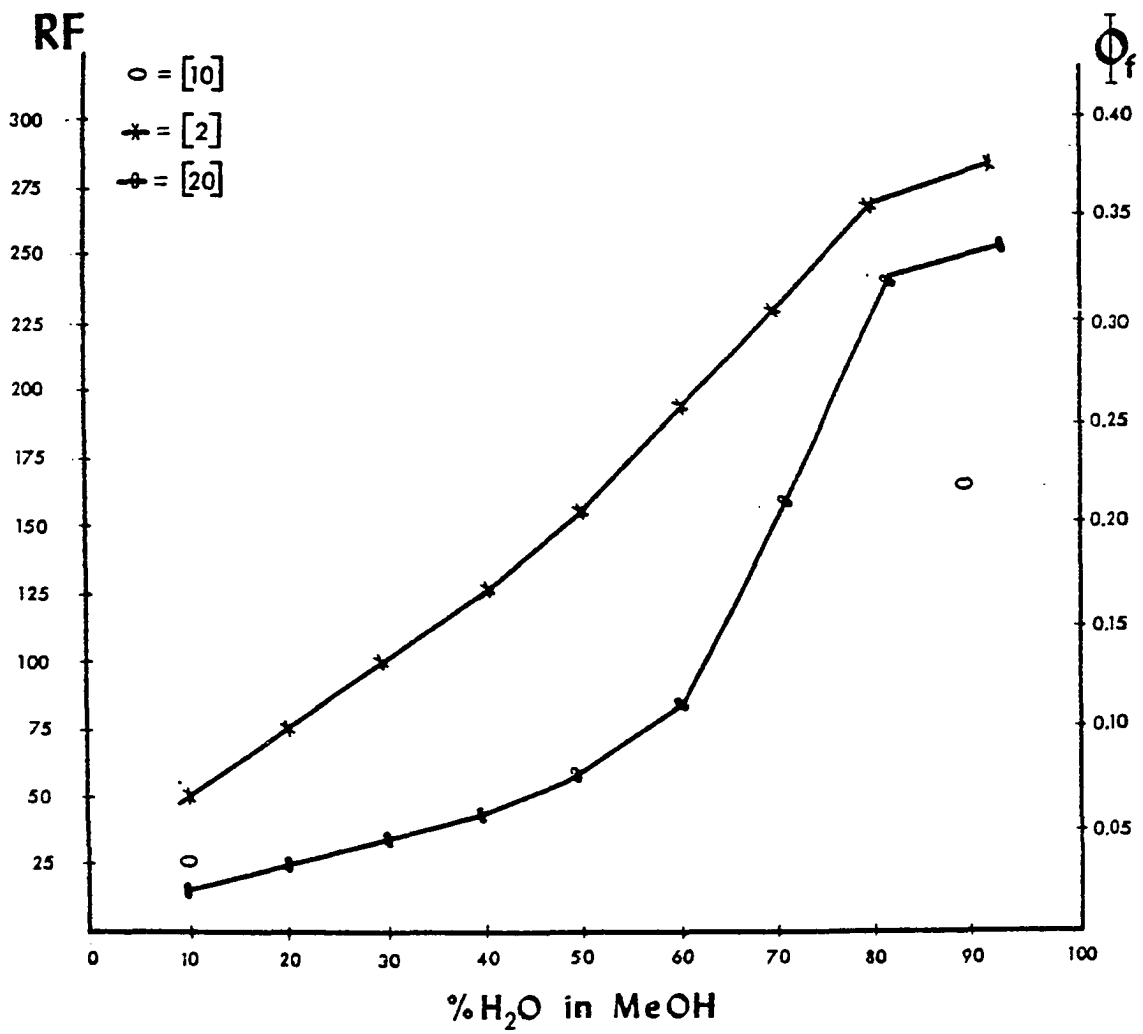

Figure 10. Relative fluorescence (RF) of 9-methylacridine [2] and (9-acridinylmethyl)trimethylammonium bromide [10] in aqueous methanol compared to the reported quantum yield (Φ_f) (27) of acridine [20].

observed for 9-methylacridine [2] versus the percent water in the solvent and the reported quantum yield for acridine [20] (27). 9-methylacridine appears to have a slightly higher quantum yield particularly at lower percentages of water in the solvent. This comparison allows one to make an estimate of the quantum yield for 9-methylacridine which, although not experimentally measured in this study, should be within 0.05 of the 0.34 reported for acridine (27) when the solvent contains 90% water. Subsequent fluorescence measurements were made in aqueous methanolic solutions of various compositions in order to determine the fluorescence characteristics of the various substrates.

The quantum yield for the acridinium cation has been measured to be 0.54 (27). It is this molecular species that is of primary interest due to its higher quantum yield relative to that of the neutral species. The ground state pKa of acridine is 5.5 but the excited state is much more basic with a pKa of approximately 10.6 (45). The red shifted fluorescence (λ max = 474 nm) of the acridinium cation becomes obvious at a pH of about 7 and protonation is complete around pH 3.5 (46). However, it was obvious early in the study that certain derivatives, such as the (9-acridinylmethyl) trimethylammonium quaternary, were much less basic than unsubstituted acridine. No fluorescence typical of the protonated species could be observed in 0.01 N H_2SO_4. However, as the concentration of acid is increased,

the expected fluorescence is observed and reaches a maximum in about 12 N H_2SO_4. The profile of fluorescence intensity versus acid concentration for [10] is given in Figure 12. Therefore, the fluorescence was determined in both 0.01 N and 12 N acid solutions to ensure that maximum protonation was obtained.

Uncorrected excitation and emission spectra for 9-methylacridine are given in Figure 11. The raw spectral data obtained are adequate for a study such as this provided that the limitations of using

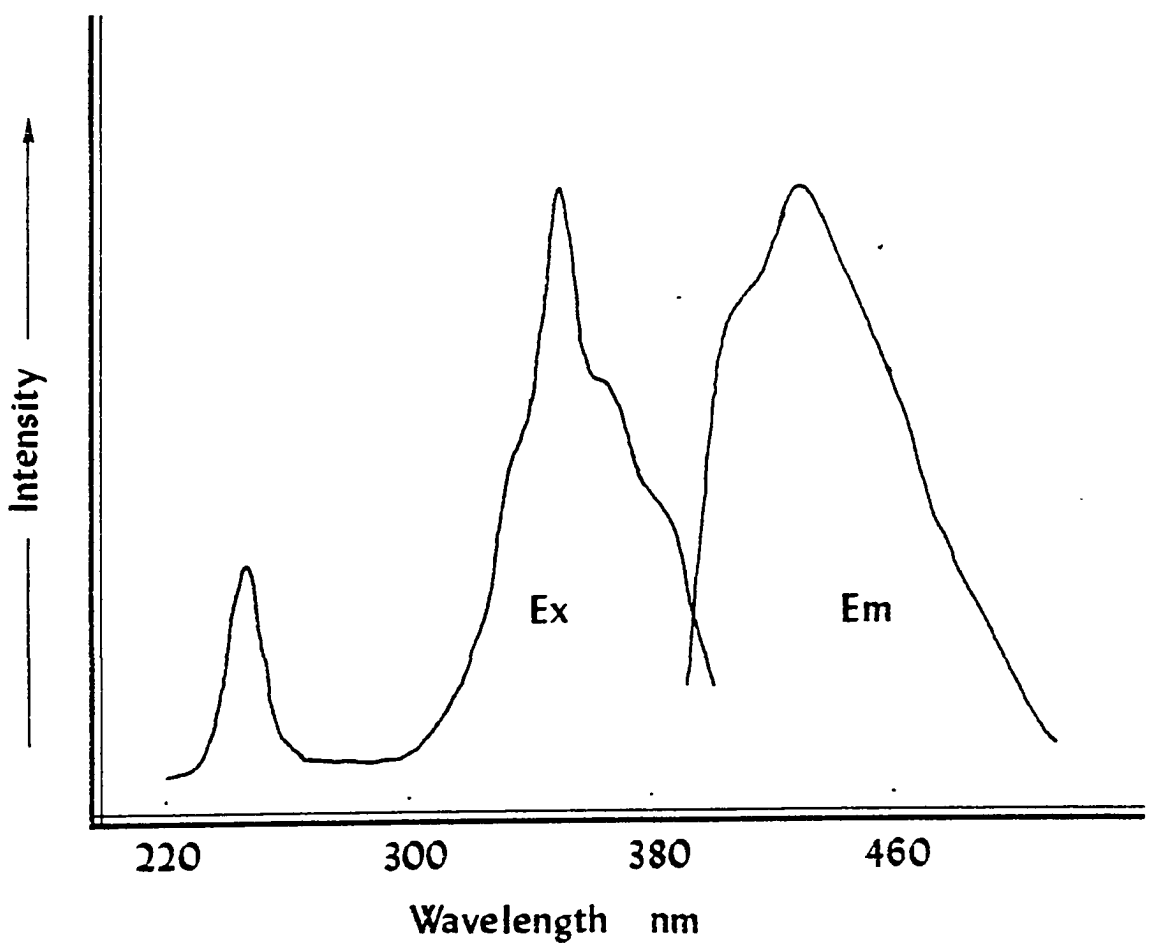

Figure 11. Fluorescence excitation and emission spectrum of 9-methylacridine in water.

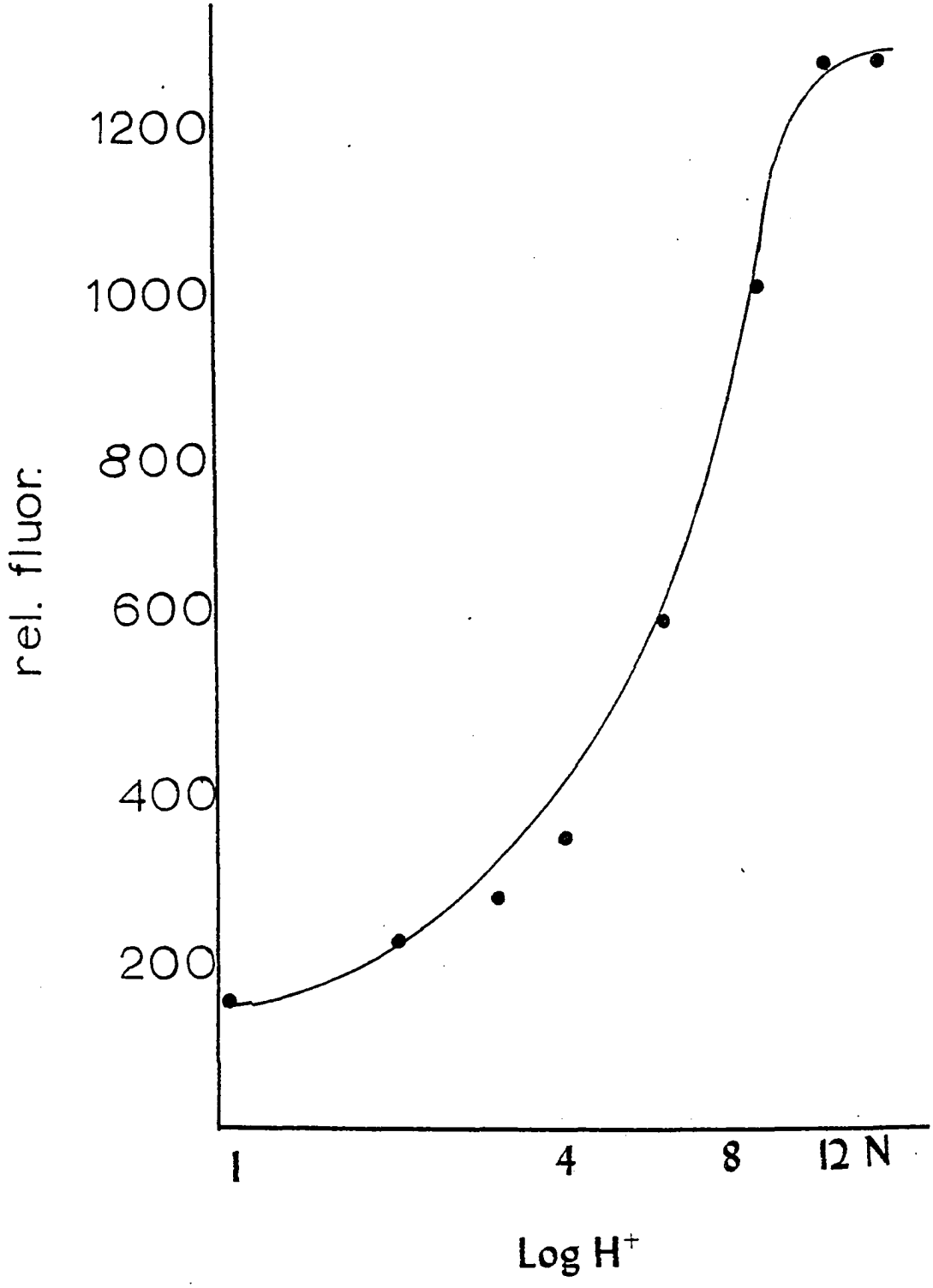

Figure 12. The effect of acid concentration on the fluorescence of (9-acridinylmethyl) trimethylammonium bromide [10].

such spectra are recognized. To obtain a corrected spectrum, there are a number of factors that must be considered. The three most important parameters which vary with wavelength and must be considered in the normalization process are: the intensity of exciting light (Figure 13) (49), attenuation due to the monochromator (Figure 14) (50) and system geometry, and the photomultiplier response. The

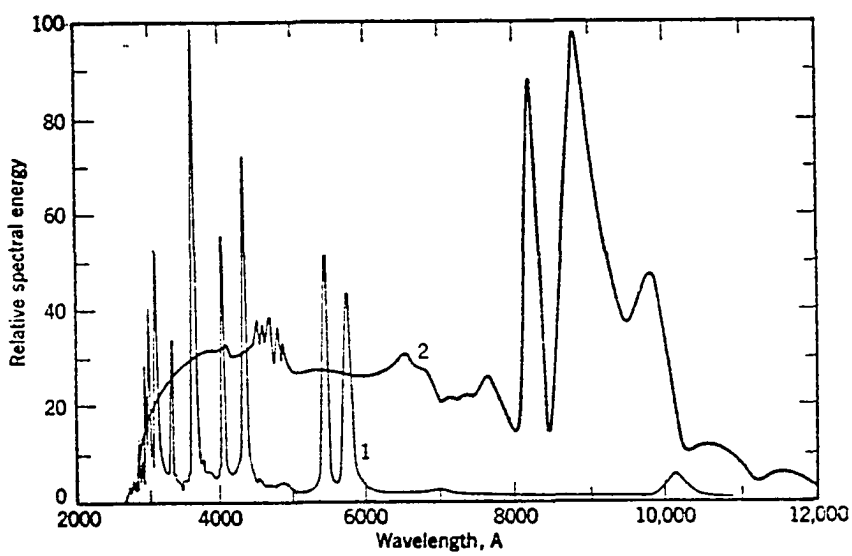

Figure 13. The energy distribution from two types of commercial point-source lamps. Curve 1 was obtained from the mercury HBO 200 lamp of Osram (Germany); curve 2, from the xenon X-75 lamp of PEK, Inc. (49).

fine structure observed in the emission spectrum also varies with the experimental parameters chosen such as slit width, concentration, solvent and temperature.

Since the emission spectra for the derivatives investigated covered only a narrow spectral range and were not significantly different, no major corrections were necessary for spectral

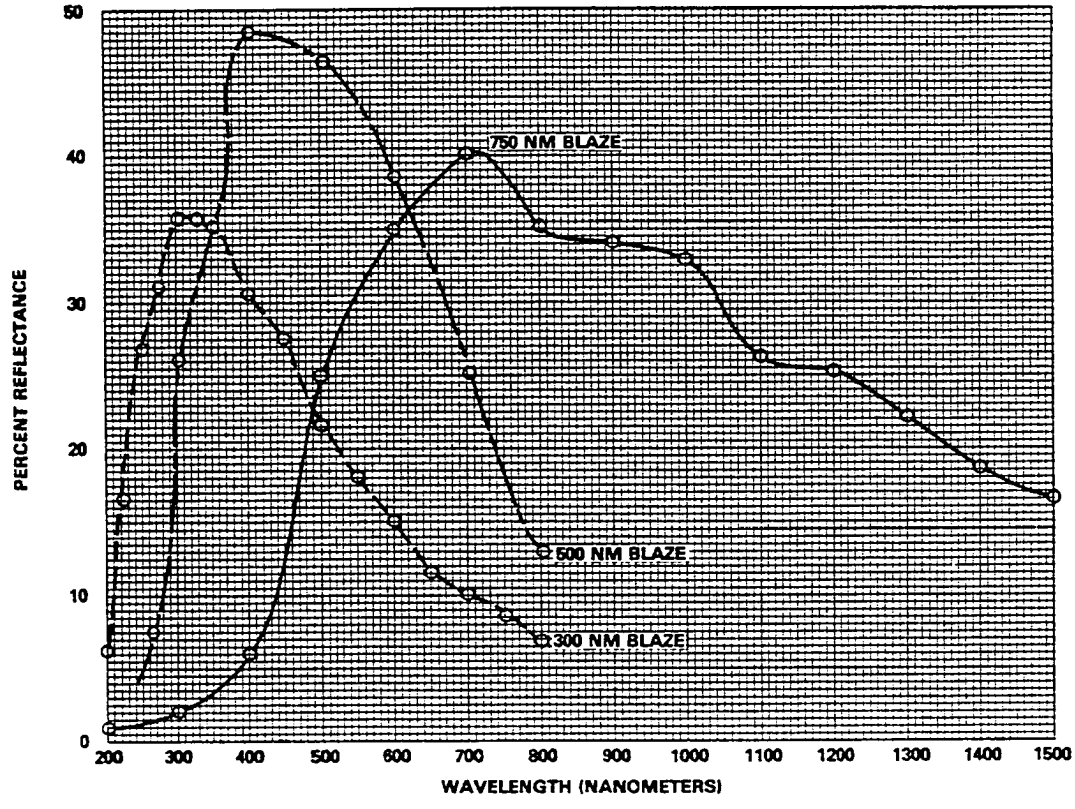

Figure 14. Reflectance curves for spectrofluorometer gratings. The maximum output occurs at the cited blaze wavelength (50).

interpretation. Of a major concern in this study were the differences in the fluorescence intensity observed from excitation at the long and short wavelength maxima.

The rate of fluorescence is given by (48):

$$I_f = [I_o(1-10^{\epsilon cl})\,\phi_f]$$

I_f = total fluorescence emitted per unit time
I_o = total flux of exciting light
c = concentration of solute
l = optical depth of solution (cm)
ϵ = molar extinction coefficient of the solute
ϕ_f = quantum yield of fluorescence.

Since previous studies (47) have indicated that the fluorescence quantum yield for acridine derivatives is independent of the excitation wavelength,

then log I_f should be proportional to ϵ if ϕ_f is independent of wavelength and I_o is constant as the wavelength of exciting light is varied. The molar extinction coefficient for 9-methylacridine is 170,000 and 8,200 at 252 nm and 355 nm respectively (see Figure 15) and clearly the fluorescence excitation spectrum presented in Figure 12 does not reflect this relationship. The differences must be related to instrumental characteristics and the ratio of peak heights are generally much different in the corrected spectrum from those in the uncorrected spectrum, particularly at wavelengths below 300 nm (Figure 16) (51), since the output of the Xenon lamp is over 4 times greater at 350 nm than at 250 nm (51). Also, the air medium significantly attenuates the exciting source at wavelengths below 300 nm. From a purely analytical point of view, where detection of very low levels of fluorescence is required, the loss of an order of magnitude of detectibility due to instrumental design factors should be re-examined. Such an instrument would use a light source that has a more intense UV emission at the excitation wavelength desired, and would use a monochromator scribed for maximum efficiency at 250 nm. Secondly, the whole excitation mechanism should be enclosed in a vacuum chamber with a quartz window to minimize air attenuation. The use of a photon counter (50) rather than the normal photomultiplier for luminescence detection would further increase sensitivity and reduce the problems of background fluorescence which is more troublesome when the shorter excitation wavelength is used.

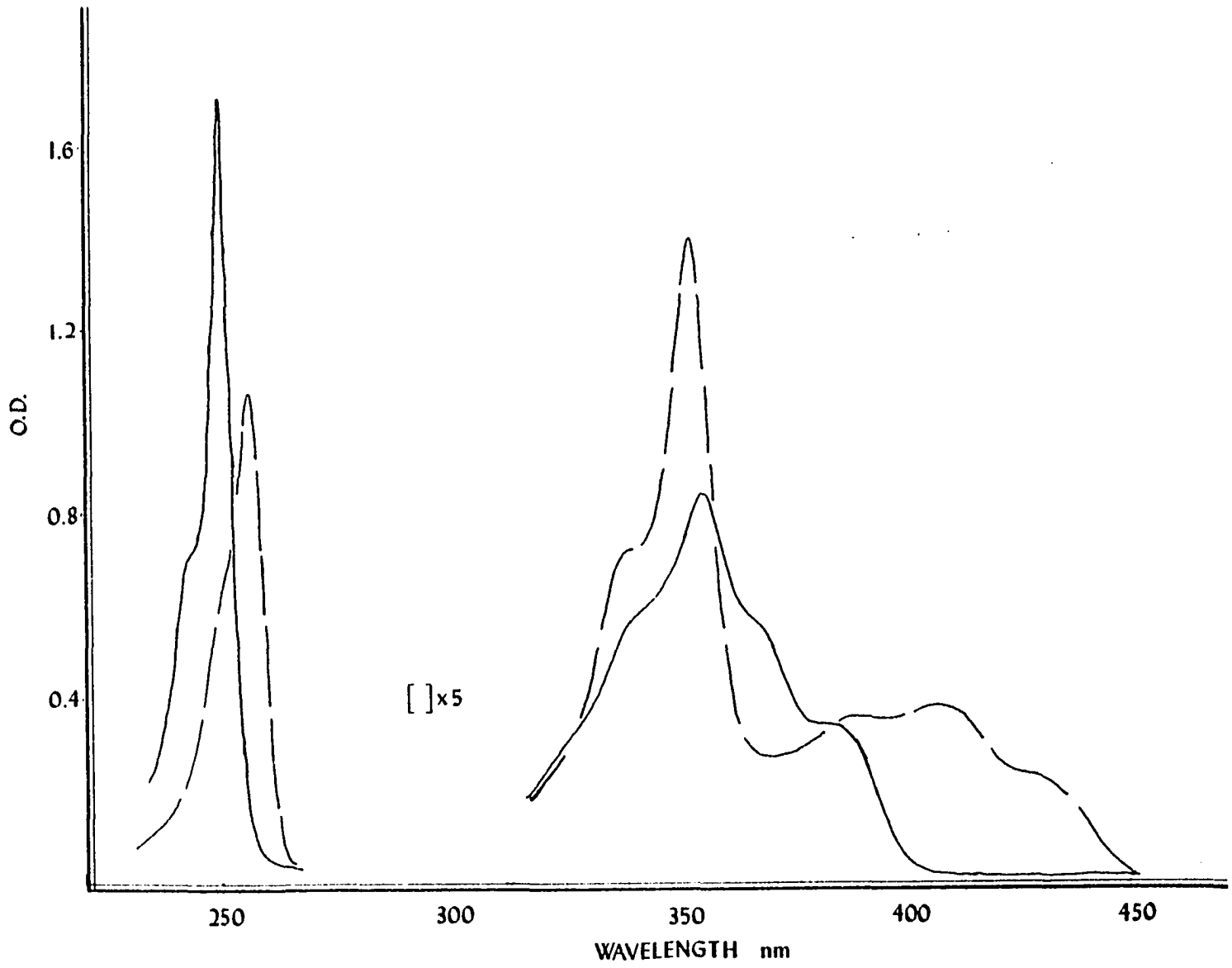

Figure 15. Absprotion spectra for 9-methylacridine [2] in ethanol (——) and ethanolic 2 N H_2SO_4 (----). Long wavelength measurements were made on solutions 5 times more concentrated than those used for the short wavelength measurements.

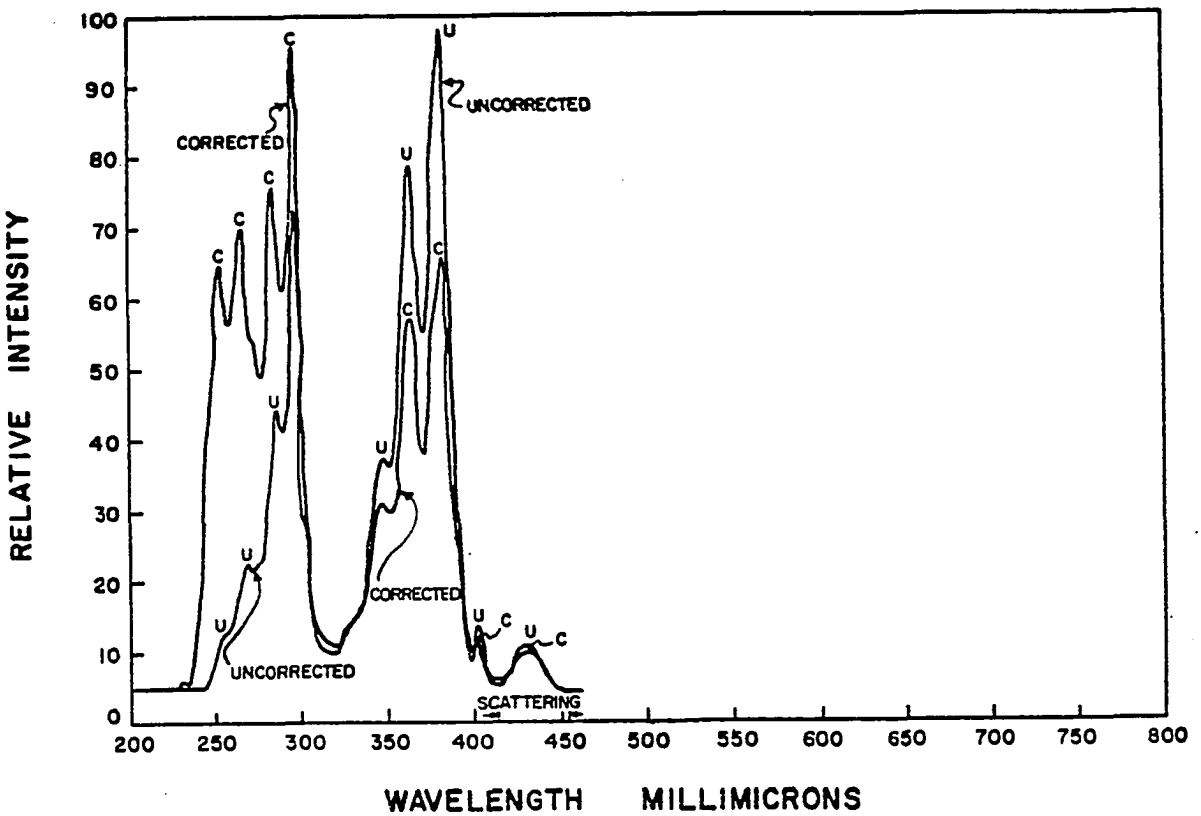

Figure 16. Energy corrected excitation spectrum of benzopyrene in ethanol. The peaks marked "C" are those of the corrected spectrum and those marked "U" are of the uncorrected spectrum (51).

Short of the development of such a special purpose analytical fluorometer, most commercial instruments, when used as fluorometric detectors, are as sensitive at the long wavelength absorption as at the short wavelength absorption even though the latter has a 10-fold greater absorptivity.

Another environmental factor which potentially could have an effect on the observed quantum yield is the use of oxygenated solvents. Although acridine fluorescence is not generally considered to be quenched by oxygen, a recent report by Olmsted (55) indicated that a 100% oxygen atmosphere could cause quenching of fluorescence.

Although the magnitude of the effect is not reported, a Stern-Volmer relationship

$$Io/_I = 1 + kq\ \tau'[O_2]$$

where kq, the quenching constant, equals $1 \times 10^{10}\ M^{-1}$ sec (55); τ', the observed lifetime, equals 0.9 nsec (53); and $[O_2]$, the oxygen concentration, equals 8.9×10^{-3} M (56), can be used to determine the reduction in fluorescence intensity in the presence of the quencher. These data indicate that the intensity (I) in the presence of the oxygen was ca. 93% of that observed in the absence of the quencher. In our hands, a 100% oxygen atmosphere was found to have no quenching effect on the fluorescence of the 9-methylacridine or (9-acridinylmethyl) trimethylammonium bromide cation and neutral molecule. The cause of this observation could be a shortened fluorescence lifetime or a reduced quenching efficiency. Oxygen quenching of fluorescence has been used to determine the lifetimes of aromatic hydrocarbons (52) where quenching is usually diffusion controlled (57, 58). Although the reasons are not clear, the quenching efficiency can vary from the diffusion controlled rate of $3.1 \times 10^{10}\ M^{-1}$ sec $^{-1}$ (59) to rates much less than that (55). These observations are in agreement with the conclusions drawn in Part I, namely when excited state quenching occurs, the information can be quite useful; however, failure to observe quenching does not necessarily infer any information about the excited state lifetime.

The summary of the standardization experiments indicate that

the spectra should be determined in absolute methanol, water, 0.01 N H_2SO_4 and 12 N H_2SO_4. Deoxygenation is not important; however, in certain instances photolysis which increases fluorescence or changes the observed maximum can occur and readings were taken immediately and one minute later to check for photolysis. All fluorescence spectra were determined at the long wavelength excitation maximum.

The absorption and fluorescence characteristics of a number of 9-substituted acridines in methanol, water and acidic solvents are given in Tables 10-12 respectively. The results obtained with this

Table 10. Spectroscopic Characteristics for 9-acridinylmethyl Derivatives in Methanol

	UV Absorption		fluorescence		
Substituent	wavelength	ϵ	excitation	emission	RF
-H	355	8,200	355	420	2.2
-Ø	356	9,600	358	420	2.2
-OH	357	9,200	358	420	1.2
$-OOCCH_3$	359	9,100	358	420	0.7
$-\overset{+}{N}(CH_3)_3$	366	10,700	368	430	0.94
-Br	363	7,900	---[a]	---[a]	0.26
$-NO_2$	362	10,600	362	412,428	0.18

[a]Photochemically degrades too rapidly for spectral characterization.

limited group of derivatives indicates that the introduction of electron withdrawing substituents generally reduces the fluorescence yield and causes a bathochromic (red) shift in both absorption and fluorescence for the non-protonated hydrogen bonded fluorescing species in methanol and water. However, the magnitude of this effect does not correlate with generally accepted substituent constants (Table 13) (60).

Table 11. Spectroscopic Characteristics for 9-acridinylmethyl[c] Derivatives in Water

Substituent	UV Absorption wavelength	UV Absorption ϵ	Fluorescence excitation	Fluorescence emission	RF
-H	same as in Table 10		355	432	20.5
-Ø			358	432	17.2
-OH			358	432	15.8
$-OOCCH_3$			358	432	16.3
$-\overset{+}{N}(CH_3)_3$			368	440	11.6
-Br			---[a]	---[a]	1.4
$-NO_2$			366	420,438	0.06

[a] Photochemically degrades too rapidly for spectral characterization.

Table 12. Spectroscopic Characteristics of 9-acridinylmethyl Derivatives in Acidic Solvent

Substituent	UV Absorption[b] wavelength	UV Absorption[b] ϵ	Fluorescence excitation	Fluorescence emission	Rel. Fluor. $0.1 N H^+$	Rel. Fluor. $12.0 N H^+$
-H	352.5	13,800	352	480	41.1	41.1
-Ø	356.5	14,200	360	490	32.9	47.5
-OH	357	14,600	360	490	32.1	32.1
$-OOCCH_3$	360	15,000	360	490	31.7	33.1
$-\overset{+}{N}(CH_3)_3$	370	16,900	375	500	1.6	17.2
-Br	363.5	11,100	---[a]	---[a]	9.2	12.5
$-NO_2$	365	15,500	370	500	9.1	55.4

[a] Photochemically degrades too rapidly for spectral characterization.
[b] Absorption spectra obtained in ethanolic 2 N H_2SO_4.

c. 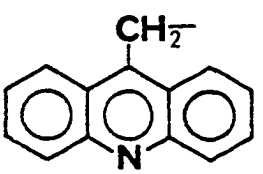

Table 13. Hammett Substituent Constants[a] for Selected Functional Groups (60)

Substituent	σ_R	σ_I
-H	0	0
-Ø	-0.11	0.10
-OH	-0.60	0.25
$-OOCCH_3$	-0.09	0.39
$-\overset{+}{N}(CH_3)_3$	0	0.86
-Br	-0.22	0.45
$-NO_2$	0.16	0.63

[a] The σ_I values are a relative measure of the effect caused by a given substituent if the effect were transmitted through sigma electrons whereas the σ_R value also includes the resonance effects.

For example, if the effects on fluorescence could be described by inductive effects, a dramatic difference between the methyl and acetate substituted compounds should be observed. On the other hand, if resonance effects were involved, there should be a large difference in the fluorescence of the alcohol and acetate derivatives. The only clear trend, as shown by the characteristic cation fluorescence, was the requirement of a higher acid concentration to effect ring nitrogen protonation for compounds substituted with electron withdrawing substituents.

One of the disappointing aspects of the structure-fluorescence study was the failure of the results to provide any reliable predictive power. For example, if the results in Table 12 were available for all compounds except (9-acridinylmethyl)trimethylammonium bromide [10], one would not predict the large relative fluorescence observed for [10] in water. Likewise, information on the same compounds in 12 N H_2SO_4

would not be useful in predicting the fluorescence characteristics of the nitro compound in that solvent either. One of the problems in describing the substituent effects on fluorescence for the above compounds exists because only inductive effects are operative for these compounds which have an alkyl methylene unit between the substituent and the aromatic ring system. No convenient valence bond (resonance) structures are useful in depicting the interaction. Furthermore, since the lone pair electrons on the ring nitrogen atom are formally orthogonal to the pi-system, sigma bond delocalization is the only way to describe the status of the lone pair electron density as well as the inductive effects of the substituents.

It must be noted, however, that even in other cases where resonance structures can be drawn, excited state behavior cannot be adequately described by this method. For example, pyridine itself is non-fluorescent but the introduction of electron donating substituents such as $-NH_2$ results in observable fluorescence (30). A similarity in the fluorescence characteristics was observed for the 2- and 3-derivatives (Table 6) (30) as well as distinct differences between the fluorescence of the 2- and 4- derivatives. Valence bond descriptions, which are useful in predicting ground state chemical properties, would suggest that the properties of the 2- and 4- derivatives should be similar. Clearly, the order of fluorescence activation due to the substituents, namely, 2>3>4, would have not been predicted by resonance

structures. Thus, these compounds exemplify the difficulty in using ground state resonance descriptions to describe excited state behavior. The mesomeric (charge-transfer) molecular orbital model more adequately describes the effects (61).

In a recent study, Bailey and Bailey (63) used CNDO molecular orbital calculations to obtain the one center core parameters to be used in PPP π-electron calculations for protonated aza-aromatics. These authors assumed that the changes in the sigma-framework caused by protonation could account for the spectral changes observed. The calculated results obtained led to a satisfactory interpretation of the experimental spectra. Similarly, such results would indicate that sigma framework changes could well account for the spectral alterations caused by various substituents. However, such a correlation does nothing more than suggest the plausibility of the proposed mechanism. It does not rule out other possible alternatives or provide a confirmed mechanistic model for the experimental observations.

The absorption spectrum of the 9-methylacridine free base and protonated species is given in Figure 15. The UV characteristics shown for 9-methylacridine are representative of the results obtained for all derivatives used in this study. It has been suggested (30) that the increased molar absorptivity of the long wave absorption upon protonation is due in part to a loss of n, π^* character (which has a very low absorptivity) in the π, π^* transition. Although this mechanistic

explanation is attractive, it is probably over-simplified in that the transition probability for the short wavelength transition is also very sensitive to substituent effects and protonation. This transition should have much less n , π^* character due to the greater energy difference between the states and thus the previous mechanistic explanation does not adequately explain the data.

In general, the UV characteristics can be summarized as follows: electron withdrawing substituents in the 9-position and protonation of the ring nitrogen tend to cause a red shift and a reduced molar extinction coefficient for the short wavelength transition. For the long wavelength absorption, the spectrum is red shifted by electron withdrawing substituents and the transition probability is increased by protonation. Also, a long wavelength shoulder appears in the spectrum of the protonated species.

The fluorescence characteristics discussed previously indicated that, although certain generalities are possible, the trends observed are not reliable enough to make predictions about particular derivatives. This observation is not surprising in light of the tremendous differences in fluorescence characteristics reported for all types of compounds and presented in the Introduction. The observed quantum yield, which is the variable of most interest from an analytical standpoint, is determined by the relative rates of the radiative and radiationless pathways. In the case of the acridines studied, the radiative transition probability can be

estimated from the UV absorption data (11) and does not vary enough to account for the differences in fluorescence observed. Of the critical parameters which determine the rates of the radiationless pathways, the energies of the $^1n, \pi^*$ and $^3n, \pi^*$ transitions are unknown because neither transition has to our knowledge ever been observed spectroscopically for any acridine derivatives. The energy of the second $^3\pi, \pi^*$ transition is also unknown and the spin-orbit coupling factors cannot be measured.

In addition to the 9-acridinylmethyl derivatives characterized in Tables 10 - 12, the fluorescence of certain 9-acridinyl derivatives (Table 14) in acidic methanol was recorded.

Table 14. Relative Fluorescence Values for Selected 9-acridinyl Derivatives in Acidic Solvents

Substituent	Relative Fluorescence 0.01 N H^+	12.0 N H^+
-H	9330	11050
$-CH_3$	12800	12800
$-OCH_3$	7000	7000
-CHO	7150	7350
p-tolyl	2080	3450

These fluorescence data indicated that the fluorescence intensity of most derivatives is within ± 20% of that of acridine except for certain notable exceptions which have very low fluorescence yields. The 9-(p-tolyl)acridine derivative was one such derivative where the low fluorescence intensity was unexpected particularly in light of the

results obtained for 9-(p-tolyl) anthracene which has a fluorescence quantum yield of 0.55 compared to 0.27 for unsubstituted anthracene (65). Even more confusing was the observation that the fluorescence intensity of 9-(p-tolyl) acridine in basic methanol is approximately twice that of 9-methylacridine.

We had hoped that this could be used as a tagging reagent after derivatization. In spite of the low fluorescence in acid of the parent compound, the bromide alkylating reagent [33] was made and reacted with chlorpromazine [16] because of the possibility of observing

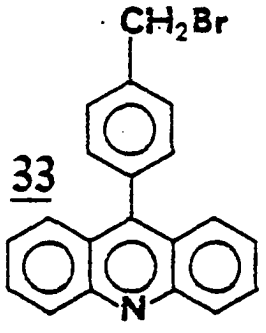

33

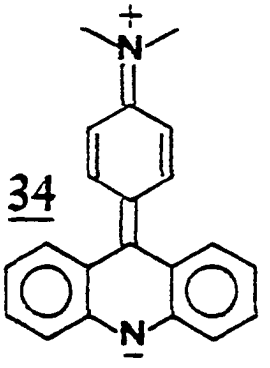

34

fluorescence in the quaternary salt. In the ground state, steric factors cause the π-system of phenyl group to be insulated from that of the acridine system. However, the quaternary salt derived from [33] and [16] was nonfluorescent and the failure of the phenyl ring to insulate the acridine nucleus from the effect of the quaternary nitrogen is not surprising since Albert (66) had previously observed that the spectral characteristics of 9-phenylacridines are consistent with conjugated resonance forms such as [34].

The difficulties in characterizing acridine excited states are

exemplified by studies of Tokumura et al. (64) who measured the amount of fluorescence, photoreduction and intersystem crossing (triplet production) occuring during flash photolysis. They found that ca. 45% of the singlet excited state could not be accounted for and its loss was ascribed to internal conversion. These results are quite different from the results obtained for anthracene derivatives where deactivation through fluorescence and intersystem crossing accounted for all of the singlet excited state produced.

In many cases, fluorescence represents only a minor pathway for excited state deactivation and therefore small changes in the rates of non-radiative transitions can result in large differences in the fluorescence yield. The non-spectroscopic nature of the transitions which seem to determine the yield of fluorescence makes systematic study of these parameters extremely difficult. Having concluded that the spectral characteristics of various 9-substituted acridines would not be particularly useful in understanding the fluorescence characteristics of the quaternary salts, a number of quaternary salts were prepared to investigate the relationship between the amine structure and the observed fluorescence. Based on the results previously discussed, the fluorescence of the quaternaries were determined in 12 N H_2SO_4 and the results are summarized in Table 15. The quaternaries were chosen for study based on previous reported structural features which might influence the fluorescence characteristics.

Table 15. Fluorescence Characteristics in 12 N H_2SO_4 in Methanol of Quaternary Salts Derived from 9-bromomethylacridine

Amine Compound	Relative Fluorescence
trimethylamine	5350
N,N-dimethyl -3-phenylpropylamine	5350
pyridine	5300
imipramine [a]	4800
amitriptyline	160
chlorpromazine	110
chlorpromazine sulfoxide	250
chlorprothixene	200
promazine	430

[a] for structures, see Figure 6, page 99.

The quaternary salts can be divided into two groups based on the relative fluorescence observed: Those that are approximately one-half as fluorescent as 9-methylacridine and those that are essentially non-fluorescent. Of the limited number of quaternaries derived from tricyclic amine drugs which were prepared and examined, only the imipramine quaternary possessed significant fluorescence. There are no apparent structural features which could be used to make a priori predictions as to the expected fluorescence characteristics of these quaternary salts. However, a promising quantitative fluorometric procedure appears possible for imipramine. This procedure would be twice as sensitive as the method developed for chlorpromazine and the other non-fluorescent quaternaries which must include the photolysis step. It appears that a productive area for further investigation would be the screening of a large number of tertiary amine drugs for which

quantification procedures are needed to identify those quaternaries which are fluorescent and thus good candidates for fluorometric quantitation. A rather simple quaternary salt synthesis procedure applicable to such a study was described in Chapter 2 which would facilitate the preparation of a large number of derivatives and thus make such a study quite feasible.

Heavy atom counterions have been implicated in fluorescence quenching mechanisms for 10-methylacridinium bromide [43] which

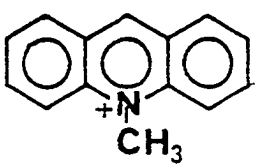

43

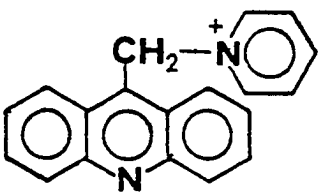

35

could be made fluorescent by changing the counterion to the perchlorate anion (67). Therefore, the perchlorate salt of [35] was made and its luminescence characteristics were determined. Since no differences in the fluorescence of the bromide or perchlorate salts of [35] were observed, it was concluded that the heavy atom quenching mechanism was not operative for these compounds. The preparation of the perchlorate salt of the chlorpromazine [15] was attempted to further confirm these results; however, the presence of silver salts decomposes [15] and thus the desired salt could not be obtained. It is interesting to note here that the anthracene analogue of [35], (9-anthranylmethyl)pyridinium

bromide, is nonfluorescent (68). After establishing that the fluorescence of anthracene is quenched at a diffusion controlled rate by N-methylpyridinium bromide, the authors concluded that the fluorescence quenching of the anthracene quaternary salt is not due to a specific substituent effect but rather a generalized collisional excited state deactivation process.

The presence of long alkyl chains which increase the vibrational degrees of freedom have been implicated as a factor affecting fluorescence characteristics (69). Also, fluorescence quenching due to intramolecular energy transfer between two chromophores connected by an alkyl chain has also been documented (70). Either one of these mechanisms could be operative in the case of the non-fluorescent quaternary adducts derived from tertiary amine drugs which are the primary thrust of this study. The quaternary salt [11], derived from the amine, N,N-dimethyl-3-phenylpropylamine was prepared as a model compound to help test this hypothesis. Since this compound had the same fluorescence characteristics as the trimethylamine derived quaternary [10], we can assume that the increased vibrational degrees of freedom do not contribute to the fluorescence quenching.

One interesting feature that exists for the N,N-dimethyl-3-phenylpropylamine quaternary [16] is the possibility of intramolecular energy transfer between the phenyl moiety and the acridine nucleus. If energy transfer were occuring, then the ratio of fluorescence intensity

observed for excitation at the long and short wavelength absorption maxima should decrease (Table 16). However, the range of ratios

Table 16. Fluorescence Characteristics of Selected Acridine Derivatives

Compound (solvent)	Relative Fluorescence Intensity Excitation Wavelength Short	Long	L/S Ratio
9-methylacridine (MeOH)	1.0	9.7	9.7
9-methylacridine (H_2O)	29.8	83.0	2.8
trimethylamine quaternary salt (H_2O)	5.4	38.5	7.1
N,N-dimethyl-3-phenylpropylamine quaternary salt (H_2O)	9.4	46.0	4.9
N,N-dimethyl-3-phenylpropylamine quaternary salt (MeOH)	0.06	1.3	21.7
1,2-bis(9-acridinylmethyl) ethane (H_2O)	0.3	0.4	1.3

observed prevents their utilization in experimentally confirming the hypothesis about energy transfer since 9-methylacridine and the trimethylamine quaternary should have had comparable ratios for making any meaningful comparisons with the N,N-dimethyl-3-phenylpropylamine quaternary. These data do, however, raise serious questions about the previous documentation (47) relating to the constancy of quantum yield as a function of excitation wavelength. Clearly, the dependence of the ratio on solvent type further supports the questions raised. Therefore, the experimental evidence obtained cannot be used to support the energy transfer hypothesis and raises more questions than it answers.

The most straightforward method of demonstrating that an

energy transfer mechanism is responsible for the fluorescence quenching in the tricyclic amine quaternaries would be the observation of luminescence characteristic of the non-acridine ring system following illumination of the acridine nucleus. Chlorpromazine has a weak fluorescence in basic aqueous solution at 460 nm (71). However, the chlorpromazine fluorescence has such a low quantum yield that it cannot be clearly observed due to the weak acridine-like fluorescence of the quaternary and the extremely rapid rate of photolysis which generates 9-methylacridine and further prevents any possible analysis of the chlorpromazine fluorescence.

The quantum yield of fluorescence observed from the phenothiazine nucleus is highly sensitive to the nature of the substituent in the 2-position. Of the derivatives readily available, those such as methiomeprazine [35] and thioridazine [36] which are 2-thiomethyl derivatives have the highest quantum yields of fluorescence (71). These derivatives were not made and investigated but it appears that a study of quaternary

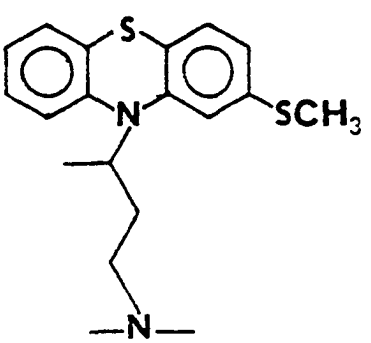

35

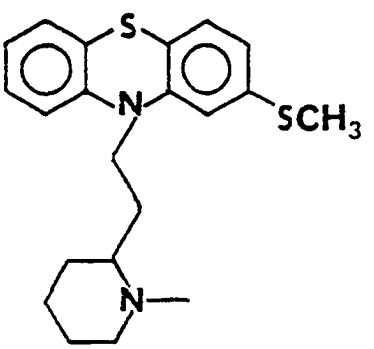

36

salts derived from these compounds could well provide information about an intramolecular energy transfer mechanism. Future work in this area using these and other derivatives should be pursued.

Another possible area of study which could be informative would be an investigation of the effect of the alkyl chain length on fluorescence characteristics. Such a study would require that the fluorescence characteristics of both fluorophores be clearly identifiable and could only be undertaken after the successful conclusion of the preceding proposed study. Such studies that investigate the relationship between transfer distance and energy transfer efficiency can be quite informative as to the mechansim of the singlet-singlet nonradiative electronic energy transfer. The proposed mechanisms and the critical parameters are presented in Table 17 (72).

Table 17. Singlet-Singlet Nonradiative Electronic Energy Transfer Mechanisms

Energy Transfer Mechanism	Distance Dependence	Comments
1. dipole-dipole transfer -Förster Mechansim	$1/R^6$	long range transfer over distances up to 50-100 Å which are present in 10^{-2}-10^{-3} M solutions
2. dipole-quadrapole transfer	$1/R^8$	intermediate range transfer with a probability of about a factor of 10 less than for the wholly allowed process above
3. exchange transfer -collisional transfer	$1/R^8$ complex	rate of transfer may not exceed the bimolecular diffusion controlled rate ($k_{diff} \sim 10^{10}$ liters/mole/sec); increasing the distance by 1 molecular diameter reduces the transfer probability by a factor of 100.

Forster's equation, also derived independently by Dexter, which gives the rate of intermolecular dipole-dipole transitions is (72):

$$k_{D^*\longrightarrow A} = \frac{9000 \ln 10 \, k^2 \, \phi_f}{128 \pi^6 n^4 N \tau_D R^6_{DA}} \int f_D(\nu) \epsilon_A(\nu) \frac{d\nu}{\nu^4}$$

where $k_{D^*\longrightarrow A}$ = the transfer rate constant

k^2 = the orientation factor (about 2/3)
ϕ_f = quantum yield of fluorescence of the donor
n = solvent refractive index
N = Avogardo's number
T_D = actual mean lifetime (sec) of the excited state
R_{DA} = intermolecular distance between donor and acceptor
$f_D(\nu)$ = spectral distribution of donor fluorescence (in quanta and normalized to unity)
$\epsilon_A(\nu)$ = molar extinction coefficient of the acceptor as a function of ν
ν = frequency in cm^{-1}

This mechanism assumes that the energy available for transfer by the donor is that which would otherwise be emitted radiatively. The transfer probability is thus stated in terms of the strengths of the individual allowed transitions and the energy overlap of the emission band of the donor and the absorption band of the acceptor.

A number of studies have looked at intramolecular electronic energy transfer. In a series of 4-(1-naphthylalkyl)-benzophenones (70), excitation of the naphthlene moiety results in singlet transfer to benzophenone. The efficiency of transfer, however, decreases as the chain length is increased from $n = 1$ to $n = 3$.

In a series of 2-(2-naphthylalkyl)-anthracenes (73), excitation

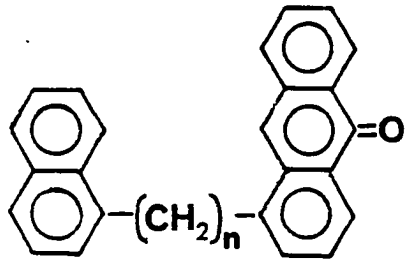

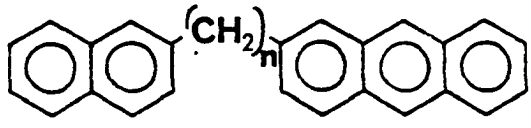

of the naphthyl group results in singlet transfer to the anthracene moiety. The authors concluded that the transfer probability was independent of alkyl chain length, however, the results of a less rigorously controlled study might have indicated that the transfer efficiency was greatest for the n = 2 derivative. Actually, the anomolously variable fluorescence yields observed for the derivatives is the complicating factor. All the derivatives proved to be more fluorescent than the standard compound, 9-methylanthracene, with the order being n = 2 > n = 3 > n = 1 > 9-methylanthracene in the ratios of 2.1, 1.6, 1.1 and 1.0, respectively. Presently, no plausible explanation exists on the basis of an energy transfer mechanism to explain the yields observed for the various anthracene derivatives.

The results would also indicate that different energy transfer mechanisms are operative for the two cases discussed.

One mechanism that was initially considered to have great potential for explaining the altered fluorescence characteristics of the quaternary adducts containing two heterocyclic chromophores was the formation of a charge transfer complex. Such an interaction fundamentally differs from the energy transfer mechanisms in that the integrity of the individual chromophores is lost through the formation of a new dimeric molecular species. There are a large number of potential molecular interactions which may occur in solution both for the ground state molecules and the excited state species. The range of potential interactions are shown schematically in Scheme IX.

Scheme IX

Potential Molecular Interactions Leading to Altered Luminescence Characteristics (74,75)

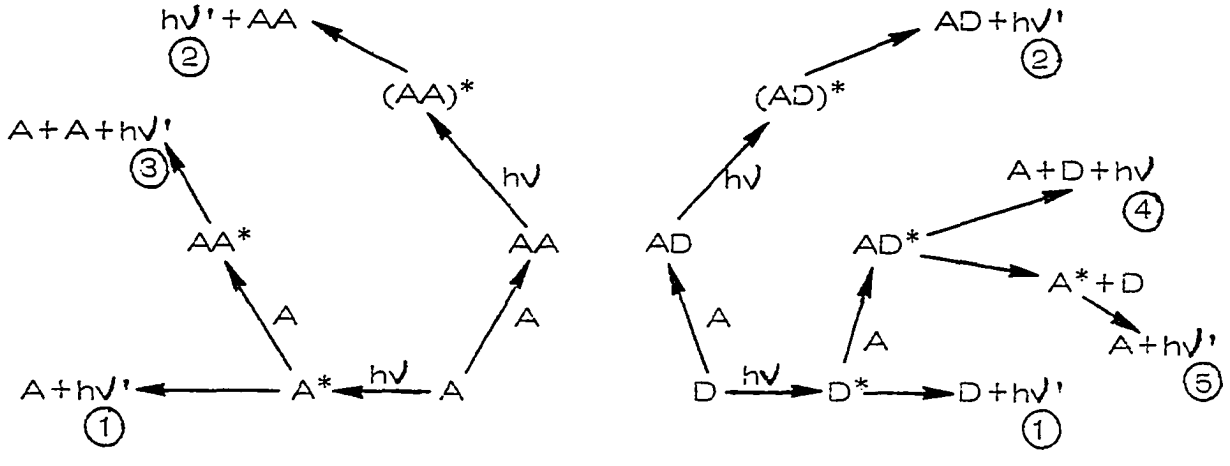

Note: In order to simplify the graphic presentation, only singlet excited state pathways are presented.

1. Excitation of the ground state molecule in a dilute solution gives rise to the singlet excited state, A^* which can fluoresce or undergo other pathways of deactivation.

2. Many compounds form ground state dimers, AA, in more concentrated solutions. A number of spectral techniques are useful in observing the dimerization such as the UV absorption and NMR spectroscopy. Excitation of the dimer to AA^*, can result in dissociation of the complex, or in some instances, in a broad structureless fluorescence that is red shifted compared to the monomer fluorescence.

3. In sufficiently concentrated solutions where the excited species can encounter a ground state molecule during its lifetime (ca. 10^{-8} sec), the encounter complex, AA^*, which is an excimer, can then fluoresce and immediately dissociate.

4. The encounter complex, AD^*, formed by the same mechanism as in (3) between chemically different molecules can give rise to exciplex fluorescence. The complex formed by this mechanism is also very short lived and dissociates simultaneously with excited state deactivation.

5. The encounter complex AD^* can also undergo an energy exchange reaction giving rise to a new excited molecule, A^*, which exhibits its typical luminescence. The transition energy of A^* must be $\leq D^*$ for this mechanism to be operative. This mechanism has previously been discussed in detail.

The mechanistic pathways describing the potential fate of the encounter complexes was presented in Scheme IX. However, a given complex is not necessarily limited to just one mechanistic pathway and the potential occurrence of one or more pathways depends upon the interaction of a large number of complex variables including the solvent environment, the chemical characteristic of the molecular species involved, and the concentration of the interacting molecules. Since the mechanisms of encounter complex formation and excited state decay

are competitive, the final luminescence characteristics observed will be the result of the relative rates of the various pathways. It must be pointed out, however, that although the mechanistic scheme was prepared to show only singlet states to maintain graphic clarity, there are an equal number of potential triplet pathways as well as a host of radiationless pathways which will compete with any observable luminescence. In fact, most encounter complexes fluoresce very weakly, if at all, and their spectrofluorometric characteristics are quite difficult to obtain experimentally.

For the purposes of this study, routine spectral techniques should provide an insight as to which mechanisms could be responsible for the non-fluorescence observed for certain acridine quaternary salts. A summary of spectral characteristics expected for each pathway is presented in Table 18.

Table 18. Expected Spectral Characteristics of Encounter Complexes

Scheme IX	AA, AD	AA*	AD*	AD*⟶A*+D
Description	Charge transfer	Excimer	Exciplex	Energy transfer
Spectral type: UV	red shifted	normal		
NMR	altered	normal		
fluorescence	quenching of normal fluorescence			
	appearance of new red shifted fluorescence			fluorescence of new species

Before presenting the results obtained for the acridine derivatives which were the subject of this investigation, a review of previously reported observations for closely related systems will be discussed.

It has been known for many years that when two different stable molecules are mixed in a suitable solvent, the color of the solution sometimes changes. Although various models for explaining these observations have been proposed by many authors, a question still remained as late as 1952 concerning the origin of the intense color brought about by the complex formation. In an attempt to clarify these problems, Mulliken (76, 77) introduced quantum mechanical language into the theory of molecular complex formation. In the simplest case a 1:1 complex, (D-A) is formed by the weak interaction of an electron donor (D) and an electronic acceptor (A). The molecule (D) has an electron which is easily removed to produce a D^+ species and the molecule A has a large tendency to accept an electron and produce an A^- species.

The wave function for the charge transfer structure $(D^+ - A^-)$ is given by $\Psi_1 = \Psi(D^+ - A^-)$ and the wave function for the nonbonding structure (van der Waals interactions) is given by $\Psi_o = \Psi(D-A)$. The ground state of the complex Ψ_N and its corresponding excited state Ψ_E are given as:

$$\Psi_N = a\,\Psi_o + b\,\Psi_1$$

$$\Psi_E = a^*\,\Psi_1 - b^*\,\Psi_o$$

Thus, the ground state Ψ_N is a mixed state of Ψ_o and Ψ_1. Using a traditional perturbational quantum mechanical approach, one can show that the strength of the complex, as well as the ratio b/a which is a

measure of the extent of charge transfer in the complex, depends upon the overlap between Ψ_o and Ψ_1, and the energies of Ψ_o and Ψ_1 where

$$S_{01} = \langle \Psi_o | \Psi_1 \rangle = \int \Psi_o \Psi_1 \, d\tau$$

$$E_o = \langle \Psi_o | \mathcal{H} | \Psi_o \rangle$$

$$E_1 = \langle \Psi_1 | \mathcal{H} | \Psi_1 \rangle$$

$$\mathcal{H}_{01} = \langle \Psi_o | \mathcal{H} | \Psi_1 \rangle$$

and the eigenvalue W is obtained by solving the appropriate secular equation. The larger S_{01} and the smaller the energy differences $(E_1 - E_o)$, the more stabilized is the complex.

In Figure 17 (78) the potential energy curves are drawn schematically to show the relationship between E_o, E_1, W_N and W_E

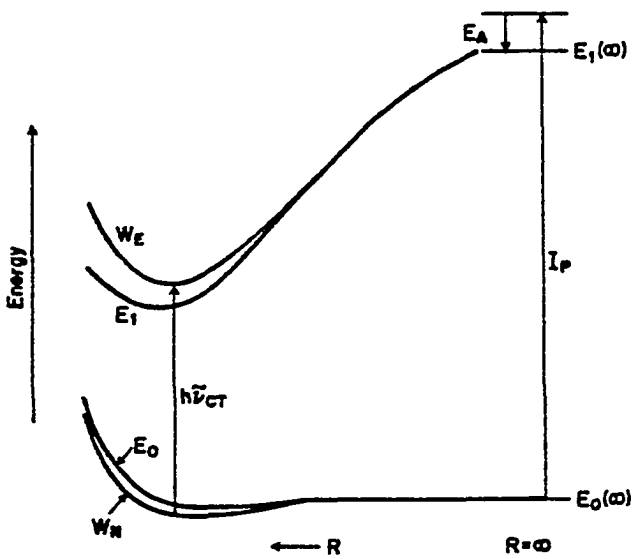

Figure 17. Schematic diagram of potential energy curves corresponding to the charge transfer excited state and ground state of the CT complexes. R, I_p, and E_a represent the intermolecular distance between donor and acceptor, the ionization potential of donor, and the electron affinity of acceptor, respectively (78).

where W_N and W_E are the eigenvalues for Ψ_N and Ψ_E respectively. As the intermolecular distance, R, decreases E_o may be stabilized by van der Waals interactions and especially by electrostatic forces for polar molecules. In the case of E_1, strong stabilization occurs because of electrostatic and covalent bonding interactions between D^+ and A^-.

The absorption spectrum arising from an electronic transition from state W_N to W_E is the charge transfer spectrum $h\nu_{CT}$. For the simplest case where A = D, the stabilization energy for the complex is given by the difference in the absorption frequencies of the monomer and dimer. In recent years, various sophisticated methods have been developed to theoretically calculate energies and mechanistically explain charge transfer complexes. One of the advances is in the inclusion of locally excited states ($A^* + D$) in the general molecular orbital description for charge transfer states. This arises because the excitation cannot be localized on only one molecule if symmetry allowed interactions are possible. This first order interaction which splits the energies of the interacting state is called exciton transfer (95).

The generic term "charge transfer" complex is widely used but can be misleading because there often is very little contribution of Ψ_1 in the total ground state wave function Ψ_N. The same is true for exciplexes and excimers. Therefore, the charge transfer label is applicable to almost any encounter complex without providing much information about the actual nature of the complex.

The range of spectral characteristics and possible molecular interactions have been extensively studied for various aromatic hydrocarbons. Anthracene exhibits a variety of spectral characteristics which all are indicative of the molecular interactions which it undergoes. Figure 18 (80) shows the fluorescence observed for both the dimer and

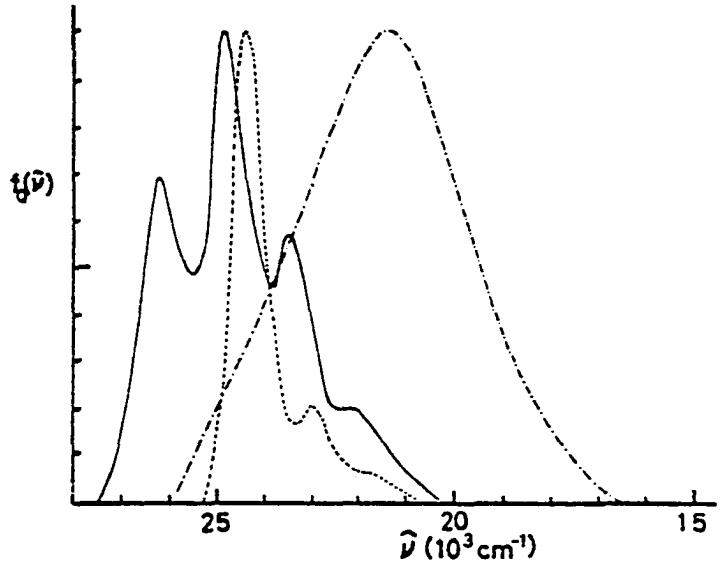

Figure 18. Fluorescence spectra of anthracene monomer (——), the dimer B (• • •), and the excimer (—• — •), respectively, in cyclohexane matrix at 77°K (80).

excimer at low temperature. The excimer fluorescence for unsubstituted anthracene cannot be observed at room temperature where photodimerization predominated (80). Using 9-substituted anthracenes which do show excimer fluorescence at room temperature, Birks et al. (81) predicted that the cis-excimer fluoresces whereas the trans-excimer dimerizes. This is based on the observation that only trans photodimers

have been isolated. To further study the geometrical requirements of anthracene fluorescence, 1,2-di(1-anthryl)ethane [37] and 1,2-di(9-anthryl)ethane [38] were prepared and investigated (82). For other

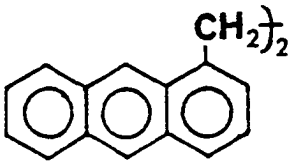

37

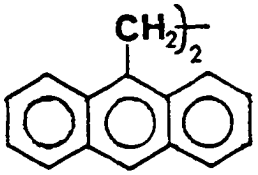

38

composite systems, $Ar-(CH_2)_n-Ar$, Ar = phenyl (83) and naphthyl (84) groups, intramolecular excimer fluorescence could be observed only when n = 3. In the case of the anthracenes where n = 2, two types of excimer fluorescence can be observed (82). Type I, observed at room temperature, comes from the non-symmetric crossed dimer whereas the type II fluorescence from the parallel sandwich dimer can only be observed at low temperature.

When mixed with aromatic molecules, N-H containing amines quench the fluorescence (85) whereas electron donor molecules like N,N-diethylaniline gives rise to a broad structureless emission band to the red of the fluorescence band of the aromatic hydrocarbon (86). Polar solvents produce a further red shift and a decrease in intensity of the exciplex band. In studying the details of the anthracene-diethylaniline exciplex, the alkyl linked intramolecular derivatives have been

made and studied (87, 88). These investigations revealed that the reduced quantum yield in polar solvents is due to the following mechanism:

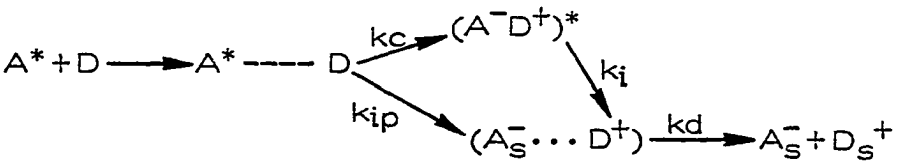

$(A^- D^+)^*$ = fluorescent exciplex
$A_s^- \cdots D^+$ = solvated ion-pair which is nonfluorescent

It is assumed that k_i and k_{ip} increase in polar solvents and solvents promote complete electron transfer resulting in the formation of a nonfluorescent solvated ion pair. The fact that the absorption spectrum is identical to an equimolar solution of anthracene and diethylaniline indicates that there is no interaction in the ground state.

Acridines also form exciplexes with anthracene and other aromatic hydrocarbons (89). However, excimer fluorescence has never been observed for acridine itself although calculations suggest that the excimer should be red shifted by approximately 6000 cm^{-1}(90). This would indicate that the acridine excimer should fluoresce at ca. 550 nm. This raises some questions since the anthracene excimer emits at ca. 480 nm (80) which is the same as the acridine cation fluorescence maximum. These data would suggest that the acridine excimer fluorescence could range from 480 - 560 nm and be solvent dependent. Furthermore, such fluorescence, if observed, might be incorrectly ascribed to the cation.

In Table 18 we described the spectral changes that might be

expected to result from various types of charge-transfer interactions. Both acridine (91) and acridine orange [39] (92) exhibit tendencies to

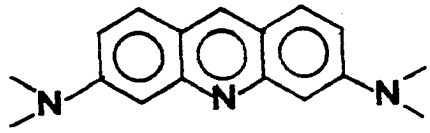

39

form ground state aggregates in concentrated solutions. The ring protons show significant shifts in d_1-chloroform solutions but not d_6-dimethyl sulfoxide solutions (91). The 100 MHz spectra of 0.129 M, 0.324 M and 0.648 M solutions of 9-methylacridine in $CDCl_3$ are given in Figure 19. The spectrum of acridine has been accurately analyzed as that of a four-spin A B C D system with the two outer rings considered independent of each other (93). A first order splitting diagram for 9-methylacridine is presented in Figure 20. The analysis breaks down slightly for J_2 and J_3 where second order or long range coupling with the methyl group is clearly evident. Also, a very critical examination of the signals for J_1 and J_4 would also reveal some further splitting not accounted for by the spin approximation.

All signals move upfield as the concentration is increased but J_1 and J_2 shift more than either J_3 or J_4. These observed shifts are consistent with those observed for acridine (91) but opposite to the direction observed for acridine orange dimers (92). However,

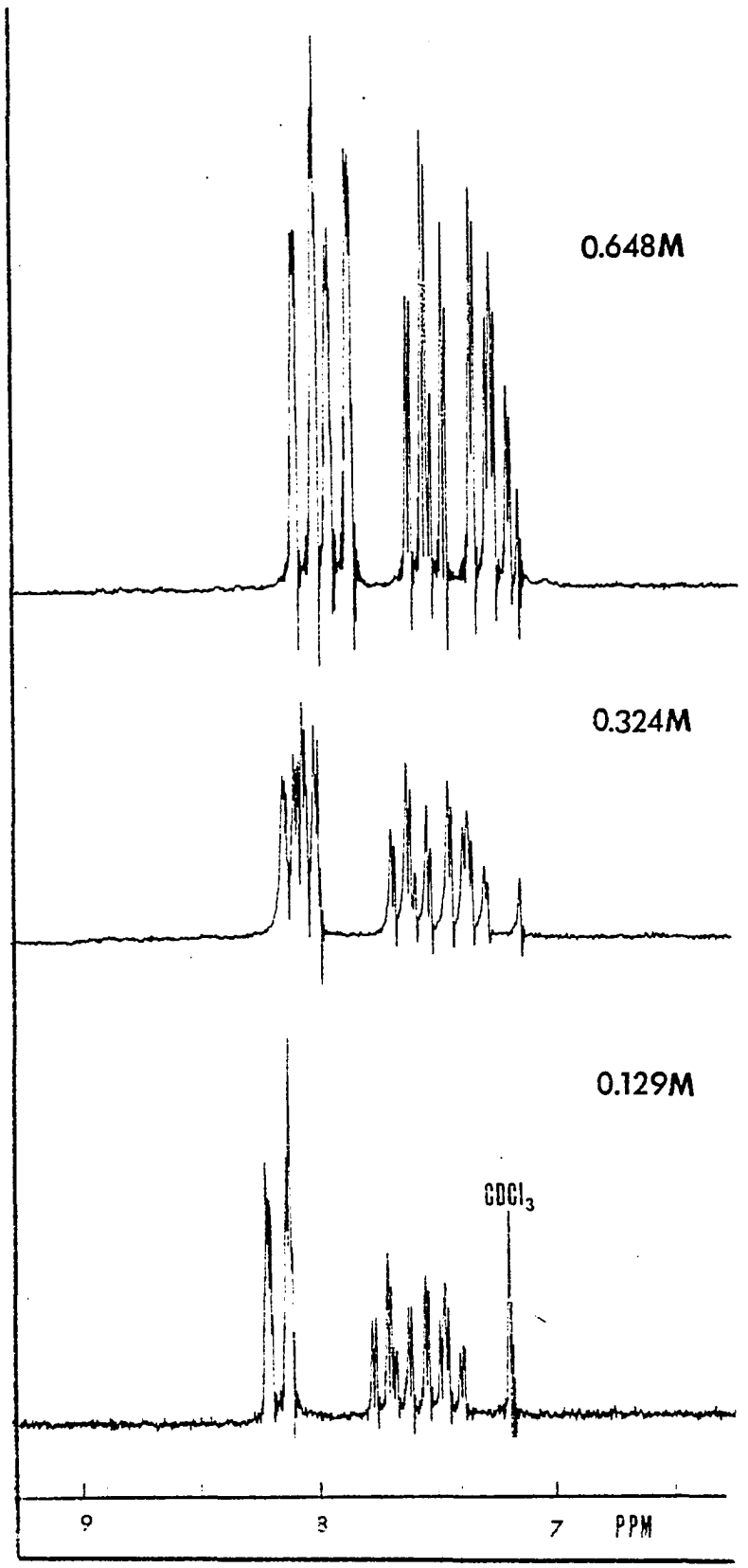

Figure 19. 100 MHz PMR signals in $CDCl_3$ for the aromatic protons of [2] as a function of concentration.

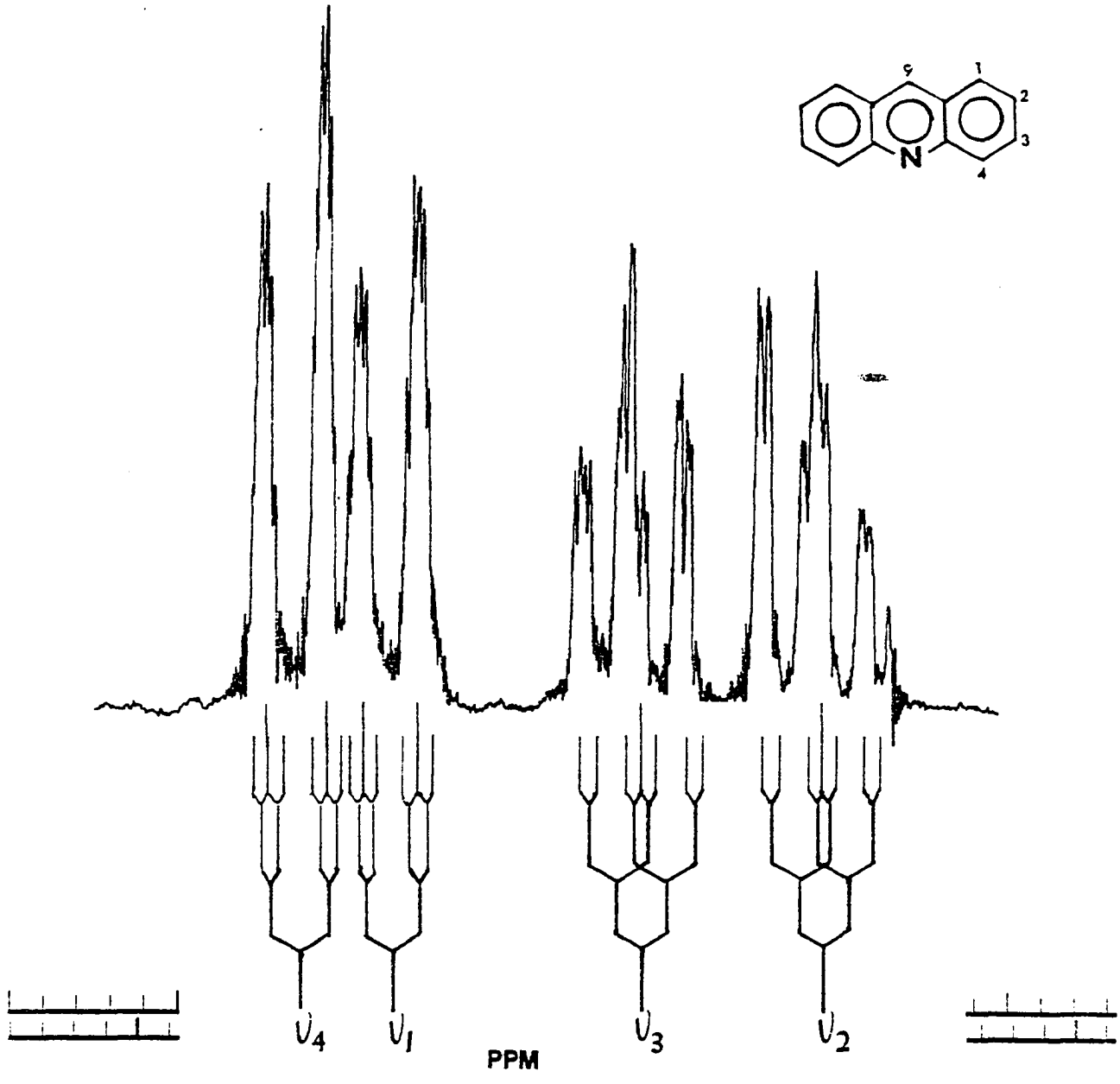

Figure 20. First order splitting diagram for 9-methylacridine.

both authors suggest that the concentration dependent spectra observed for each compound are a result of the formation of asymmetric dimers where the nitrogen atoms are antiparallel and the rings are not directly over each other. The shift differences appear to be a result

of the positioning of protons of one molecule in the ring current of the other interacting molecule.

The NMR spectrum of the dimer, 1,2-bis-(9-acridinyl) ethane [6] in dilute (0.065 M) solutions (Part I, Figure 1) would indicate that there is a ground state interaction because the ν_1 and ν_4 proton signals, extrapolated to infinite dilution, appear similar to those of the intermediate concentration signals for 9-methylacridine. In much more concentrated solutions (0.325 M), the spectrum observed is similar to that observed for a concentrated solution of 9-methylacridine. These data suggest that there is some type of interaction between the two aromatic nuclei that comprise this compound and thus the 0.065 M solution spectrum does not change significantly upon dilution.

In another attempt to verify the NMR shift changes which might occur with complexed acridine, another interacting system was investigated. Diphenylamine co-crystallizes with 9-methylacridine to form a 1:1 adduct and fractional crystallization cannot be used to separate these two compounds. However, no change in the spectrum of a 0.129 M solution of 9-methylacridine in $CDCl_3$ was observed when diphenylamine (0.148 - 0.780 M) was added.

The NMR chemical shift changes that accompany the charge transfer complexation of 1,4-dinitrobenzene with various phenothiazine derivatives including chlorpromazine has been documented (94). However, the chemical shift data for the acceptor alone was reported and

not that for the phenothiazine nucleus. Therefore, in investigating the potential complex formation between the acridine and phenothiazine nuclei, the applicability of the NMR technique has been documented but the chemical shift changes expected cannot be predicted.

The effect of chlorpromazine on the NMR spectrum of the trimethylamine quaternary salt [10] is presented in Figure 21 and no significant changes in the spectrum can be seen. However, there is also very little concentration dependence observable in the NMR spectrum of [10] in d_4-methanol (Figure 22). If a ground state interaction existed, the asymmetric substitution on the phenothiazine ring should be quite effective in reducing the NMR degeneracy of the acridine

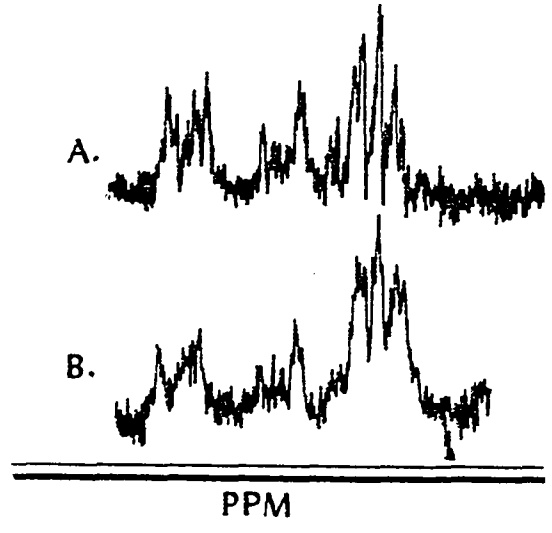

Figure 21. 60 MHz PPM signal (CD_3OD) for the aromatic protons of a 0.075M solution of (9-acridinylmethyl) trimethylammonium bromide [10] separately (curve A) and in the presence of 0.378M chlorpromazine [16] (curve B).

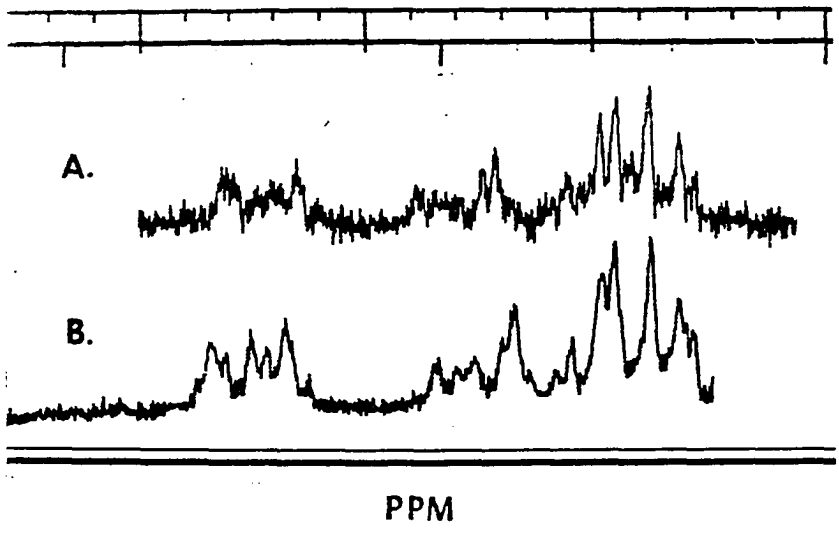

Figure 22. 60 MHz PMR signal (250 Hz sweep width in CD_3OD) for the aromatic protons of (9-acridinylmethyl) trimethylammonium bromide [10] at 0.075 (A) and 0.375 M (B).

signals and be quite obvious. Therefore, we conclude that a ground state complex is quite unlikely.

The apparent preference for the formation of acridine-acridine dimers rather than heterocomplexes is provided by the crystal structure determined by single crystal x-ray crystallography (95). The structure is shown in Figures 23 and 24.

It has been previously mentioned that excimer fluorescence has not been observed in concentrated acridine solutions (90). As is the case with anthracene derivatives (82), the 9-acridinylmethyl "dimer" [6] should serve as an optimum model for excimer fluorescence. The fluorescence of the "dimer" is very weak. The intensity in methanol is

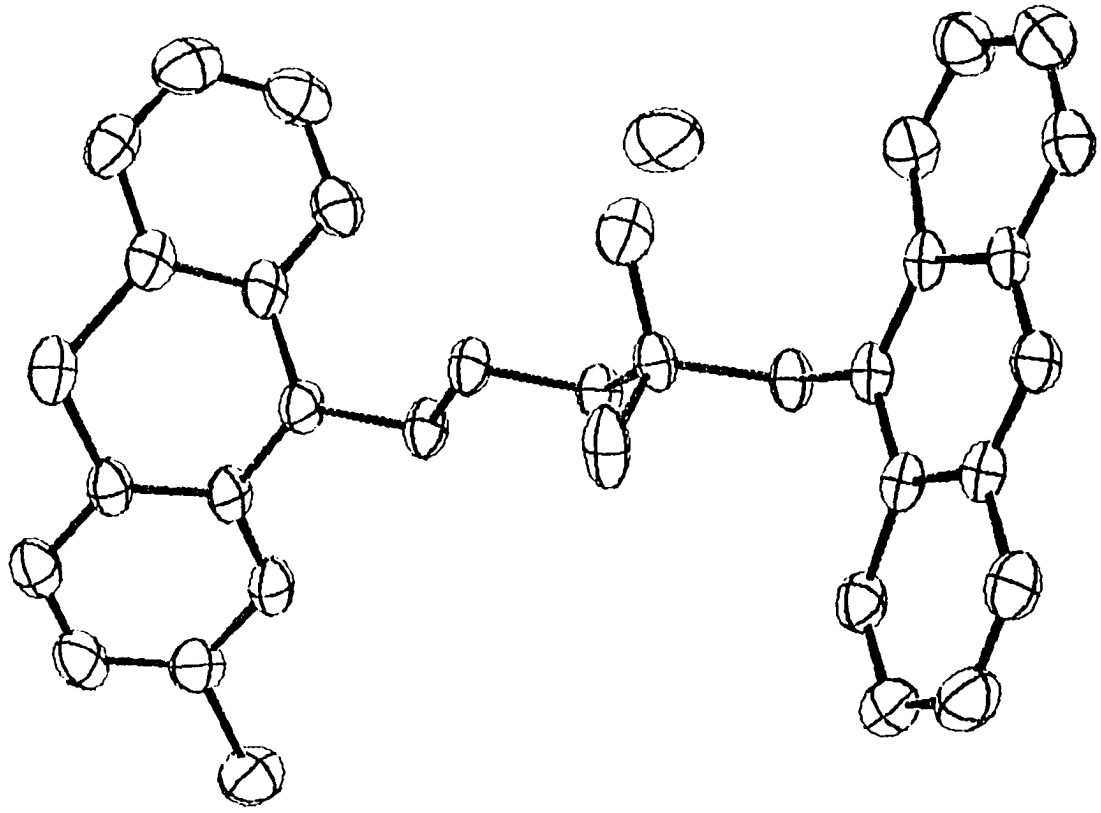

Figure 23. Computer drawing of a single molecule of the quaternary ammonium salt derived from 9 bromomethylacridine and chlorpromazine (95).

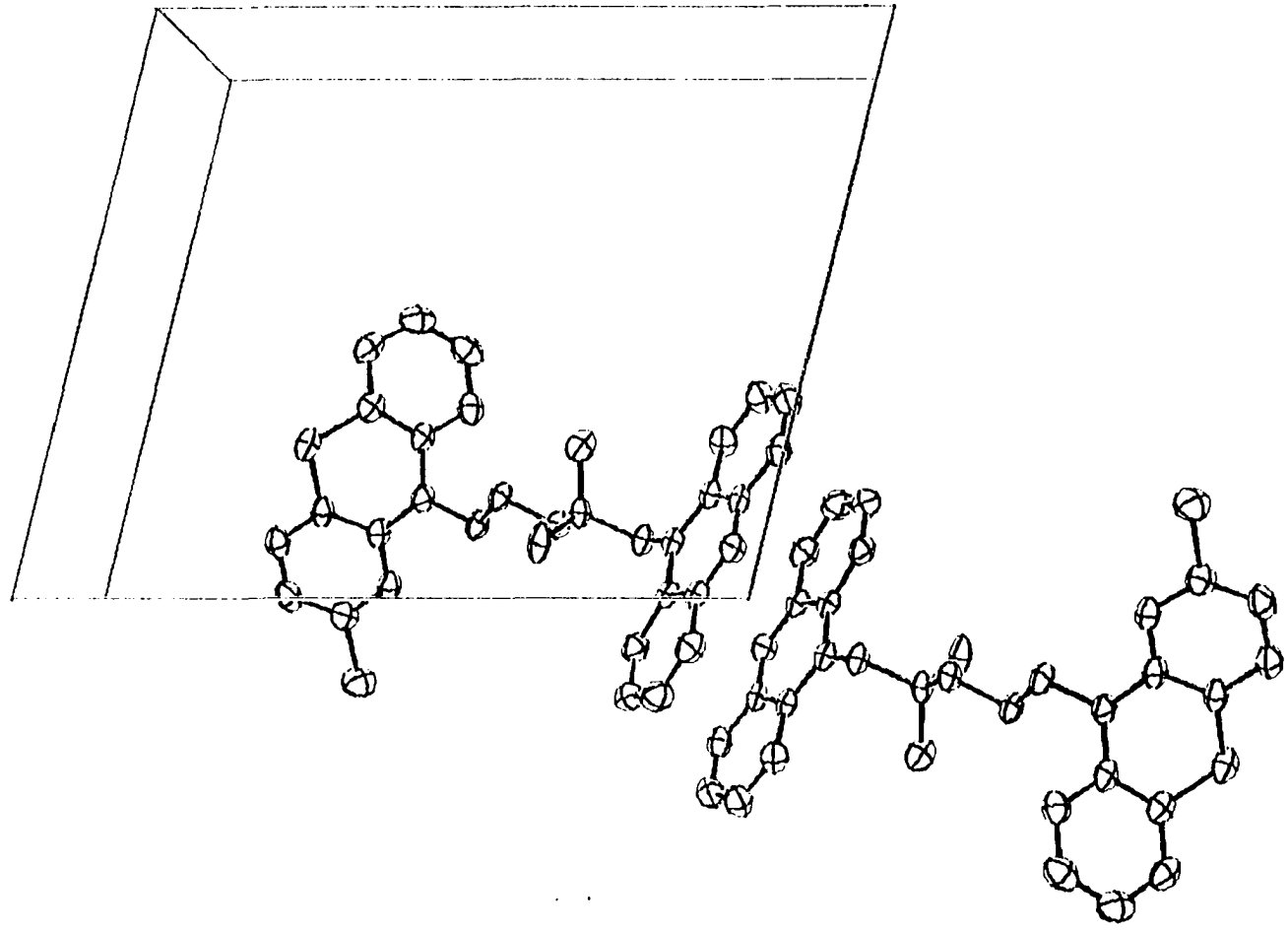

Figure 24. Computer drawing showing the acridine-acridine antiparrallel stacking about the center symmetry at 0, 1/2, 0. The box represents the unit cell boundaries (95).

only 15% of that observed for 9-methylacridine and further decreases in water to 27% of the methanol value. The relative intensity observed in methanol is not increased by the addition of acid although the expected bathochromic shift for the fluorescence maxima is observed. The fluorescence spectrum was recorded in cyclohexane, methanol and water and there was no clear evidence for excimer fluorescence. The emission spectrum obtained in water was very broad with maxima at ca. 420 and 440 nm. However, excimer fluorescence should have occurred from ca. 480 - 550 nm in this solvent (90) and was not observed. The very low quantum yield would indicate that some molecular interaction which enhances radiationless pathways is occuring but the spectral characteristics observed provide no insight as to the cause of this anomolous fluorescence behavior.

The results obtained in this study indicate that certain quaternary salts of trimethylamine drugs are nonfluorescent but no clear mechanistic description for this behavior could be experimentally confirmed. The results obtained for the "dimer" [6] indicate that acridine excimers, if they exist, are nonfluorescent. Furthermore, charge transfer complexes or exciplexes are also likely to be nonfluorescent. A recent report in Chemical Abstracts (101) from some Italian workers indicated that certain acridine-phenothiazine complexes had been observed but no details about the experimental approach were given. It now appears likely that, although no mechanistic information

could be obtained from the derivatives investigated by the described experimental approach, certain model compounds such as (9-acridinyl-methyl)[3-(9-anthryl) propyl]dimethylammonium bromide could yield information about potential exciplex formation and the quaternary salt of methiomeprazine might yield information about possible energy transfer.

CHAPTER 4

EXPERIMENTAL

Ultraviolet spectra were obtained on a Cary 14 spectrophotometer. NMR spectra were obtained on a Varian Associates T-60 or XL-100 spectrometer. Mass spectra were obtained on a Hitachi-Perkin Elmer RMU-7 spectrometer. Fluorescence spectra were obtained on either an Aminco Bowman or Perkin-Elmer MPF-3L spectrofluorometer. IR spectra were recorded on a Beckman IR-8 or Beckman IR-3. Melting points were determined on a Gallenkampf MF 370 capillary melting point apparatus and are uncorrected. Merck $PF_{254+366}$ silica gel was used for column and general thin layer chromatography (TLC) while 100μ terephthalate backed silica gel plates without indicator, Eastman Kodak, were used for the quantitative analyses. Microanalyses were performed by Galbraith Laboratories, Inc., Knoxville, Tenn.

All solvents used for fluorescence characterization were Nanograde or Analytical grade, twice glass redistilled, and were checked for the presence of fluorescent contaminants by obtaining the blank fluorescence spectrum at an excitation wavelength of 350 nm.

The absorbance and fluorescence characteristics of the compounds were described in text and are not repeated in the experimental section.

The primary criteria of compound purity for spectral purposes was a singlet spot by TLC examination. The following solvent systems for silica gel plates could be used to identify the purity of the compounds used in this study: dichloromethane, benzene-acetone (95:5) and acetonitrile-water (9:1). By examining a sample in these three systems where all the known derivatives had identifible R_f values, the purity could be ascertained.

9-methylacridine [2] was obtained by a modified Bernthsen synthesis described in Chapter 2 and 9-bromomethylacridine [1] was prepared by the method of Campbell et al. (6). Acridine, Merck commercial grade, was purified by an initial sublimation at ca.90° followed by repeated recrystallization from alcohol. 9-chloroacridine was prepared by the method of Albert (33). Collectively, these compounds plus diphenylamine of various origins and recrystallized from alcohol-water served as the starting meterials for the preparation of the acridine derivatives used for this study. Samples of tertiary amine drugs were kindly supplied by the manufacturers or the National Institute of Mental Health.

Preparation of 9-acridinyl nitromethane [40]

The compound [40] was prepared essentially according to the method of Krohnke and Honig (96) by the route given in scheme X.

Scheme X

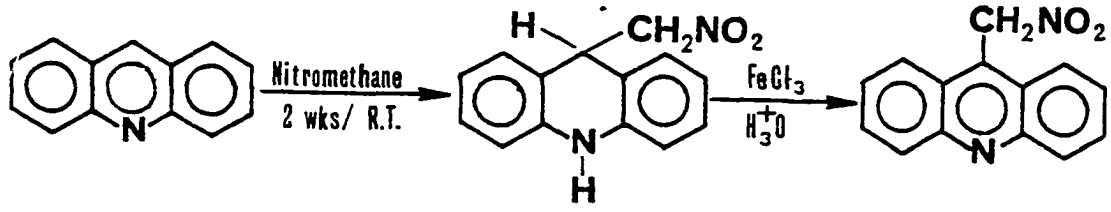

The crude product from the nitromethane reaction was recrystallized from ethanol and oxidized in dilute HCl-$FeCl_3$ (2.7 gm/10 mL H_2O) for 30 minutes.

The crude product which crystallized from the aqueous oxidizing mixture was sublimed yielding semipurified [40] (19% based on the amount of acridine). The product was dissolved in water, neutralized with Na_2CO_3 and extracted into $CHCl_3$, evaporated to dryness and recrystallized from benzene and melted at 155-156° (lit. mp. = 156-157°) and gave a single spot on TLC in benzene-acetone (95:5). The NMR spectrum of the acridan intermediate and the final product and mass spectrum was obtained to confirm product identity. 60 MHz PMR of 9-acridanylnitromethane: ($CDCl_3$, TMS, delta): 6.7-7.3 (8H, m) 6.2 (1H, br s) 4.85 (1H, t) 4.3 (2H, d). 60 MHz PMR spectrum of 9-acridinylnitromethane [40]: (d_6-benzene, TMS, delta): 7.0-8.6 (8H, m) 5.55 (2H, s). Mass spectrum (70 ev, relative abundance): 238 (M^+, 8), 192 (base peak).

Synthesis of 9-acridinylmethanol [4]

Method I (6): via 9-acridinylmethyl acetate [41].

9-acridinylmethyl acetate [41] was prepared in good yield by reacting [1] (100 mg 0.37 mmole) with an equal weight (100 mg) of potassium acetate in refluxing ethanol for 2 hr. The reaction mixture was concentrated to ca. 5 mL, 20 mL of water was added and extracted with ether. The crude product was recrystallized from 50% ethanol giving 34 mg of product melting at 124.5-125° (lit. mp. = 124°). The product was found to be a single component by TLC in benzene-acetone (95:5). 60 MHz PMR of [41]: ($CDCl_3$, TMS, delta): 7.45-8.5 (8H, m) 6.1 (2H, s) 2.1 (3H, s). If the desired product is [4], 2 equivalents of 1 N NaOH in H_2O was added and the above reaction mixture was allowed to sit at room temperature for 24 hrs. The mixture can then be worked up by adding an equal volume of ether and sufficient water to get two layers. The organic layer is removed, evaporated to dryness and washed 3 times with ether leaving a product that melts at ca. 160° when preheated to 158° (lit. mp. = 164-165° dec).

Method II (97): via 9-acridinylcarboxaldehyde [3].

To a warmed solution of 9-methylacridine [2] (1 gm, 5.2 mmole) in ca. 150 mL xylene, 0.6 gm (5.5 mmole) of selenium dioxide was added and the mixture refluxed for 1 hr. The xylene was evaporated to near dryness, ca. 50 mL water/K_2CO_3 was added and extracted exhaustively with ether. The organic layer was dried over Na_2SO_4 and concentrated.

The crude product was chromatographed on a silica gel preparative layer plate with benzene-acetone (95:5), eluted from the plate with CCl_4 and recrystallized from the same solvent yielding 455 mg (42.5% of theory) of [3]. The product was then twice recrystallized from hexane and melted at 144-145° (lit. mp. = 150°). The aldehyde prepared above was dissolved in ca. 50 mL methanol and 100 mg (2.6 mmoles) $NaBH_4$ was added. The reaction was over within 5 min and 5 mL 2 N NaOH was added and the mixture refluxed for 1 hr to hydrolyze the borate ester (98). The mixture was cooled and 280 mg (62% yield) of 9-acridinylmethanol [4] was collected by filtration. The precipitate was washed with cold ether and shown to be pure by TLC in benzene-acetone (95:5). The melting point was 166-167° when preheated to 158° (lit. mp. = 164-165°). Mass spectrum (70 ev, relative intensity) 209 (M^+, base peak), 192 (20), 178 (84). All of the above are known compounds and were characterized only to the extent necessary to confirm the product identity.

Preparation of Quaternary Salts.

All salts were prepared by the following general procedure: The hydrochloride salt of the tertiary amine drug was dissolved in a minimum amount of water, neutralized with solid K_2CO_3 and extracted into either hexane or chloroform. The extract was dried over anhydrous Na_2SO_4 and evaporated to dryness. The free base was then added to a nearly saturated warm solution of 9-bromomethylacridine [1] in acetonitrile

and left at room temperature for 24 hrs and then in the freezer (-20°) for 24 hrs. The crystals were collected and washed with a minimum volume of acetone-ether (1:1). In cases where the initial crystallization was low yielding, the reaction mixture was concentrated to ca. one half the original volume and put in the freezer (-20°) for 24 hrs. The products were recrystallized from acetonitrile or acetonitrile containing up to 15% methanol depending on solubility. Specific details for the compounds are given:

(9-acridinylmethyl) trimethylammonium bromide [10]: Preparation described in Part I.

(9-acridinylmethyl)(3-phenylpropyl)dimethylammonium bromide [11]: Preparation described in Part I.

(9-acridinylmethyl)[3-(2-chlorophenothiazine-10-yl)propyl] dimethyl-ammonium bromide [15]: Preparation described in Part I.

(9-acridinylmethyl)[3-(2-chlorothiozanthen-9-yl- $\Delta^{9,\gamma}$)propyl]dimethyl-ammonium bromide [31]: Starting with ca. 500 mg (1.42 mmole) of chlorprothixene HCl, 840 mg (ca. 100% of theory) of crude [31] crystallized from the reaction mixture. The crystals were washed with acetone and then recrystallized from 15% methanolic acetonitrile, (mp. = 156-159° dec). The 60 MHz PMR spectrum (Figure 25) and IR spectrum (Figure 26) were consistent with the proposed product. Analysis for $C_{32}H_{28}N_2S_1Cl_1Br_1$: calculated, C 65.37, H 4.80, N 4.76; found, C 65.20, H 4.93, N 5.00.

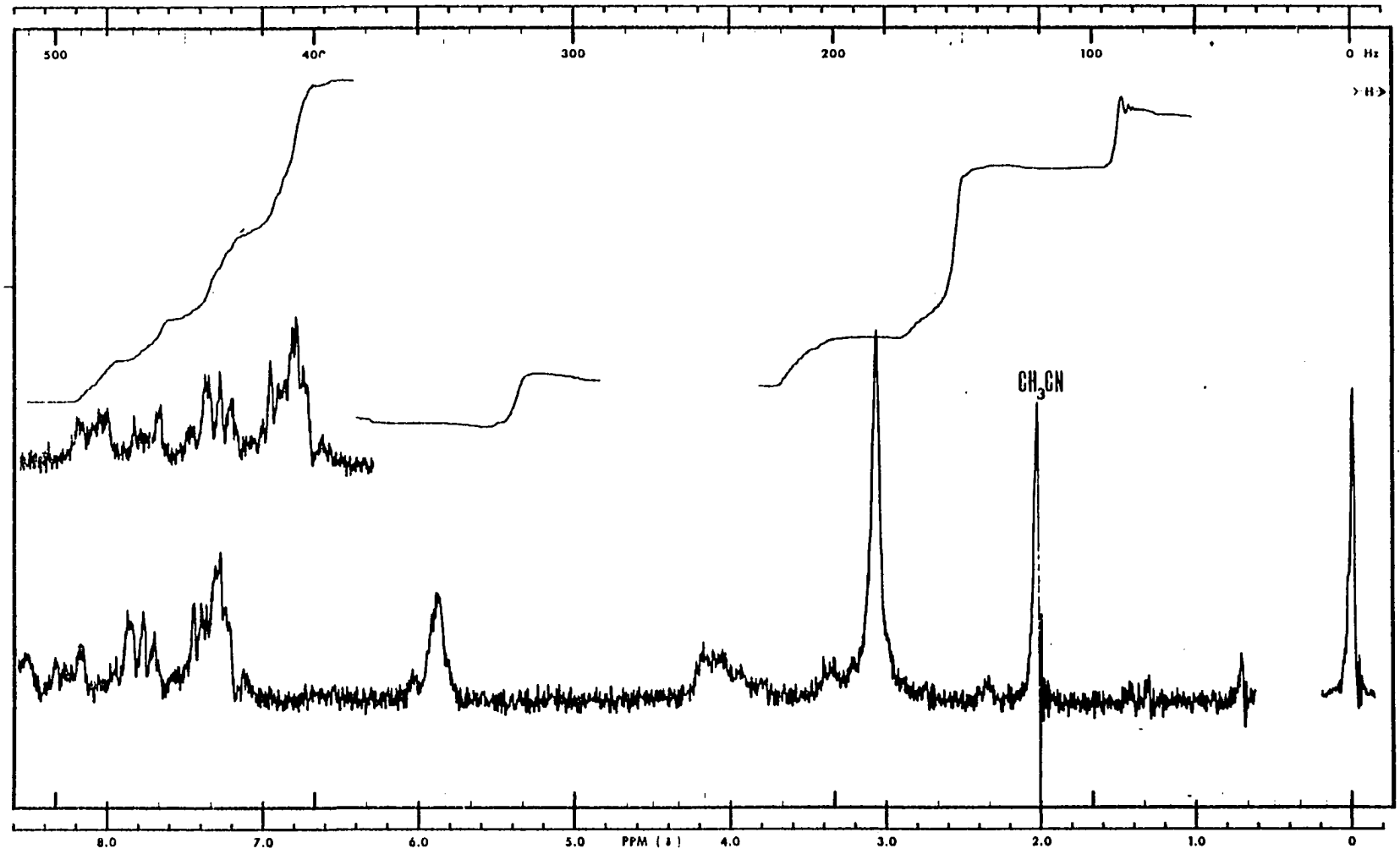

Figure 25. 60 MHz PMR ($CDCl_3 + CD_3OD$) of the chlorprothixene quaternary [31].

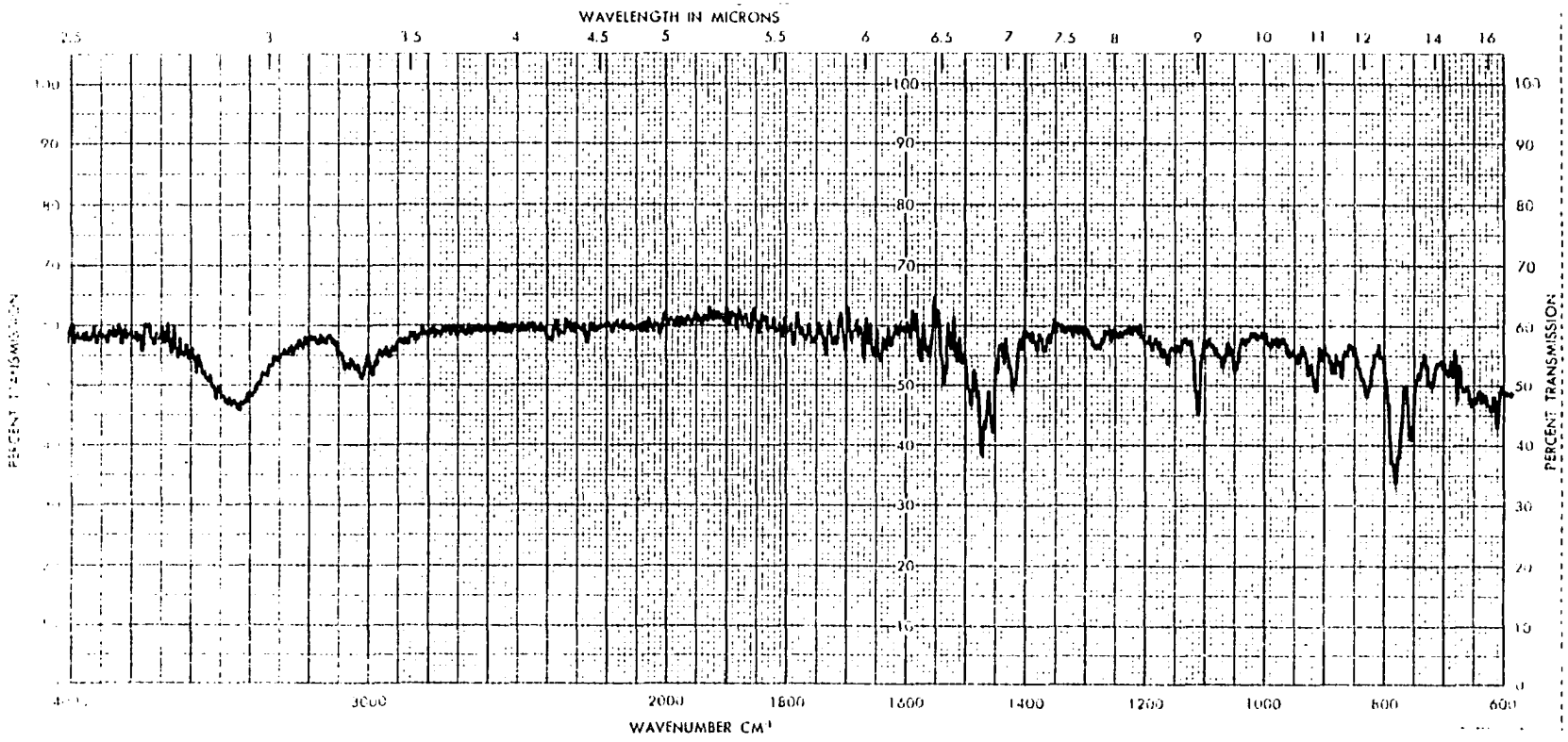

Figure 26. IR spectrum (KBr) of the chlorprothixene quaternary [31].

(9-acridinylmethyl)[3-(phenothiazin-10-yl) propyl] dimethylammonium bromide [32]: Starting with ca. 300 mg (1.05 mmole) promazine HCl ca. 430 mg (75% of theory) of crude [32] crystallized from the reaction mixture. The crystals were washed with acetone-ether (1:1) and recrystallized from 10% methanolic acetonitrile. The 100 MHz PMR (Figure 27) and IR spectrum (Figure 28) were consistent with the proposed compound. Analysis for $C_{31}H_{30}N_3SBr \cdot 1.5\ H_2O$: calculated, C 63.80, H 5.70, N 7.19; found, C 63.79, H 5.50, N 7.01.

(9-acridinylmethyl)[3-(10,11 dihydro-5H-dibenzo [a,d] cyclohepten-5-yl- $\Delta^{5,\gamma}$)propyl] dimethylammonium bromide [29]: Starting with ca. 500 mg (1.6 mmole) of amitriptyline·HCl, 730 mg (83% of theory) of crude [29] crystallized from the reaction mixture. The crystals were washed with acetone and recrystallized from 10% methanolic acetonitrile (mp. = 168.5-170° dec). The 100 MHz PMR interpretation has previously been discussed in text (Figures 27, 28). The best analysis obtained for $C_{34}H_{33}N_2Br \cdot CH_3CN$, although not within acceptable limits was: calculated, C 73.21, H 6.14, N 7.12; found, C 74.62, H 6.13, N 7.20.

(9-acridinylmethyl)[3-(2-chlorophenothiazine-10-yl-5-oxide)propyl] dimethylammonium bromide [30]: Only trace amounts of starting material, chlorpromazine sulfoxide·HCl, was available and therefore the quaternary salt [30] was not chemically characterized. The R_f value in acetonitrile-H_2O (9:1) was consistent with that expected for a quaternary salt.

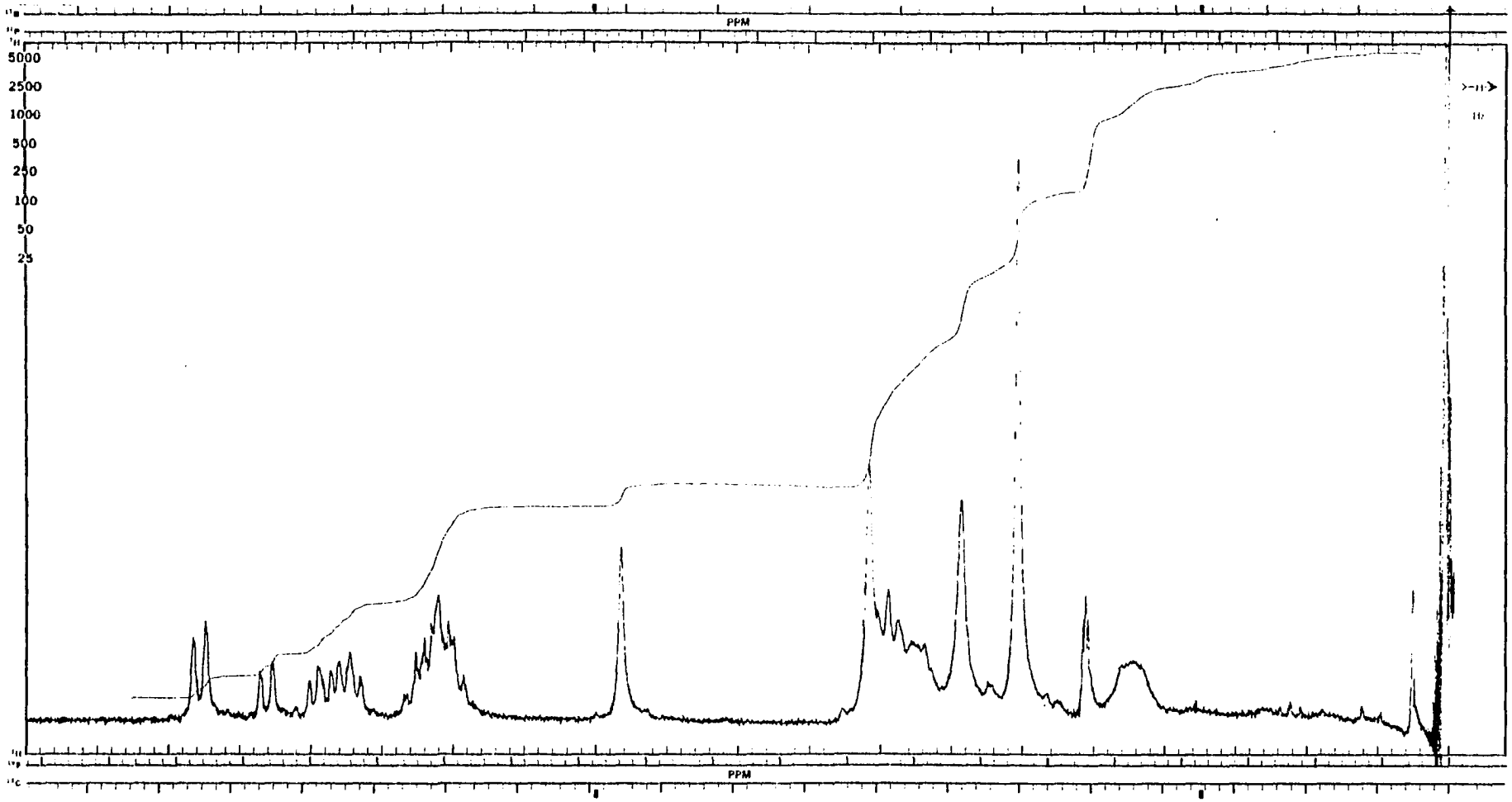

Figure 27. 100 MHz PMR spectrum (d_6-DMSO) of the promazine quaternary [32].

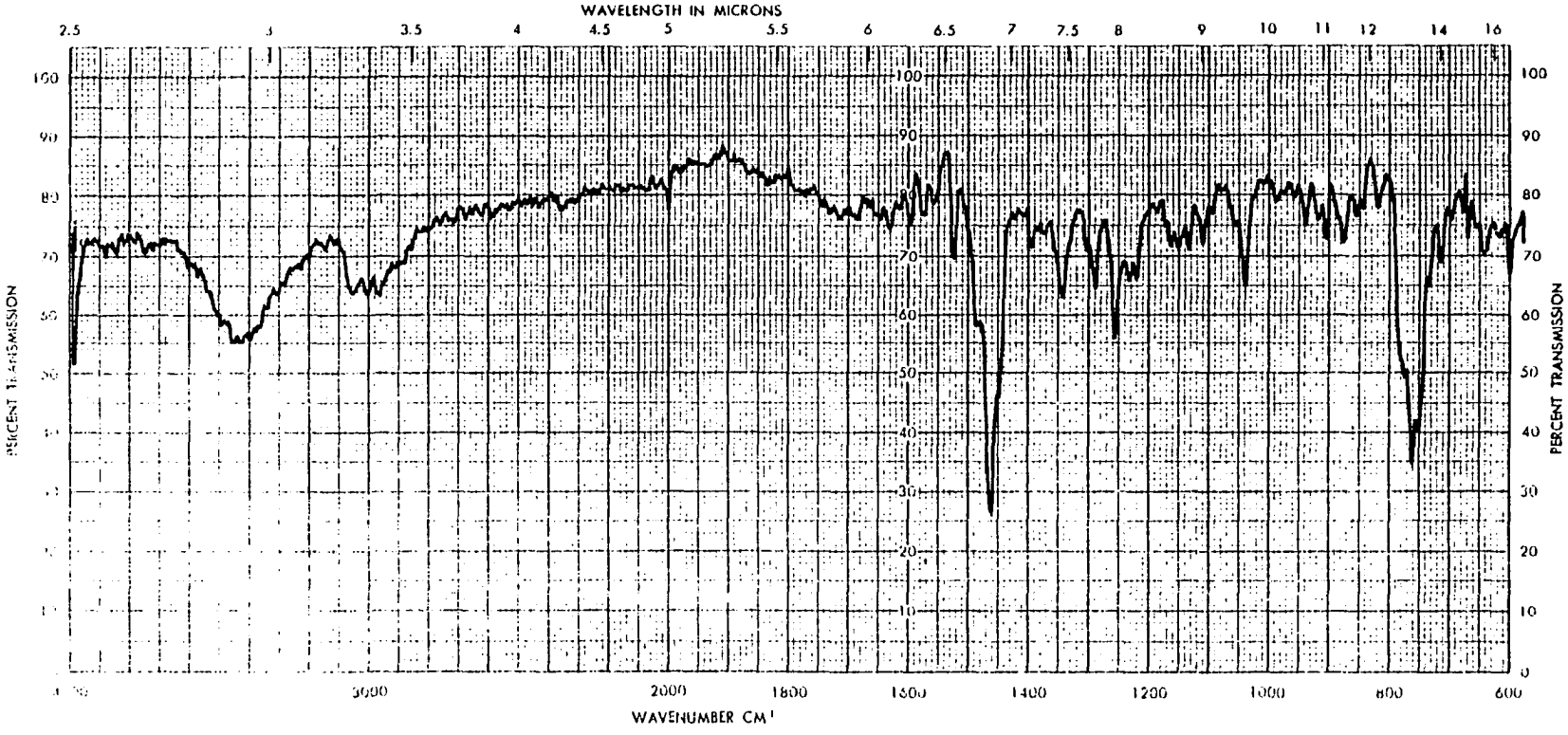

Figure 28. IR spectrum (KBr) of the promazine quaternary [32].

9-acridinylmethylpyridinium perchlorate: A sample, 28 mg (0.08 mmole) of 9-acridinylmethylpyridinium bromide previously prepared in our laboratory was dissolved in methanol-water (1:1) in a centrifuge tube and silver perchlorate (0.08 mmole) dissolved in the same solvent was added to the reaction mixture and let stand in the dark for 1 hr. The supernatant was removed after centrifugation and put in the freezer (-20°) and the product crystallized out. Following recrystallization from acetonitrile, the characteristic perchlorate IR absorption at 625 and 1100 cm^{-1} (Figure 29) was observed.

(9-acridinylmethyl)[3-(10,11-dihydro-5H-dibenz[b,f] azepin-5-yl) propyl] dimethylammonium bromide [28]: The compound [28] was previously prepared in our laboratory by the following procedure. Imipramine free base (472 mg, 1.68 mmole) and [1] (520 mg, 1.93 mmole) in 30 mL acetonitrile were reacted over night and the reaction mixture evaporated to dryness. The crude powder was dissolved in a minimum volume of dichloromethane and ether was added to precipitate the quaternary salt [28]. The fine flocculant precipitate (ca. 600 mg, 65% of theory) was collected by centrifugation and gave a single spot by TLC in acetonitrile-water (1:1). The 60 MHz PMR (Figure 30) was consistent with the proposed product.

Preparation of 9-benzylacridine [42] (99): To a glass pressure bomb was added 1 gm phenylacetic acid, 1.3 gm dry $ZnCl_2$ and 0.8 gm diphenylamine. The reaction was heated to 200° for 6 hr. After

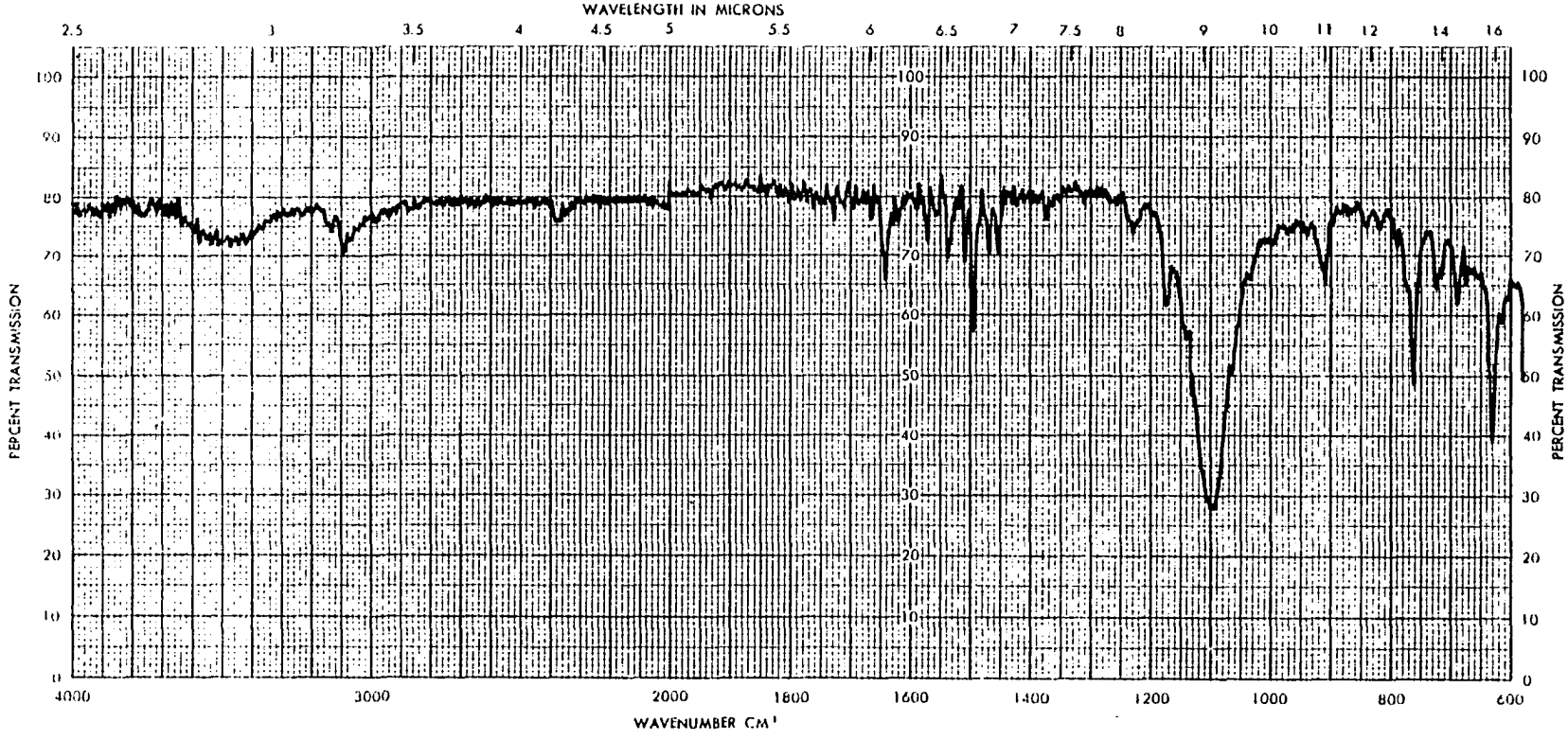

Figure 29. IR spectrum (KBr) of 9-acridinylmethylpyridinium perchlorate.

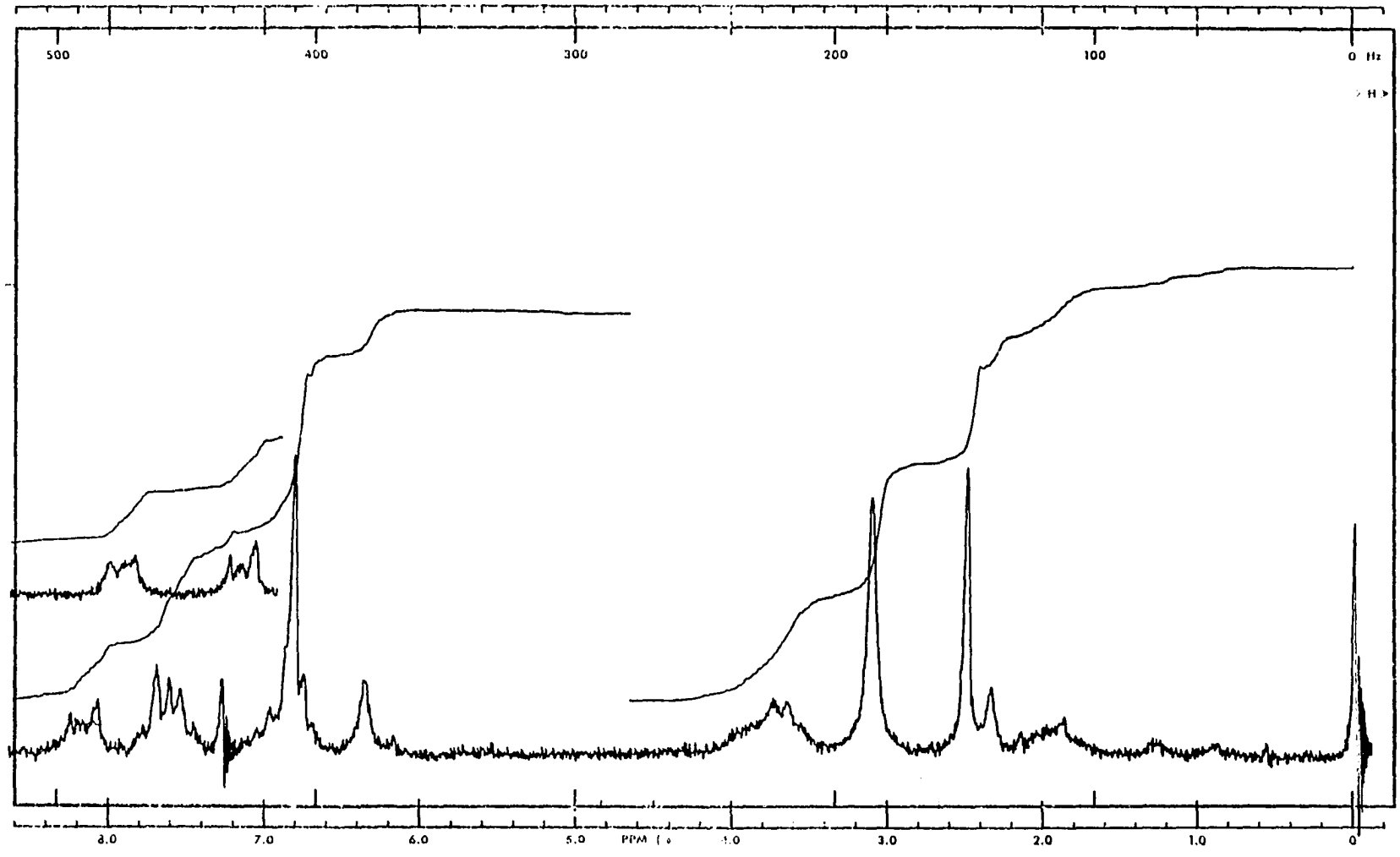

Figure 30. 60 MHz PMR spectrum ($CDCl_3$) of the imipramine quaternary [28].

cooling, ca. 150 mL $CHCl_3$ was added and the mass digested on a steam bath. The $CHCl_3$ layer was washed with basic water and evaporated to dryness and the product was sublimed to yield 270 mg (21% of theory). The product was recrystallized from ethanol and melted at 174-175° (lit. mp. = 173°). The 60 MHz PMR spectrum: ($CDCl_3$, TMS, delta) 7.0-8.4 (13H, m) 5.0 (2H, s). Mass spectrum (70 ev, relative intensity) 269 (M^+, base peak) 192 (10) were consistent with the proposed product.

Preparation of 9-(p-bromomethylphenyl) acridine [33]: 9-(p-tolyl) acridine previously prepared in our laboratory was recrystallized from ethanol-hexane (1:1) and melted at 187-188° (lit. mp. = 189-190°). 60 MHz PMR (CCl_4, TMS, delta):7.2-8.35 (12H, m) 2.55 (3H, s). To the tolyl derivative (640 mg, 2.49 mmole) in ca. 30 mL dry CCl_4 was added 480 mg N-bromosuccinimide and 10 mg benzoyl peroxide. The reaction at reflux temperatures was initiated with light and the reaction allowed to proceed for 2.5 hr. The progress of the reaction could not be followed by TLC because the starting material and product have identical R_f values in all solvents investigated. The progress of the reaction could be followed by NMR by looking for the appearance of a signal at 4.62 delta (Figure 31) and the disappearance of the signal at 2.55 delta. The reaction mixture was filtered hot and then evaporated to dryness. The crude solid could be recrystallized from CCl_4, methanol or ether in varying yields but all samples still had small amounts of acridine starting material by NMR. The IR (Figure 32)

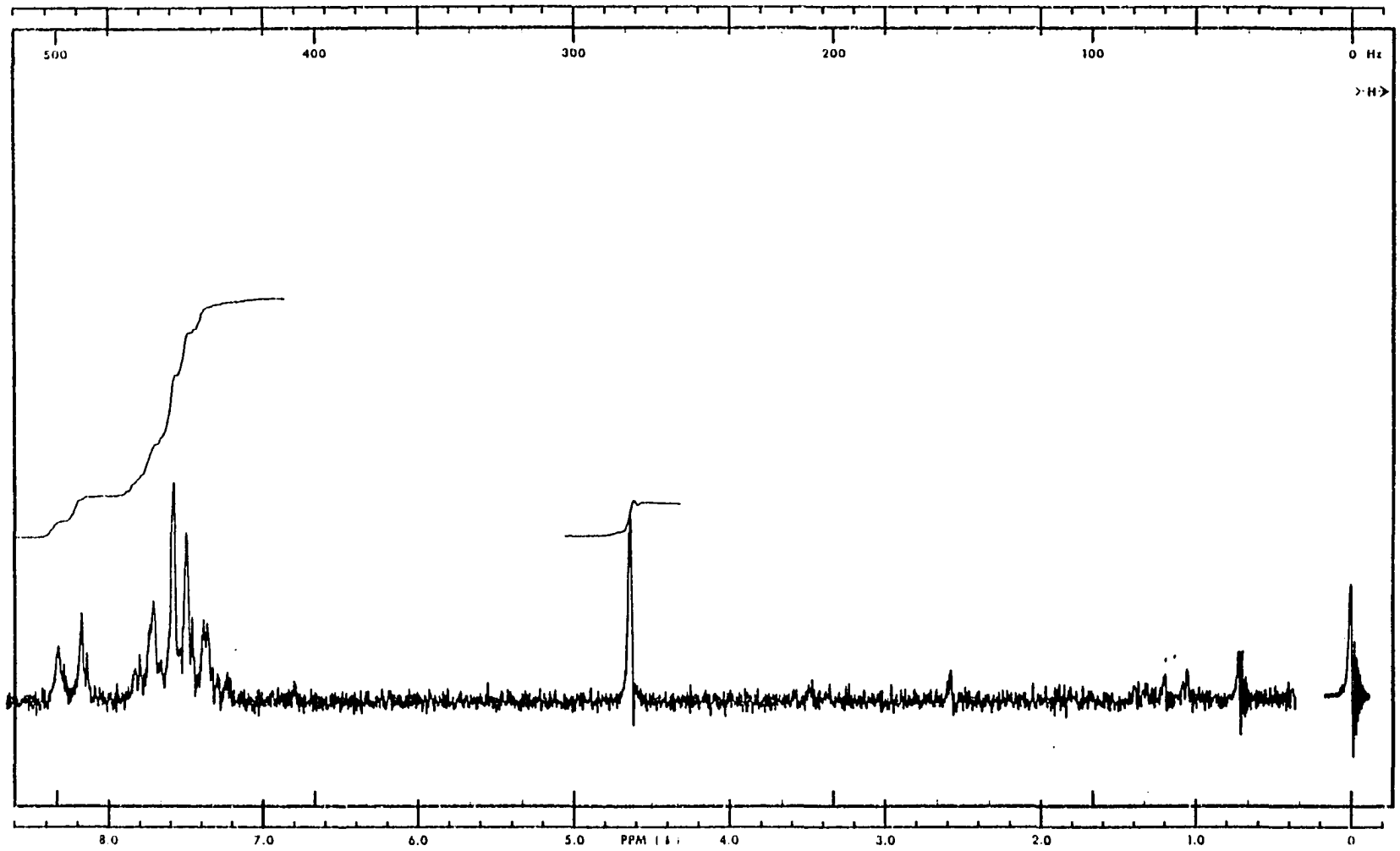

Figure 31. 60 MHz PMR spectrum ($CDCl_3$) of 9-(p-bromomethylphenyl) acridine [33].

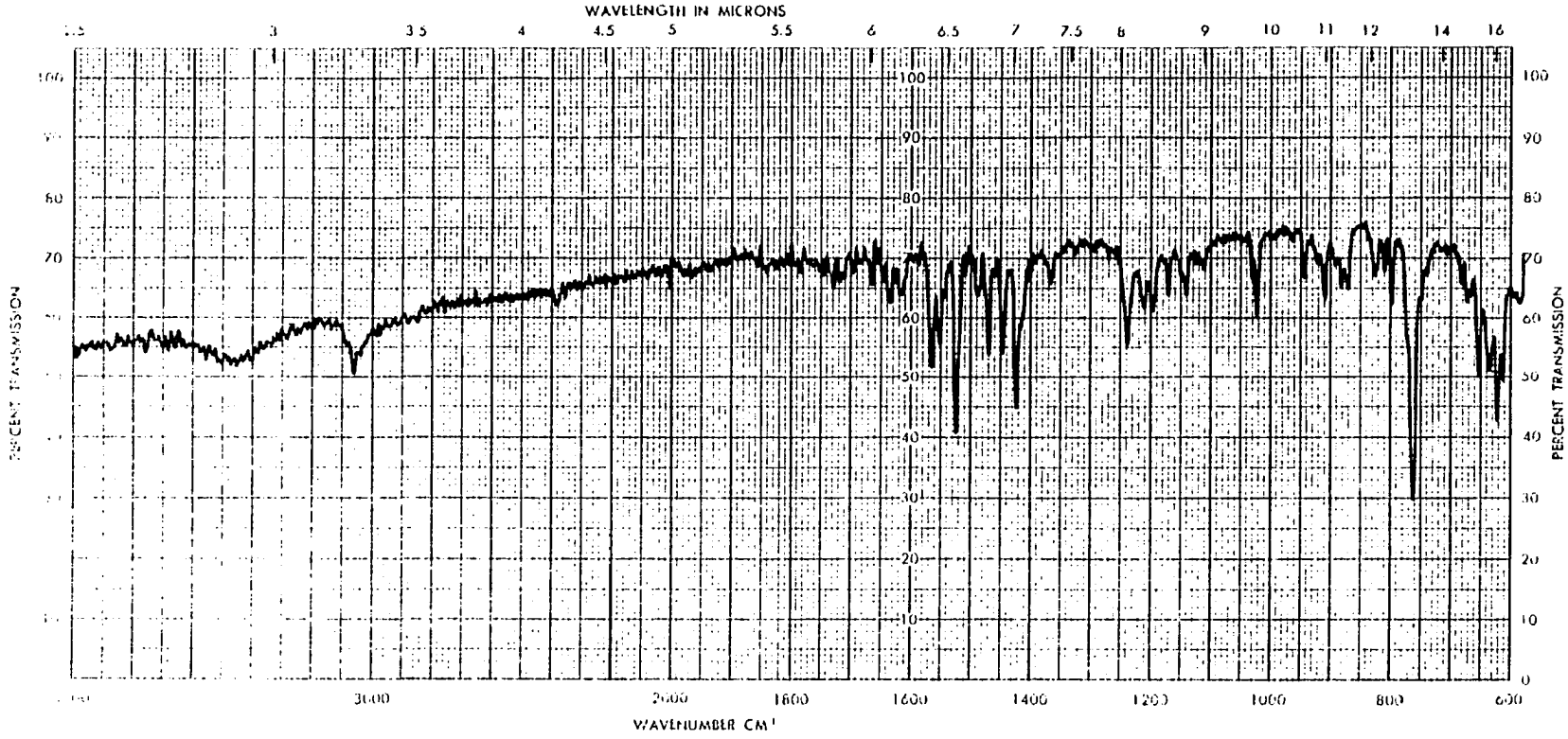

Figure 32. IR spectrum (KBr) of 9-(p-bromomethylphenyl) acridine [33].

and NMR spectra (Figure 31) were consistent with the brominated compound being the major component.

A preliminary attempt was made to evaluate the alkylating reagent [33] by reacting an equal weight amount of [33] with chlorpromazine [16] in acetonitrile. A quaternary product was formed (by TLC examination) and appeared nonfluorescent on the TLC plate. Since the observation of fluorescence on the TLC plate had proven very reliable as a screening method for determining if a particular quaternary would possess analytically useful fluorescence, this adduct was judged to be a nonfluorescent quaternary and the product was not characterized further. Thus, this area of investigation was terminated.

Preparation of 9-acridinylcarboxylic acid [9]: The various routes leading to [9] have previously been described in text and only the details of synthesis via 9-cyanoacridine will be described in detail in this section. Crude 9-chloroacridine [27] (ca. 1.0 gm) was refluxed in ca. 75 mL benzene and filtered hot through a medium fritted glass filter to remove much of the acridone present and the solution evaporated to dryness. The resulting 0.8 gm of [27] plus 0.3 gm potassium cyanide and 0.17 gm CuCN in ca. 15 mL methanol were heated for 4 hr at 150-170° in a pressure bomb. The hot reaction mixture was filtered and concentrated to ca. 1/2 the original volume which yielded 537 mg (74% of theory) of crude 9-cyanoacridine which was recrystallized twice from methanol and melted at 170-174° (lit. mp. = 179-180°). 9-cyanoacridine

(142 mg, 0.66 mmole) was dissolved in 1.5 mL 90% H_2SO_4 and heated to 110° for 3 hr. After cooling, 0.4 gm $NaNO_2$ was slowly added and the reaction continued for 3 hrs more at 140°. The reaction mixture was cooled and diluted with 25 mL water and the solid collected by filtration. The solid was dissolved in basic water, filtered and the filtrate acidified. The crude [9] (92 mg, 62% of theory) was collected and dried. The R_f value of [9] in acetonitrile-water (9:1) is 0.45 and certain impurities having lower R_f values were still present. The recommended recrystallization from a large volume of ethanol is extremely low yielding and the purity of the product (mp. = 285-290° dec., lit. mp. = 289-290°) was not significantly improved.

LITERATURE CITED

1. P. N. Kaul, M. W. Conway and M. L. Clark, Nature, 224, 327, (1970).

2. P. N. Kaul, M. W. Conway, M. K. Ticku and M. L. Clark, P. Pharm. Sci., 61, 581, (1972).

3. P. N. Kaul, M. W. Conway, M. L. Clark, Adv. Biochem. Phychopharm., 9, 391, (1974).

4. L. F. Fieser and M. Fieser,"Reagents for Organic Synthesis", 1, John Wiley and Sons, (1967), p. 685.

5. D. H. Efron, S. R. Harris, A. A. Manian and L. E. Gaudette, Psychoparhmacologia (Ber.), 19, 207, (1971).

6. A. Campbell, C. S. Franklin, E. H. Morgan and D. J. Tivey, J. Chem. Soc., 1145, (1958).

7. A. A. Albert, "The Acridines". 1st ed., Edward Arnold, London, (1951), p. 337.

8. L. Whitfield, P. N. Kaul, and M. L. Clark, J. Pharmacokin. Biopharm., 6, in press, (1978).

9. J. G. Calvert and J. N. Pitts, Jr., "Photochemistry", John Wiley and Sons, N.W., (1966), p. 176.

10. Ibid, p. 274

11. S. J. Strickler and R. A. Berg, J. Chem. Phys., 37, 814, (1962).

12. M. Kasha in "Fluorescence, Theory, Instrumentation and Practice", G. G. Guilbault ed., Marcel Dekker, Inc., N. Y., (1967), p. 203.

13. Reference 9, p. 295.

14. N. Mataga and T. Kubota, "Molecular Interactions and Electronic Spectra", Marcel Dekker, Inc., N. Y., (1970), p. 143.

15. S. K. Lower and M. A. El-Sayed, Chem. Rev., 66, 199, (1966).

16. Reference 14, p. 142.

17. E. L. Wehry in "Fluorescence, Theory, Instrumentation and Practice", G. G. Guilbault ed., Marcel Dekker, Inc., N. Y., (1967), chapter 2.

18. B. R. Henry and W. Siebrand, J. Chim. Phys., 20th Annual Report, 33 , (1969).

19. G. W. Robinson and R. P. Frosch, J. Chem. Phys., 38, 1187, (1963).

20. G. W. Robinson and R. P. Frosch, J. Chem. Phys., 37, 1962, (1962).

21. M. Gouterman, J. Chem. Phys., 36, 2848, (1962).

22. A. Rosencwaig, Anal. Chem., 47, 592A, (1975).

23. A. Kearvell and F. Wilkinson, J. Chim. Phys., 20th Annual Report, 125, (1969).

24. S. R. Veljkovic, Trans. Faraday Soc., 53, 1181, (1957).

25. B. L. van Duuren, Anal. Chem., 32, 1436, (1960).

26. B. L. van Duuren, Chem. Rev., 63, 325, (1963).

27. E. J. Bowen, N. J. Holder and G. B. Woodger, J. Phys. Chem., 66, 2491, (1962).

28. N. Mataga, Y. Kaita and M. Koizumi, Bull. Chem. Soc. Jpn., 29, 373, (1956).

29. M. A. El-Sayed, Acta. Phys. Pol., 34, 649, (1968).

30. A. Weisstuch, Fluorescence of Pyridine Derivatives, Ph. D. Dissertation, St. Johns University, (1969).

31. J. E. Adams, W. W. Mantulin and J. R. Huber, J. Am. Chem. Soc., 95, 5477, (1973).

32. Reference 7, p. 151.

33. A. A. Albert, "The Acridines", 2nd ed., Edward Arnold, London, (1966).

34. Ibid, p. 34.

35. Ibid, p. 93.

36. H. Jensen and F. Rethwisch, J. Am. Chem. Soc., 50, 1144, (1928).

37. A. E. Porai-Koshits and A. A. Kharkharov, Bull. Acad. Sci. USSR classes Sci. Chim., 243, (1944). (Chem. Abst. 39:1631).

38. Reference 4, vol. 3, p. 50.

39. H. M. R. Hoffman, J. Chem. Soc., 6748, (1965).

40. R. M. Coates and J. P. Chen, Tet. Lett., 2705, (1969).

41. M. W. Conway, Nanodetermination of Chlorpromazine and its Metabolites, M. S. Thesis, University of Oklahoma, (1971).

42. Lloyd Whitfield, Development of a New Nanoassay for Chlorpromazine and Chlorpromazine Sulfoxide, M. S. Thesis, University of Oklahoma, (1975).

43. R. E. Lehr, personal communications.

44. Reference 33, p. 282.

45. E. Vander Donckt in "Progress in Reaction Kinetics", G. Porter ed., 5, Pergamon Press, Oxford, (1970), p. 273.

46. K. Nakamaru, S. Niizuma and M. Koizumi, Bull Chem. Soc. Jpn., 42, 255, (1969).

47. G. Weber and F. W. J. Teal, Trans. Faraday Soc., 54, 640, (1958).

48. Reference 9, p. 278.

49. Ibid, p. 704.

50. "Aminco Fluorescence Accessories", American Instrument Co., Silver Springs, Md., (1977), p. 26.

51. H. K. Howerton in "Fluorescence, Theory, Instrumentation and Practice", G. G. Guilbault, Marcel Dekker, Inc., N. Y., (1967), p. 248.

52. I. B. Berlman, "Handbook of Fluorescence Spectra of Aromatic Molecules", Academic Press, N. Y., (1965), p. 35.

53. Ibid, p. 122.

54. R. M. Acheson in "The Chemistry of Heterocyclic Compounds", vol. 9, 2nd ed., A. Weissberger and E. C. Taylor eds., Wiley Interscience, N. Y., (1973).

55. J. Olmsted, Chem. Phys. Lett., 26, 33, (1974).

56. Gmelins "Handbuch der Anorganischen. Chemic.", 8 Auf. Verlag Chemie GMB II, (1958).

57. W. R. Ware, J. Phys. Chem., 66, 455, (1962).

58. B. Stevens and J. T. Dubois, Trans. Faraday Soc., 59, 2819, (1963).

59. P. B. Merkel and D. R. Kearns, J. Chem. Phys., 58, 398, (1973).

60. J. March, "Advanced Organic Chemistry", McGraw-Hill, N. Y., (1968), p. 243.

61. J. N. Murrell, "The Theory of the Electronic Spectra of Organic Molecules", Wiley and Sons, N. Y., (1963).

62. A. A. Albert and J. N. Phillips, J. Chem. Soc., 1294, (1956).

63. M. L. Bailey and J. P. M. Bailey, Theoret. Chim. Acta., (Berl.), 16, 303, (1970).

64. K. Tokumura, K. Kikuchi and M. Koizumi, Bull. Chem. Soc. Jpn., 46, 1309, (1973).

65. T. M. Vember, L. A. Kiyanskaya and A. S. Cherkasor, Zh. Obsheh. Khim., 33, 2342, (1963). (Chem. Abstr. 59:13784g).

66. Reference 33, p. 186.

67. T. G. Beaumont and K. M. C. Davis, J. Chem. Soc., 456, (1970).

68. R. A. Hann, D. R. Rosseinsky and T. P. White, J. Chem. Soc., Faraday Trans-2, 70, 1522, (1974).

69. C. A. Parker, "Photoluminescence in Solutions", Elsevier, N. Y., (1968), p. 436.

70. P. A. Leermakers, G. W. Byers, A. A. Lamola and G. S. Hammond, J. Am. Chem. Soc., 85, 2670, (1963).

71. J. B. Ragland and V. J. Kinross-Wright, Anal. Chem., 36, 1356, (1964).

72. Reference 9, p. 340.

73. O. Schnepp and M. Levy, J. Am. Chem. Soc., 84, 172, (1962).

74. "The Exciplex", M. Gordon and W. R. Ware eds., Academic Press, N. Y., (1975).

75. N. Mataga and T. Kubota "Molecular Interactions and Electronic Spectra", Marcel Dekker, Inc., N. Y., (1970).

76. R. S. Mulliken, J. Am. Chem. Soc., 74, 811, (1952).

77. R. S. Mulliken and W. B. Person, Ann. Rev. Phys. Chem., 13, 107, (1962) and references contained therein.

78. Reference 75, p. 205

79. Reference 75, p. 95

80. Reference 75, p. 424

81. J. B. Birks in "The Exciplex", M. Gordon and W. R. Ware eds., Academic Press, N. Y., (1975), p. 58.

82. T. Hayashi, T. Suzuki, N. Mataga, Y. Sakata and S. Misumi, Chem. Phys. Lett., 38, 599, (1976).

83. F. Hirayama, J. Chem. Phys., 42, 3163, (1965).

84. E. A. Chandross and C. J. Dempster, J. Am. Chem. Soc., 92, 3586, (1970).

85. N. Mataga in "The Exciplex", M, Gordon and W. R. Ware eds. Academic Press, N. Y., (1975), p. 127.

86. K. G. Rao, V. V. Bhujle and C. N. R. Rao., Spectrochim Acta., 31, 885, (1975).

87. T. Okada, T. Fujita, M. Kubota, S. Masaki, N. Mataga, R. Ide, Y. Sakata and S. Misumi, Chem. Phys. Lett., 14, 563, (1972).

88. S. Masaki, T. Okada, N. Mataga, Y. Sakata and S. Misumi, Bull. Chem. Soc. Jpn., 49, 1277, (1976).

89. I. E. Obyknovennaya and A. S. Cherkasov, Dokl. Akad. Nauk. SSSR, 173, 867, (1967). (Chem. Abst. 67:69183).

90. T. Azumi and H. Azumi, Bull. Chem. Soc. Jpn., 40, 279, (1967).

91. J. P. Kokko and J. H. Goldstein, Spectrochim. Acta., 19, 1119, (1963).

92. D. J. Blears and S. S. Danyluk, J. Am. Chem. Soc., 89, 21, (1967).

93. O. Sciacovelli and W. von Philipsborn, Org. Magn. Reson., 3, 339, (1971).

94. R. Foster and C. A. Fyfe, Biochem. et Biphys. Acta., 112, 490, (1966).

95. S. E. Elich, D. van der Helm, C. Barkley and R. E. Lehr, submitted to Cryst. Struct. Comm., (1978).

96. F. Krohnke and H. L. Honig, Justus Liebigs Ann. der Chemie., 624, 97, (1959).

97. L. Monti, Atti. Accad. Lincei., 24, 145, (1936). (Chem. Abst. 31:4321).

98. S. W. Chaikin and W. G. Brown, J. Am. Chem. Soc., 71, 122, (1949).

99. N. P. Buu-Hoi and J. Lecocq, Fec. Des. Trav. Chim. des Pays-Bas, 64, 251, (1945).

100. J. E. Sinsheimer, V. Jagodic, L. J. Polak, D. D. Hong and J. H. Burckhalter, J. Pharm Sci., 64, 925, (1975).

101. M. R. Gasco, Atti-Accad. Sci. Torino, Cl-Sci. Fis. Mat.-Nat., 773, (1974). (Chem. Abst. 84:121747s).